DANMARKS OG GRØNLANDS GEOLOGISKE UNDERSØGELSE RAPPORT 2010/47

Controls of hydrothermal quartz vein mineralisation and wall rock alteration between Sermilik and Grædefjord, southern West Greenland

Jochen Kolb, Annika Dziggel, Martin Koppelberg, Nicolas B. Stoltz, Alexander F. M. Kisters & Anders Bergen

GEOLOGICAL SURVEY OF DENMARK AND GREENLAND
MINISTRY OF CLIMATE AND ENERGY

G E U S

DANMARKS OG GRØNLANDS GEOLOGISKE UNDERSØGELSE RAPPORT 2010/47

Controls of hydrothermal quartz vein mineralisation and wall rock alteration between Sermilik and Grædefjord, southern West Greenland

Jochen Kolb, Annika Dziggel, Martin Koppelberg, Nicolas B. Stoltz,
Alexander F. M. Kisters & Anders Bergen

GEOLOGICAL SURVEY OF DENMARK AND GREENLAND
MINISTRY OF CLIMATE AND ENERGY

GEUS

Content

Content 3

Abstract 4

Introduction 5

Regional geological setting 6

Metamorphism 8
Structural geology 8

Geology of the Sermilik area 12

Lithology 12
Structural geology 13
Hydrothermal mineralisation 19

Geology of the Ilivertalik granite north of Sermilik 22

Lithology 22
Structural geology 23

Geology of the high strain zone between Grædefjord and Quvnerup ilua 25

Lithology 25
Structural geology 26
Hydrothermal mineralisation 29

Geology of the Sarfaat Aariaat area 32

Lithology 32
Structural geology 34
Hydrothermal mineralisation 37

Structural reconnaissance mapping and mineralisation of the Graedefjord region 38

Abstract 38
Introduction 39
Geological background 40
Results 40
Camp I: S of the Graedefjord 40
Camp II: Ikerasarssup Island, at the mouth of the Graedefjord. 47
Camp III: N of Graedefjord, ... 50
Camp IV: N of Graedefjord 54
Camp V: S of Graedefjord, Camp V was located some 10-12 km to the E of Camp I 58
Summary and Discussion 63
Structural Geology 63
Mineralisation 65

Summary and discussion 66

Conclusions and future work 68

References 70

Abstract

This field report describes localities studied in 2009 in the Buksefjorden and Grædefjord map sheet areas. The localities studied in the field were chosen with the aim to locate and interpret hydrothermal mineralisation and alteration. Two hydrothermal alteration and mineralisation types were identified in the field: (1) Quartz veins with associated hydrothermal alteration halos and (2) breccias in brittle-ductile faults.

The quartz veins are widespread, normally 5–20 cm wide and can be followed over 200–2000 m along strike. They are generally only weakly enriched in Au with values in the ppb range. Only north of Sermilik, the quartz veins and the alteration zones record Au grades of up to 6 ppm. The quartz veins are structurally controlled by the F_{2b} and F_3 folds that are obvious from the map pattern. Regionally, hydrothermal quartz veins and alteration systems are probably related to the 2720-2670 Ma deformation in the amphibolite facies that is considered to represent collision tectonics of the Tasiusarsuaq terrane with the northern Archaean terranes. The structural control of quartz veins and hydrothermal alteration and alteration assemblages comprising mainly Bt-Grt-Qtz-Po±Au indicate that the Au mineralisation is classified as hypozonal orogenic gold class of Au deposits.

The breccias in the brittle-ductile faults (probably D_5) show gossan weathering at the surface, however, do not return economically interesting metal enrichment.

The study area was investigated to a great detail and significant hydrothermal mineralisation has been found in the quartz veins. The gold values, also from the examples studied in 2008, are variable and only locally in the ppm range. Therefore, the potential for economic orogenic gold mineralisation in the studied areas (2008 and 2009) cannot be estimated. The location of hydrothermal quartz veins and their hydrothermal alteration halos is, on the other hand, well understood and can be predicted from the data presented in this report.

Introduction

This is a field report covering localities studied in June–July 2009 in SW-Greenland between the fjords Alangordlia and Sermilik on the Buksefjorden 1:100 000 geological map sheet and along Grædefjord on the Grædefjord 1:100 000 geological map sheet. Additionally, two areas south of Midgaard were mapped in detail. The field expedition and the follow up research work is co-financed by GEUS and the Bureau of Minerals and Petroleum (BMP), Nuuk, Greenland under the project entitled “Strukturelt kontrolleret hydrotermal omdannelse og mineralisering på regional skala og detaljestudie af udvalgte grønstensbælter i Sydvestgrønland 61°30’ – 64°00’”. The aim of this report is to document the field investigations and the data collected during fieldwork and combining and discussing this new data together with previous investigations and published accounts. A special focus is drawn on the potential for hydrothermal mineralisation and the documentation of the studied occurrences.
Three teams of two geologists each worked in different areas supported by helicopter: (1) J.Kolb (GEUS, project leader) and A.Dziggel (RWTH Aachen university) started fieldwork in Sermilik, moved to locations south of Grædefjord the 7th July and finally joined team 3 to discuss the results of the mapping program; (2) A.F.M.Kisters (University of Stellenbosch) and A.Bergen (University of Copenhagen) concentrated on the area north and south of Grædeford; and (3) N.B.Stoltz and M.Koppelberg (both RWTH Aachen University) mapped two areas of the Fiskenæsset complex as part of their M.Sc. (Diplom) mapping program. As a basis, not only the 1:100 000 geological map sheets were used but also the detailed field maps and field reports of the geologists that worked in the area before were taken into account and were found to be very useful. The field maps turned out to be very detailed and no major discrepancy between the maps and our investigations were found. However, outcrops of the Ilivertalik granite north of Sermilik close to the eastern map boundary of the Buksefjorden 1:100 000 geological map sheet didn’t show the characteristic porphyritic fabric that otherwise defines the Ilivertalik granite. On the Grædefjord 1:100 000 geological map sheet, the mapping of late leucocratic granitoid intrusions was found to be inconsistent with detailed mapping in some areas and no distinction between these leucocratic rocks and the earlier TTG gneiss in other areas. This is addressed in discussions with the colleagues from the mapping department in GEUS in their own project with the BMP, and will be subject to amendments on the digital geological map.

Regional geological setting

The study area is situated in the Tasiusarsuaq terrane of the North Atlantic craton of southern West Greenland (Fig. 1). The Tasiusarsuaq terrane extends from approximately Ameralik in the north to the Frederikshåb Isblink in the south (Fig. 1). This report describes field data collected in the area between Sermilik and Fiskenæsset and, therefore, the regional geology description is focused on that part of the Tasiusarsuaq terrane.

Supracrustal rocks occur as small lenses and belts in TTG gneiss and are dominated by amphibolite and mafic granulite with minor meta-sedimentary and meta-ultramafic rocks (Chadwick & Coe 1983; Friend *et al.* 1996). Meta-rhyolite from Nunatak 1390 yields an age of 2876 ± 5 Ma (Næraa & Scherstén 2008), however a correlation of these rocks with those from the main land is, to date, not straight forward (Windley & Garde 2009). The amphibolite and the mafic granulite are mainly tholeiitic and picritic basaltic rocks with a subalkaline affinity (Kolb *et al.*, in prep.). Meta-ultramafic rocks form dykes and sheets within the supracrustal units. They represent meta-pyroxenites and meta-peridotites and have similar trace element systematic as the amphibolite and mafic granulite, which suggests that the dykes and sheets represent feeder structures (Kolb *et al.*, in prep.). The trace element pattern indicate that the mafic and ultramafic lithologies represent oceanic crust in an intra oceanic island arc or back arc setting (Kolb et al., in prep.).

The Fiskenæsset complex represents a ca. 2970 Ma metamorphosed layered igneous complex that is up to 2 km wide, comprising anorthosite, leucogabbro, gabbro, peridotite and up to 20 m thick chromite seams (Fig. 1, Ghisler 1970; Myers 1985; Polat *et al.* 2009; Windley *et al.* 1973). The rocks intruded as sills into amphibolite showing pillow structures (Escher & Myers 1975; Polat *et al.* 2009). Major and trace element data suggest a petrogenetic link, through a tholeiitic differentiation trend, between the Fiskenæsset complex and bordering basaltic rocks (amphibolite/mafic granulite) (Polat *et al.* 2009). The composition of the Fiskenæsset complex and surrounding amphibolite/mafic granulite is consistent with a subduction zone geodynamic setting. The rocks are, therefore, interpreted to represent remnants of Neoarchaean oceanic island arc similar to anorthosite complexes developed in Phanerozoic magmatic arc systems (Polat *et al.* 2009). TTG gneiss forms lit-par-lit intrusions into the rocks of the Fiskenæsset complex (Myers 1976; Polat *et al.* 2009).

The TTG gneiss yield zircon U–Pb ages between 2.92–2.81 Ga with a maximum between 2.86–2.84 Ga (Crowley 2002; Friend & Nutman 2001; Næraa & Scherstén 2008; Nutman & Friend 2007; Schjøtte *et al.* 1989). The gneiss commonly has migmatitic fabrics and contains numerous later felsic intrusions in the form of pegmatites and larger intrusive bodies.

Conformable layers of porphyritic granitoids, the Ilivertalik granite, occur in a zone that extends about 50 km in E–W direction and 20 km in N–S direction (Fig. 1). The syn- to late-tectonic granitoid locally contains Opx owing to its intrusion into the deeper crust at 2795 +11/-7 Ma (Pidgeon & Kalsbeek 1978).

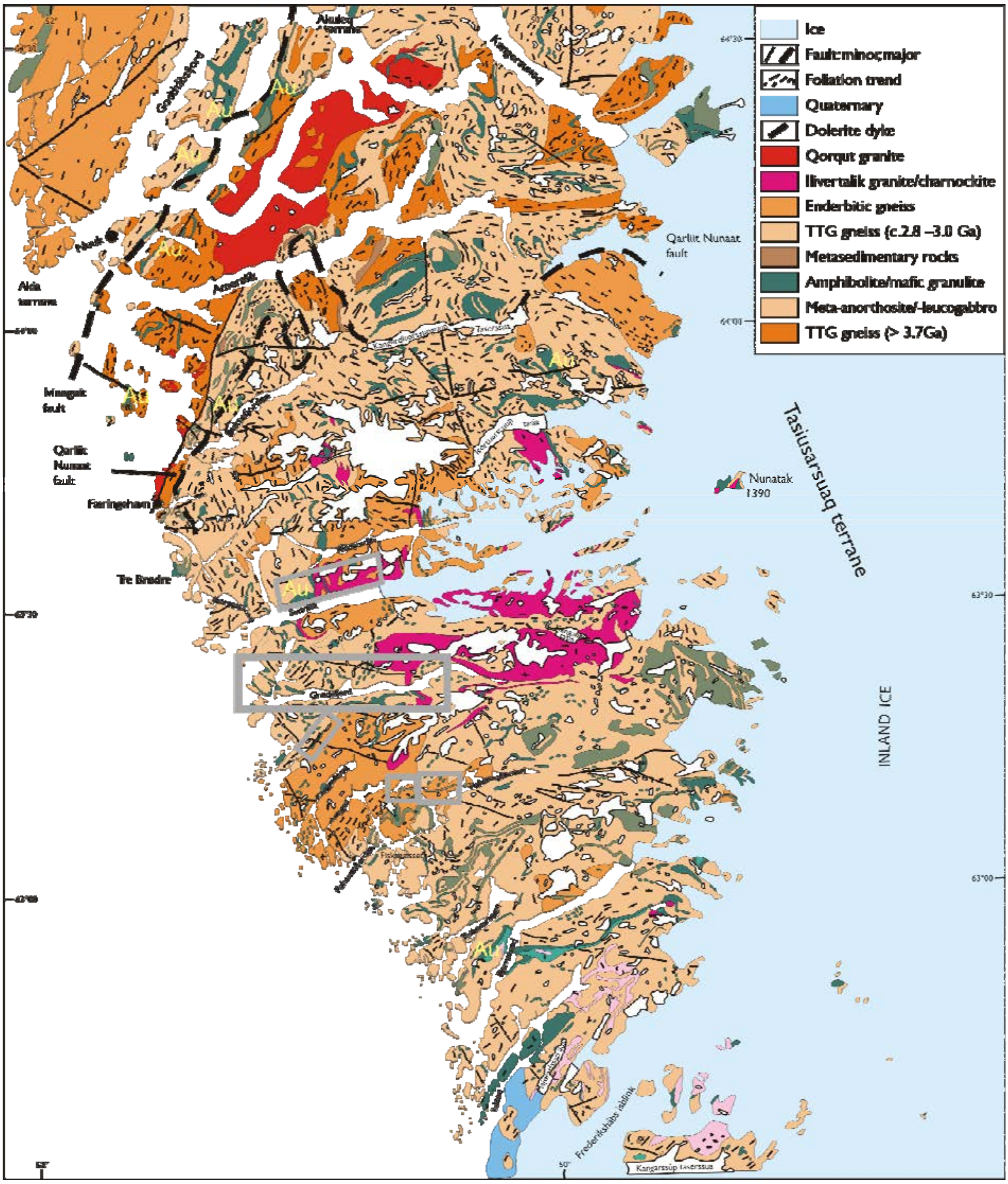

Figure 1. *Geological map of southern West Greenland and location of the study area covered by field work in 2009 (modified after, Escher & Pulvertaft 1995). "Au" in yellow shows different gold occurrences.*

Metamorphism

Granulite-facies metamorphism is the characteristic metamorphic facies of the Tasiusarsuaq terrane (Chadwick & Coe 1983). The peak metamorphic conditions were estimated at about 10.5 kbar and 810°C in gneiss and mafic granulite (Riciputi *et al.* 1990; Wells 1976). Granulite-facies metamorphism was dated on a metamorphic zircon at 2795 +11/-7 Ma in the south (Pidgeon & Kalsbeek 1978) and at the northern terrane boundary by U–Pb zircon dating of an Opx-bearing pegmatite at 2805 ± 2 Ma (Crowley 2002). Both ages are similar within error and suggest that the peak of granulite-facies metamorphism occurred at ca. 2800 Ma. The metamorphic peak was followed by locally extensive amphibolite-facies retrogression, most notably in a several km wide zone at the northern margin of the terrane (Friend *et al.* 1987, 1988; Kolb *et al.* 2009; Nutman *et al.* 1989a; Windley & Garde 2009). In meta-sedimentary rocks close to the Ilivertalik granitoid, retrograde metamorphic conditions are estimated at 7 kbar and 630°C (Riciputi *et al.* 1990; Wells 1976). Based on U-Pb dating of metamorphic Zrn, Tnt and Mnz, the amphibolite-facies retrogression was dated at ca. 2740–2700 Ma (Crowley 2002). A similar metamorphic age was established based on a 2719 ± 5 Ma zircon age from further southeast (Næraa & Scherstén 2008). An even younger tectono-metamorphic event, dated at ca. 2630-2610 Ma, was established for a NNW-SSE trending shear zone close to Isortuarrsuup tasia (Fig. 1, Nutman & Friend 2007).

Structural geology

The general map pattern of the study area is characterised by the outline of the supracrustal rocks and the rocks of the Fiskenæsset complex, which display an open to close fold pattern with southeast to south trending axial traces, locally fold interference pattern, and the massive intrusion of the Ilivertalik and the Taserssuatsiait granitoids in the south (Fig. 1). The aim of the structural study is to define relative age relationships between different deformation stages and between deformation, metamorphism and magmatism as well as to identify the structures that are related to the exhumation of the granulite facies rocks. In detail, the rock fabrics indicate five different deformation stages (D_1–D_5; Table 1) (Kolb *et al.* 2009).

D_1 fabrics are preserved in low strain enclaves, where a S_1 foliation and/or S_1-parallel aplitic dykes are preserved in later isoclinal folds. This is mainly observed in the TTG gneiss in the northern part of the terrane.

During D_2, the S_1 foliation was isoclinally folded (F_{2a}) and an axial planar S_2 foliation developed that strikes mainly NE-SW and dips moderately SE. Early isoclinal F_{2a} folds form rootless, intrafolial folds in S_2 or, in low strain enclaves, form up to 50 cm wide (half wavelength) rootless folds. The axial plane is always parallel to S_2, however, the b_{2a} fold axes are variable and show no distinct orientation maximum. The S_2 foliation is the penetrative foliation in the northern area (Fig. 1). Shear sense indicators such as σ-, δ-clasts and S-C fabrics point to a reverse sense of movement broadly to the NW. Away from these shear zones, the S_2 foliation is locally folded into upright, open to close F_{2b} folds with a wavelength of up to 3 km. The F_{2b} fold axis is oriented approximately perpendicular to the mineral stretching lineation and plunges at shallow angle to the ENE.

The D_3 stage represents the regional-scale fold stage that is obvious from the map pattern (Fig. 1). The S_2 foliation is folded into upright, open to tight folds with NW–SE trending axial traces on a km-scale. The b_3 fold axes mainly plunge at shallow to moderate angles (5°–25°) SE, but non-cylindrical folds were also observed with b_3 plunging both SE and at around 20° NW. Locally, type 2 fold interference patterns incorporating F_{2b} and F_3 folds form weak mushroom-like patterns on the map (Fig. 1), because the relief of the area is too high to show the ideal pattern (Ramsay & Huber 1987). The F_3 folds show a progressive decrease in wavelength from gentle to isoclinal, which is connected to an increase in amplitude at various scales. The limbs of the tight to isoclinal F_3 folds are sheared off. This is also observed at all scales: higher order folds are sheared off by up to 2 m wide shear zones, whereas map-scale folds are sheared off by 20–100 m and, locally, up to 1 km wide shear zones (Fig. 1). The most abundant shear zones are characterised by a closely spaced, near vertical, NW–SE trending S_3 foliation. The L_3 mineral stretching lineation plunges predominantly at 5°–20° to the SE. If both sinistral and dextral sense are observed the indicators of sinistral sense of shearing dominate by approximately 80:20, but often are dextral shear sense indicators conspicuous by their absence. However, locally shear zones with predominant dextral shear sense indicators are observed. No systematic difference in the orientation of the shear zones, S_3 foliation or L_3 lineation is related to the different shear sense indicators. Recumbent, WSW-verging F_3 folds are locally observed, where the foot wall limb of anticlines is activated as up to 1 m wide, near horizontal reverse shear zones. The reverse deformation is directed to the WSW.

Locally, several metre wide low-angle D_4 faults are observed (Fig. 2). The faults dip at about 25° to the WNW and have a down-dip striation on the fault surface. Dragging fabrics of the regional foliation indicate normal sense of movement and a displacement in the order of 10-50 m.

Figure 2. *Photograph of the southern shore of Sermilik with D_4 normal faults characterising the topography. White arrows mark the sense of shear.*

The D_5 stage is characterised by several sets of faults that were not studied in detail and are therefore grouped here. The main orientations of faults are NW–SE, N–S and E–W (Fig. 1). They show a lateral displacement of marker horizons on the map by up to 1 km. Dolerite dykes are often parallel to the E–W-trending faults (Fig. 1).

Comparing this structural interpretation by Kolb et al. (2009) with older published interpretations, shows that they are similar in many respects (Table 1, Andersen & Friend 1973;

Chadwick & Coe 1983; Hopgood 1976; Kalsbeek & Myers 1973; Kolb *et al.* 2009). Only the study by Hopgood (1976) is from a local area, very detailed and not easy compatible to all others and a correlation is vague (cf.; Table 1). Most of the authors agree on three main deformation stages: D_1 represented by intrafolial folds and a first S_1 foliation; D_2 characterised by larger-scale folds, a penetrative S_2 foliation and NW-directed reverse shearing; and D_3 comprising folds with southerly-dipping fold axes and near-vertical NNW-SSE trending shear zones (Table 1). The regional-scale D_4 dome and basin structures of Chadwick and Coe (1983) most probably represent D_2-D_3 fold interference pattern and/or non-cylindrical D_3 folds of Kolb et al. (2009).

Table 1: Compilation of structural data published for the Tasiusarsuaq terrane and possible correlations.

	Kolb et al. (2009)	Chadwick and Coe (1983)	Kalsbeek and Myers (1973): NW domain	Kalsbeek and Myers (1973): SE domain	Andersen and Friend (1973)	Hopgood AM (1976)	possible correlation
D_1	first foliation, parallel aplitic dykes	intrafolial folds, first folding	isoclinal folds, recumbent		small-scale folds	intrafolial folds, isoclinal, detached	D_1
D_2	general NW-SE compression	large-scale folds, penetrative foliation	isoclinal folds, sub-vertical axial planes, trending NE-SW	tight to isoclinal folds, near-vertical axial planes, trending E-W to NE-SW, locally overturned	penetrative foliation, trending NE-SW, major folds	isoclinal folds, foliation, boudinage	D_1
F_{2a}	isoclinal folds, axial planar foliation, no regular orientation of fabrics: transposed later						
S_2	penetrative foliation, locally mylonitic, dipping S-SE, down-dip mineral stretching lineation, NW thrusting						
F_{2b}	open, upright folds, fold axis perpendicular to mineral stretching lineation (NE/E-W/SW): stacking						
D_3	general E-W compression	large-scale folds, penetrative foliation, fold axes plunging S-SSE	tight folds, sub-vertical axial planes, trending NW-SE		small- to medium-scale folds, overturned, axial planes gently dipping S	asymmetrical folds, recumbent, weak axial planar foliation, dipping gently SW: N-S compression	F_{2a}
F_3	upright folds, fold axes plunging S-SSE						
S_3	near-vertical NNW-SSE trending strike-slip shear zones, mainly sinistral, but dextral also observed; locally m-scale reverse shear zones, top to the W						
D_4	low-angle normal faults, dipping WNW	regional-scale dome and basin structures			folds, near-vertical axial planes, trending SE-NW	asymetrical, inclined, tight folds, axial planes dipping SE: NW-SE compression	D_2
D_5	NW-SE, N-S, E-W faults (Proterozoic)					upright, moderately tight folds, trending ESE-WNW: NNE-SSW compression	F_{2b}
D_6						open, upright folds, trending SSE-NNW: ENE-WSW compression	D_3
D_7						open, upright folds, trending NNE-SSW: WNW-ESE compression	
D_8						low-angle thrusts, pseudotachylite, dipping SE: NW-SE compression	D_4

Geology of the Sermilik area

Lithology

The Sermilik area consists of three major components, including ca. 3.0 to 2.8 Ga TTG gneiss, a larger, mainly E-W trending supracrustal belt dominated by mafic granulite, and granitoid gneisses of the Ilivertalik granite/charnockite (Fig. 1). The study area (camp II) is dominated by TTG gneiss and the several hundred metres thick supracrustal sequence of mainly mafic metavolcanic rocks that are intercalated with minor layers of aluminous felsic schist. The rocks are metamorphosed to granulite facies conditions and have been intruded by abundant pegmatite dykes.

The fine- to medium-grained TTG gneiss has a well-developed subvertical and E-W trending foliation, which is locally mylonitic (Fig. 3a). The rocks mainly consist of quartz, plagioclase, clinopyroxene and hornblende, with local retrogression to biotite and epidote. Locally developed leucosomes containing clino- and orthopyroxene crosscut the mylonitic fabric, indicating that granulite-facies metamorphism outlasted deformation. The contact between the TTG gneiss and the mafic granulites is tectonic, primary intrusive contact relationships between the two rock types were not observed (Fig. 3b). However, the contact is marked by the intrusion of abundant leucocratic (Ilivertalik?) granitoids that contain xenoliths of mafic granulite and the older gneisses. The mafic granulites are relatively massive rocks that contain variable proportions of clinopyroxene, garnet, plagioclase, hornblende, quartz, opaque phases and, locally, orthopyroxen and/or titanite. They commonly display a fine layering between relatively mafic and felsic layers. Up to several cm wide leucosomes containing large crystals of garnet and clinopyroxene are developed both parallel and at an angle to the foliation. Clinopyroxene is often replaced by hornblende or fine-grained symplectites made up of epidote and quartz. The intercalated aluminous felsic schists consist of quartz, plagioclase, biotite, garnet and, locally, sillimanite and kyanite (Fig. 3c). At one locality (09JKOL014), the aluminous felsic schist contains an up to ca. 0.5 m thick, boudinaged layer of bright-green clinopyroxenite. Individual boudins are unfoliated and cut by numerous quartz-veinlets. The rocks mainly consist of clinopyroxene, plagioclase, quartz and, locally, hornblende, titanite and rare garnet. The leucocratic granitoids at the contact between the TTG gneiss and the supracrustal belt, as well as the numerous pegmatite dykes within the mafic granulite sequence crosscut the earlier-formed fabrics (Fig. 3d). The pegmatite dykes are variable in orientation with moderate to steep dips to the NE and SW. The NE dipping pegmatites are strongly schistose to mylonitic. Both leucocratic granitoids and pegmatite dykes have a similar mineralogy and consist of quartz, plagioclase, K-feldspar, garnet, biotite, opaque phases, as well as epidote and/or muscovite. The mineral assemblage in the pegmatites points to amphibolite facies conditions during their emplacement.

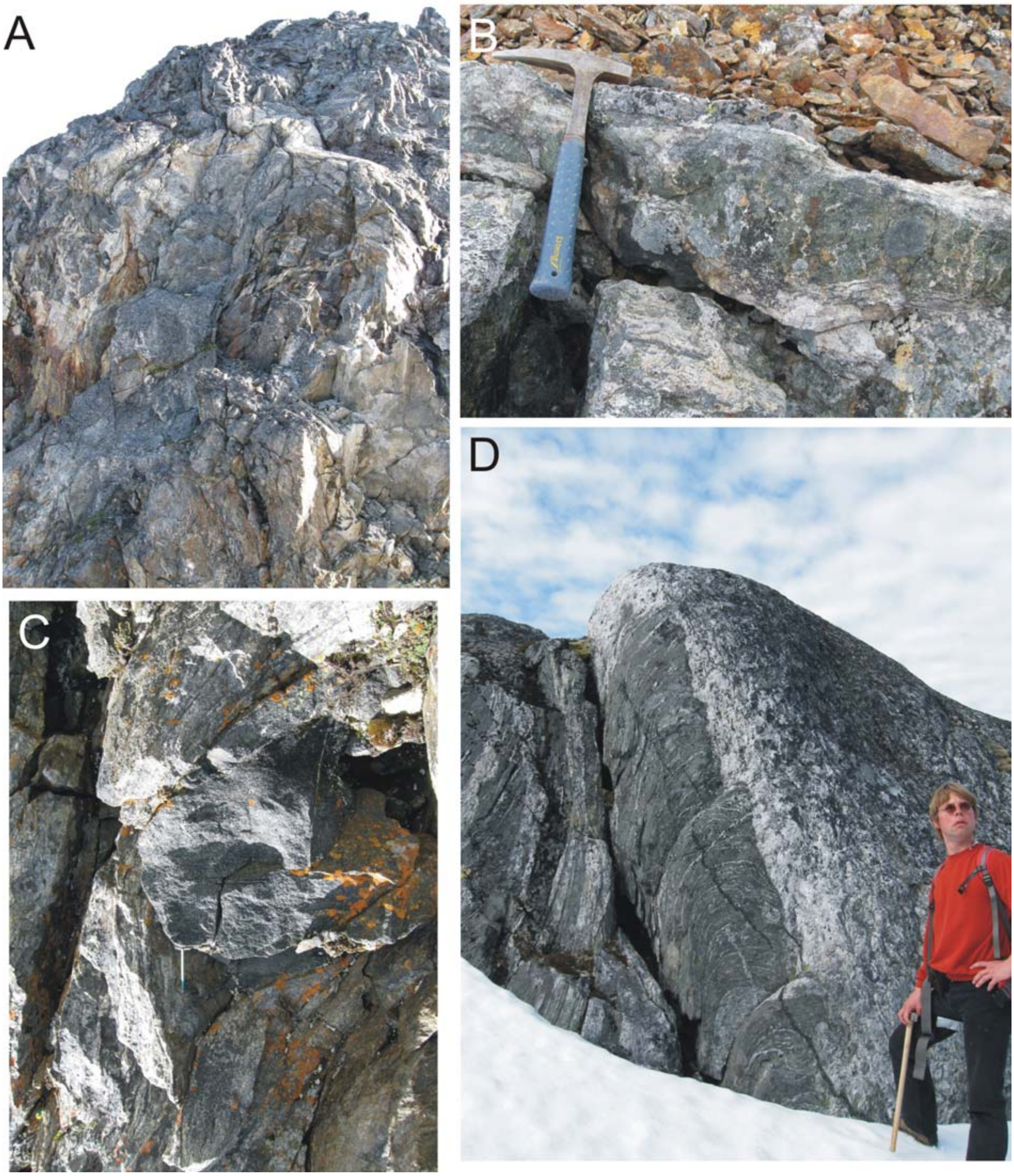

Figure 3. *(a) Grey TTG gneiss with closely-spaced foliation and locally cross cutting leucosome; (b) Tectonic contact between TTG gneiss and mafic granulite; (c) Aluminous felsic schist; (d) Pegmatite intruded into mafic granulite transposing the $S_{1/2}$ foliation.*

Structural geology

The larger supracrustal belt on the northern shore of Sermilik shows a fold interference pattern with ENE-WSW trending axial traces refolded by later folds with N-S trending axial traces (Fig. 1). These two fold stages are correlated with F_{2b} and F_3, respectively. The eastern boundary to the porphyritic Ilivertalik granite is represented by a N-S trending D_3 reverse shear zone. In the massive Ilivertalik granite lacking the porphyritic fabric, three foliations are distinguished.

D_1 fabrics are represented by a S_1 foliation that is defined by Hbl, Bt, Opx and Cpx in the gneiss, by Bt and Sil in meta-sedimentary rock and by Opx, Cpx and Hbl in the mafic granulites. These mineral assemblages suggest that the D_1 deformation stage occurred in the granulite facies. Felsic veinlets and pegmatites are also parallel to S_1. Some of these dykes and sills are undeformed, indicating that their intrusion postdates the D_1 deformation. The S_1 foliation is folded into moderately to steeply plunging, close to isoclinal F_{2a} folds (Fig. 4a). The fold axes have variable orientations due to later refolding (Fig. 5). The wave-length varies between about 1 m to cm-scale in intrafolial folds (Fig. 4a, b). The axial planar foliation is a penetrative S_2 foliation that is mainly parallel to S_1 and in the absence of F_{2a} folds often impossible to distinguish from S_1 (Fig. 4a, 5, 6). The S_2 foliation is defined by Hbl and Bt in the gneiss, by Bt and Sil in meta-sedimentary rock and by Cpx, Bt and Hbl in the mafic granulites, suggesting that the D_2 stage occurred under amphibolite facies conditions. Felsic pegmatitic dykes parallel to the S_2 foliation also contain an amphibolite facies Hbl-Pl-Kfs-Qtz mineral assemblage. No preferred orientation of S_2 is observed due to folding of the foliation in two subsequent stages (Fig. 5-7). The mineral stretching lineation is down-dip to slightly oblique (Fig. 6d) and mainly defined by Hbl, Cpx and stretched Qtz and Fsp. Locally, a L>S fabric is developed in the gneiss and the pegmatite. Shear sense indicators such as σ-, δ-clasts, S-C fabrics and transposition fabrics are inconsistently showing both reverse and normal sense of movement (Fig. 6d). This ambiguous data is interpreted to be the result of multiple reactivations of the S_2 foliation planes during the later stages of deformation, e.g. F_{2b} flexural slip folding. The S_2 foliation is folded into gently to moderately plunging, open to close F_{2b} folds (Fig. 6a-c). The F_{2b} fold axes mainly plunge to the SE, but northwesterly plunges are also observed and explained by later refolding. The amplitude and wavelength of F_{2b} is generally at an m-scale (Fig. 4c). Pegmatites are parallel to S_2 and, locally, folded by F_{2b}, but also cross cut S_2 and F_{2b} folds (Fig. 3d, 6c, 7c). Some of the cross cutting pegmatites are axial planar to F_{2b} folds and some form a conjugate pattern, where the intersection is close to parallel to the F_{2b} fold axis. On a map-scale, the brown band of meta-sedimentary rock shows an F_{2b} fold (Fig. 1).

The D_3 deformation stage folded the S_2 foliation into upright, open, gently plunging F_3 folds (Fig. 7). The F_3 fold axes plunge gently to the SW, which can be seen on the map-scale at the gneiss-mafic granulite contact (Fig. 1). Locally, pegmatites intruded F_3 folds parallel to S_2 and in ac-orientation, indicating that they intruded during the D_3 deformation stage (Fig. 7c). A weak axial planar S_3 foliation is developed in places (Fig. 7). The foliation trends NE-SW and is near-vertical. Narrow, up to 1 m wide shear zones are parallel to the S_3 axial planar foliation. Mylonites in these shear zones show steep dips either to the NW or to the SE (Fig. 7d). Shear sense indicators such as σ-, δ-clasts, S-C fabrics and transposition fabrics indicate reverse sense of movement for both orientations.

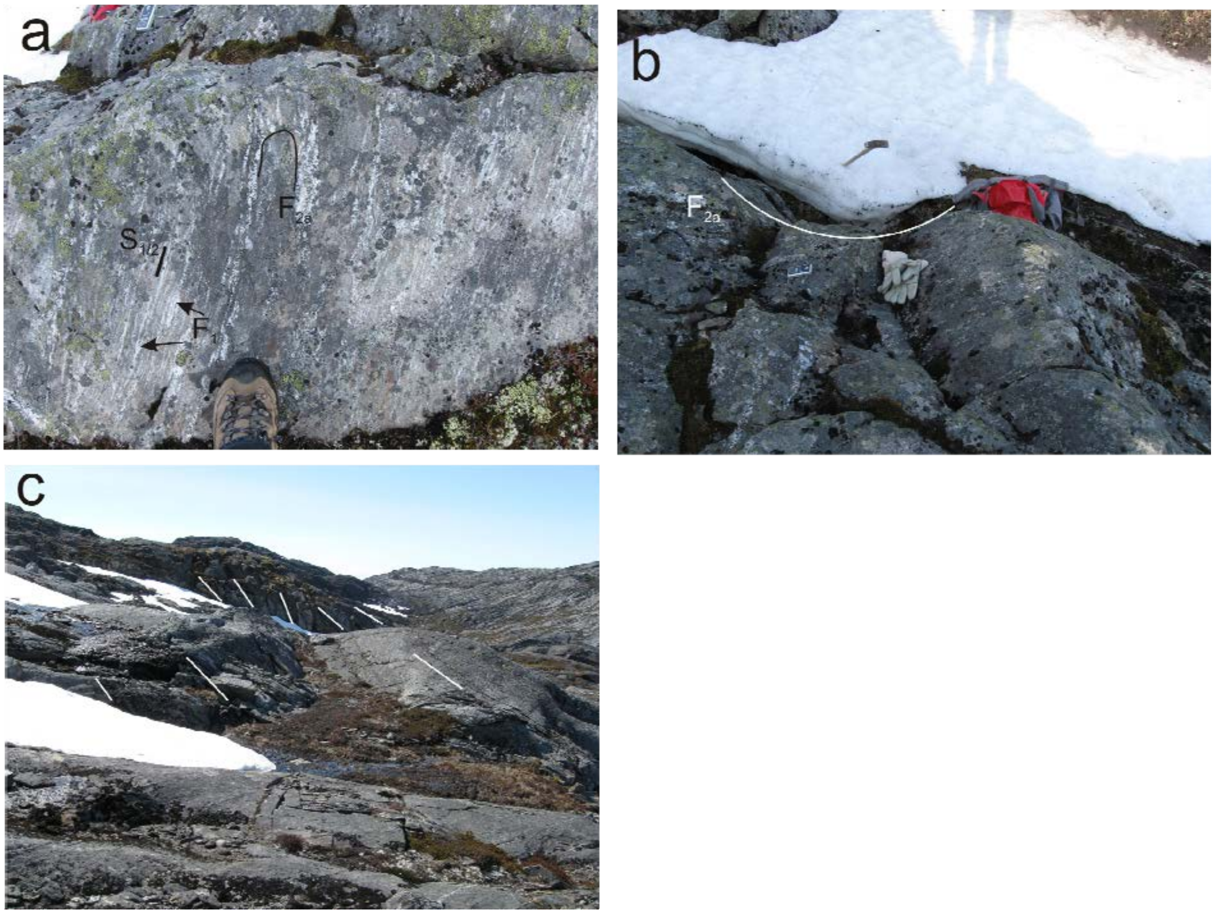

Figure 4. *(a) F_1 intrafolial folds, closely-spaced $S_{1/2}$ foliation defined by leucosome banding in the TTG gneiss and cm-scale F_{2a} fold; (b) M-scale F_{2a} fold in TTG gneiss with a near-vertical fold axis; (c) Variation in S_2 orientation due to open F_{2b} folds with shallow-plunging, NW-SE trending fold axes.*

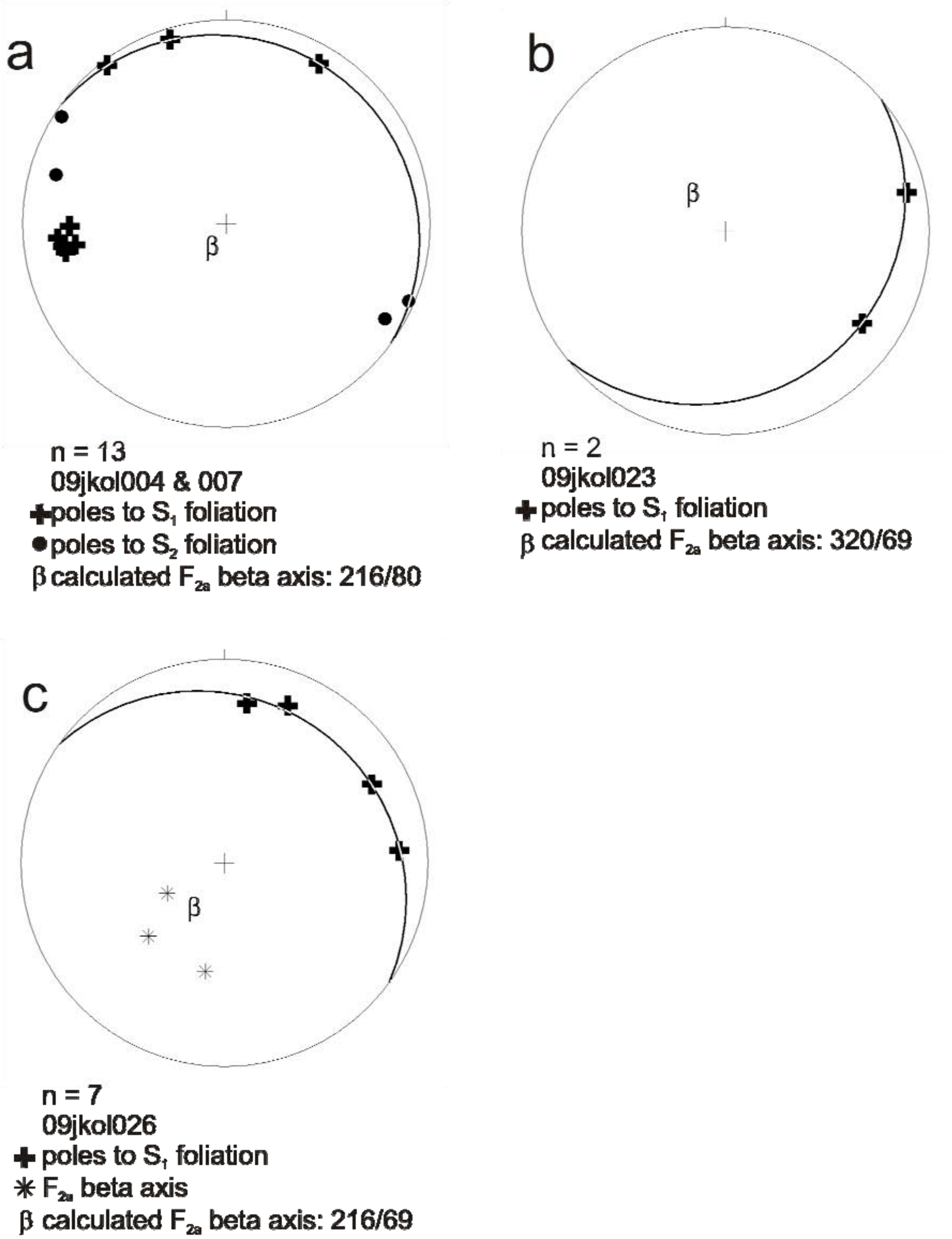

Figure 5. *(a) Poles to S_1 and S_2 forming a great circle characteristic of F_{2a} folds, locality 09jkol004 & 007; (b) Poles to S_1 forming a great circle characteristic of F_{2a} folds, locality 09jkol023; (c) Poles to S_1 forming a great circle characteristic of F_{2a} folds and measured F_{2a} beta axes, locality 09jkol026.*

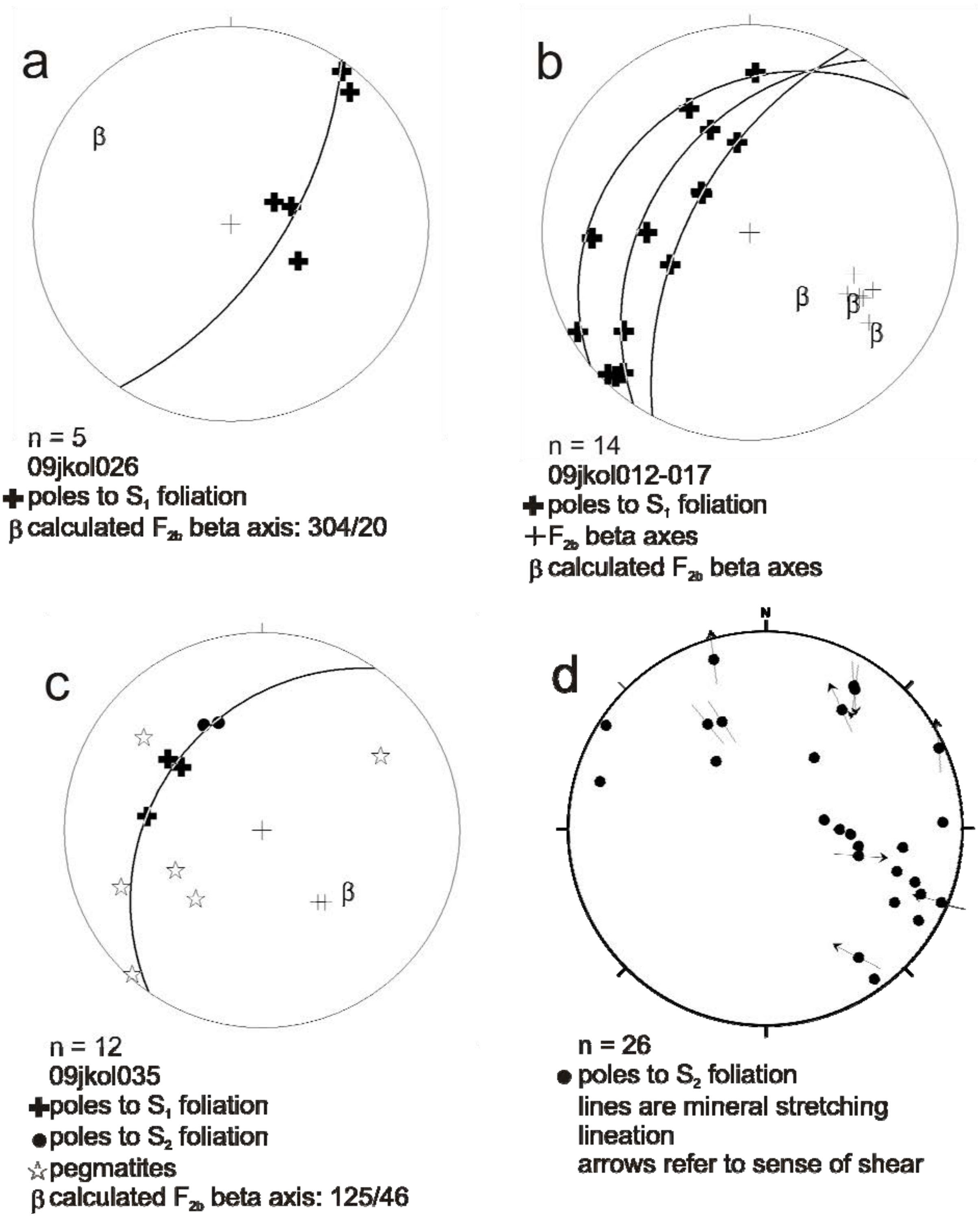

Figure 6. *(a) Poles to S_1 forming a great circle characteristic of F_{2b} folds, locality 09jkol026; (b) Poles to S_1 forming a great circle characteristic of F_{2b} folds and measured F_{2b} beta axes, locality 09jkol012 - 017; (c) Poles to S_1 and S_2 forming a great circle characteristic of F_{2b} folds, locality 09jkol035. Note the orientation of measured F_{2b} beta axes and pegmatites; (d) Hoeppener diagram showing poles of S_2 foliation together with L_2 mineral stretching lineation and sense of shear.*

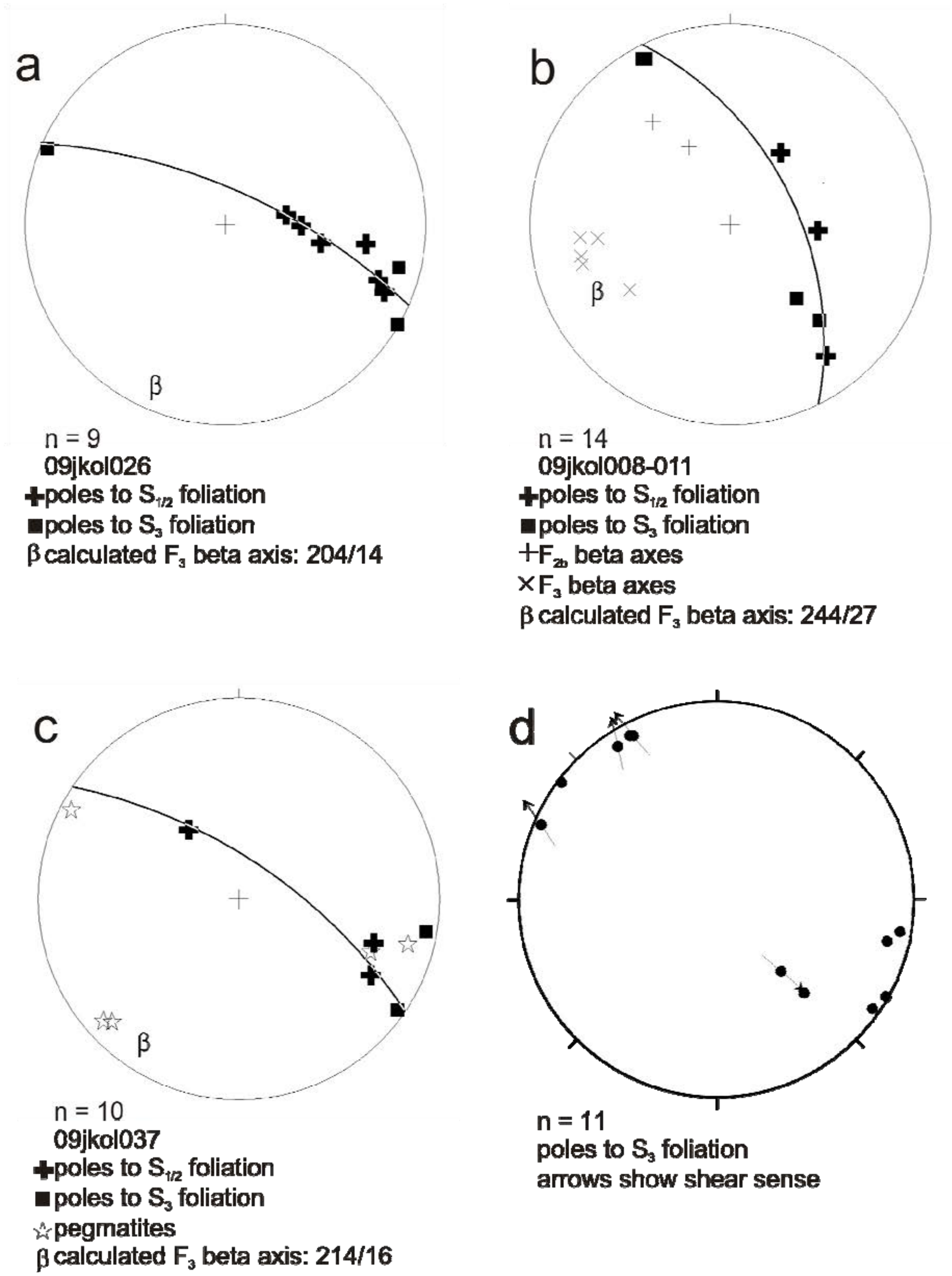

Figure 7. *(a) Poles to $S_{1/2}$ and S_3 forming a great circle characteristic of F_3 folds, locality 09jkol026. Note the axial planar orientation for S_3; (b) Structural inventory of locality 09jkol008 – 011 showing transposition of earlier fabrics by D_3 fabrics; (c) Poles to foliations and pegmatites indicating F_3 folding and ac-orientation of two pegmatites, locality 09jkol037; (d) Hoeppener diagram showing poles of S_3 foliation together with L_3 mineral stretching lineation and sense of shear.*

Hydrothermal mineralisation

Two areas containing quartz veins and hydrothermal alteration halos can be defined: (1) The hinge zone of a F_3 syncline with a thickened meta-sedimentary rock unit and (2) the southern limb of the F_{2b} fold defined by the band of meta-sedimentary rock. The hydrothermal quartz veins in both locations are either parallel to the S_2 foliation or cross cut the foliation (Fig. 8). The cross cutting quartz veins form axial planar veins and veins in ac-orientation with respect to the F_{2b} folds (Fig. 9). This suggests that the quartz veins formed during the late stages of the D_2 deformation contemporaneous with F_{2b} folding. The quartz veins cross cut pegmatites that intruded during the D_2 deformation stage parallel to the S_2 foliation.

The quartz veins are up to 50 cm wide, comprise Qtz and minor Fsp and Py, and have a 20 – 100 cm wide hydrothermal alteration halo. S_2 parallel quartz veins form pinch-and-swell fabrics and are, locally, folded into gentle folds. In places, several parallel quartz veins form a laminated set of veins.

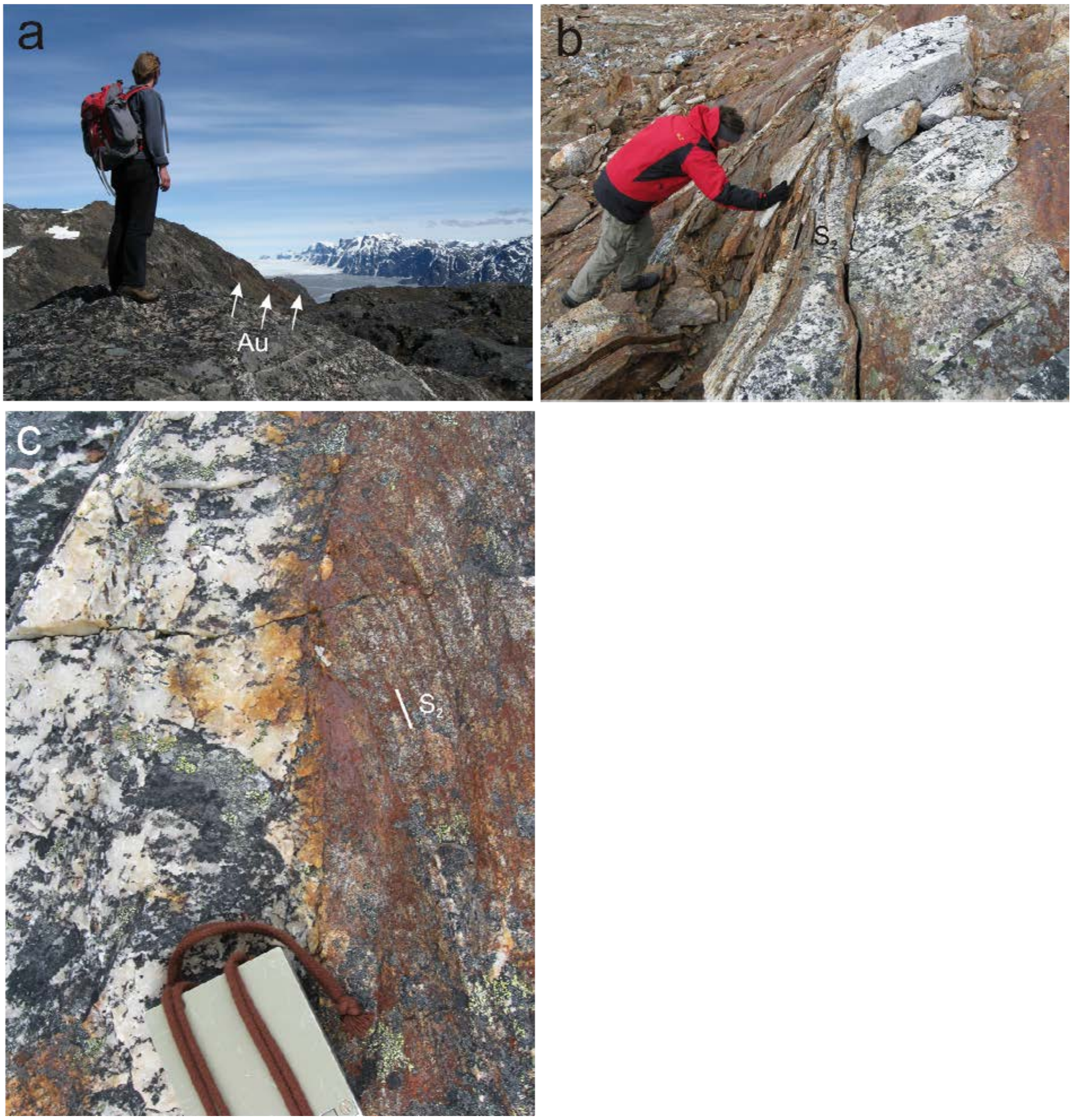

Figure 8. *(a) Gossan zones north of Sermilik, marking the hydrothermal alteration zones around the auriferous quartz veins; (b) S_2 foliation parallel quartz veins; (c) Quartz vein cross cutting the S_2 foliation.*

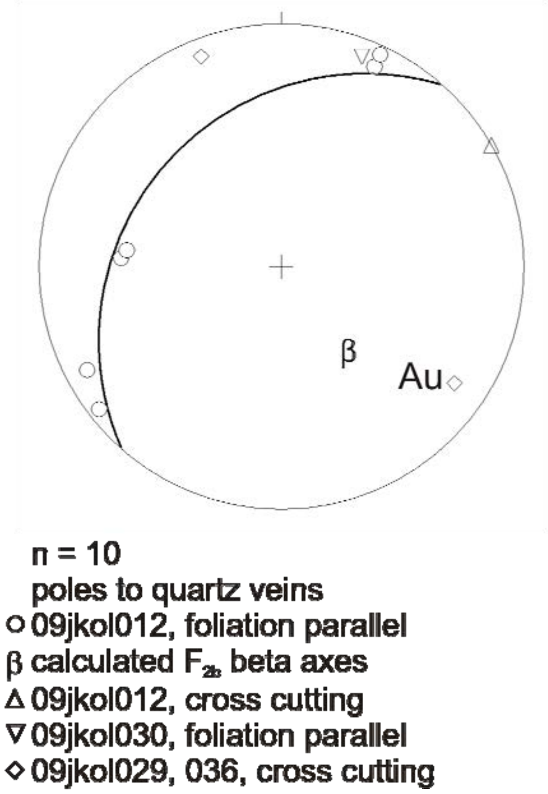

Figure 9. *Poles to quartz veins. The foliation-parallel quartz veins form a great circle characteristic of F2b folds. Note, that the quartz vein containing 6 ppm Au is in ac-orientation to the fold structure.*

In the mafic granulite, the alteration assemblage comprises Bt-Grt-Kfs-Hbl-Qtz-Py. The meta-sedimentary rocks are characterised by a Bt-Grt-Sil-Qtz-Py alteration assemblage. In both host rock lithologies, the hydrothermal alteration is Pl-destructive. Geochemical analysis of 7 quartz vein samples yields gold contents between 2 – 30 ppb and one exception at 6370 ppb Au. The variation is possibly explained by a combination of unsystematic sampling, the nugget effect and supergene depletion and/or enrichment of the samples. Since all the veins have a similar hydrothermal alteration halo, it is likely that they all belong to the same hydrothermal systems including hydrothermal gold. The structural control of the hydrothermal mineralisation together with the syn-metamorphic, post peak metamorphic nature of hydrothermal alteration point to an orogenic gold mineralisation style.

During a reconnaissance stop south of Sermilik, a very similar quartz vein system was studied. The host rock is a mafic granulite comprising an Opx-Cpx-Pl-Qtz-ore peak assemblage and a Hbl-Pl-Qtz-ore retrograde assemblage. Quartz veins are 30 – 50 cm wide, comprise Qtz and minor Pl and form pinch-and-swell fabrics parallel to the S_2 foliation. On either side of the veins, an about 40 cm wide hydrothermal Qtz-Hbl-Bt-Ep-Pl-Po-Rt-Ccp alteration halo is developed. The quartz veins and the hydrothermal alteration zones form 3 – 5 parallel zones that can be followed over 400 m along strike. One quartz vein sample and one hydrothermal alteration zone sample yield 2 ppb and < 2 ppb Au, respectively. The quartz veins have a very similar alteration halo and are in the same structural position as the gold-bearing quartz vein described above. It is, therefore, not clear why gold was only detected in one single sample analysed. Further studies will be directed towards answering this important question.

Geology of the Ilivertalik granite north of Sermilik

Lithology

The geology of the Ilivertalik granite was investigated at a locality N of Sermilik fjord, some 10 km east of the Camp II area (Fig. 1). During the 2009 field season, a large proportion of the area was still covered by snow, such that only a reconnaissance study could be carried out. Two main rock types were distinguished: older TTG gneiss and rocks belonging to the Ilivertalik granite (Fig. 10). The TTG gneiss is a leucocratic, fine-grained rock that often displays a fine lithological layering (Fig. 10a). They have an amphibolite facies mineral assemblage of quartz, plagioclase, biotite and, locally, hornblende. The granitoid rocks of the Ilivertalik granite are not easily distinguished in the field (Fig. 10b). This is because the Ilivertalik-type "granites" are variable in grain-size and composition and contain relatively few K-feldspar. However, in contrast to the TTG gneiss, the rocks are characterised by the presence of clinopyroxene and orthopyroxene, pointing to granulite facies conditions during their emplacement. The typical mineral assemblage is quartz, plagioclase, K-feldspar, garnet, clinpyroxene, orthopyroxene and magnetite. Locally, the granulite facies mafic phases have been retrogressed to biotite and hornblende.

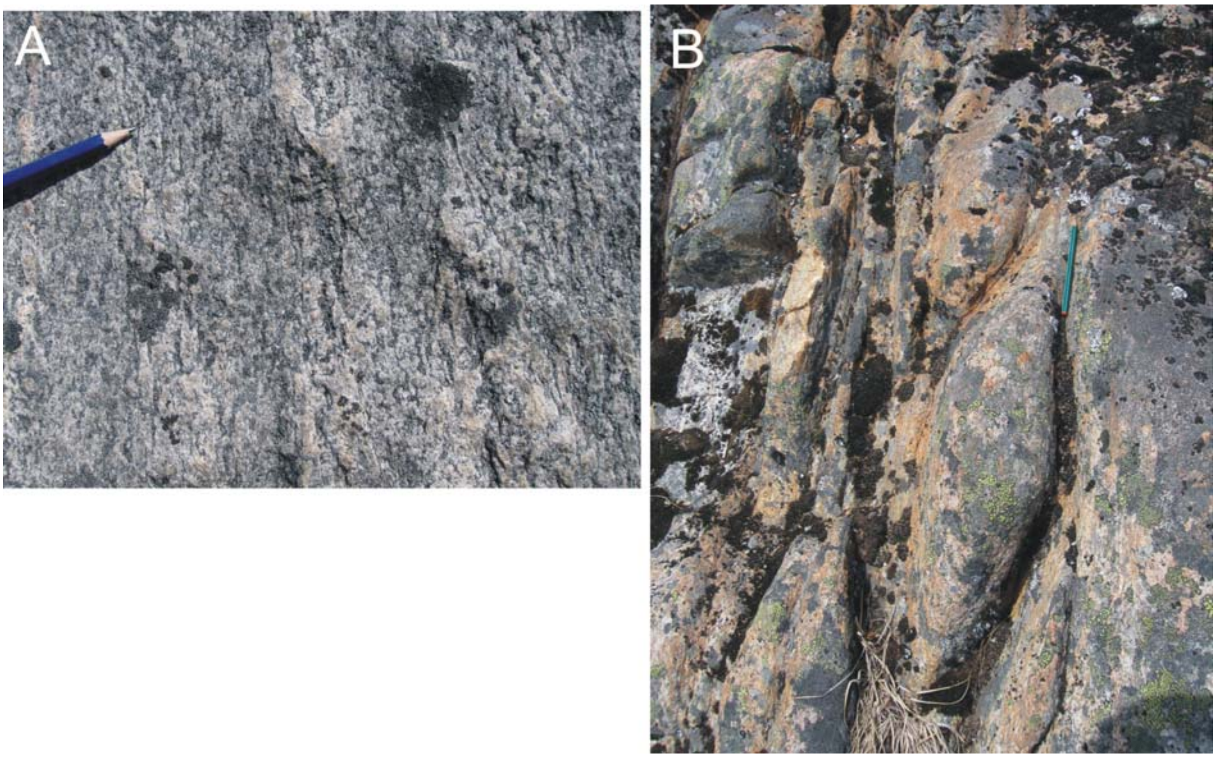

Figure 10. *(a) Grey TTG gneiss with a closely-spaced S_2 foliation marked by the fine banding; (b) Typical brownish weathering colour of the Ilivertalik granitoid gneisses, probably due to weathering of magnetite.*

Structural geology

In the Ilivertalik granite as well as the TTG gneiss, the penetrative foliation mainly dips moderately to the SSE (Fig. 11). In both lithologies, F_{2a} folds are observed that fold the S_1 foliation into tight to isoclinal folds (Fig. 12). The axial planar S_2 foliation is parallel to S_1 and, therefore, hard to distinguish from S_1 where F_{2a} folds are not observed. The S_1 and/or S_2 foliation is defined by Bt, Hbl and Px. The F_{2a} fold axes plunge moderately to the SW (Fig. 11). Locally open F_{2b} folds are developed with near-horizontal E-W trending fold axes (Fig. 12). They are close to perpendicular to the mineral stretching lineation on S_2, which plunges down-dip, moderately to the SE (Fig. 11). Shear sense indicators such as σ-, δ-clasts and S-C fabrics show reverse sense of movement to the NW on D_2 shear zones, very similar to the situation further north in the Kangiata Nuna area (Kolb *et al.* 2009).
During the D_3 stage of deformation, S_2 is folded into upright, open to tight folds with gently SE-plunging fold axes (Fig. 11). These F_3 folds are related to near-vertical D_3 shear zones that are up to 2 m wide and have a moderately SE-plunging lineation. The sense of shear could not be determined due to the lack of shear sense indicators.

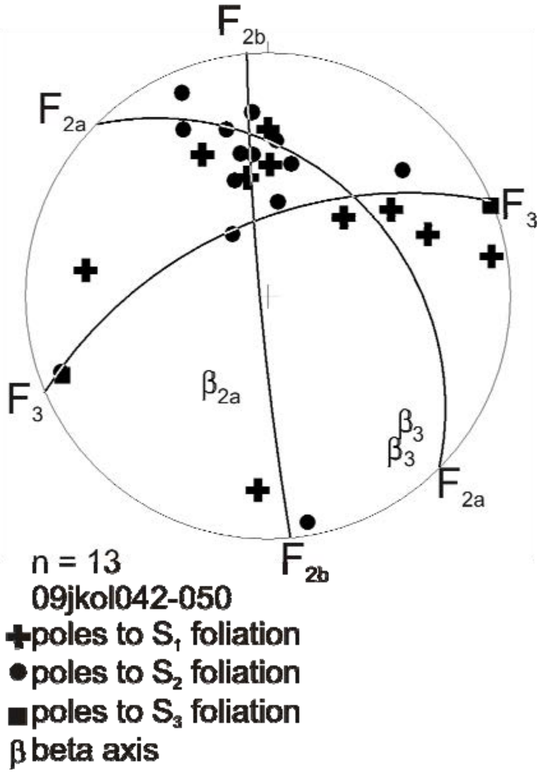

Figure 11. *Poles to the various foliations and measured fold axes. Great circles are labelled with the relevant indices for the various stages of deformation.*

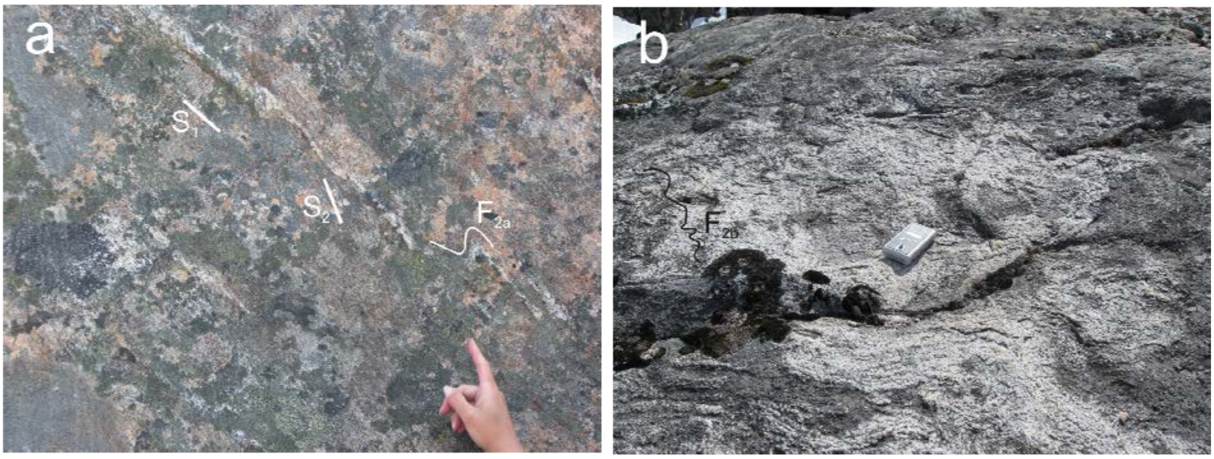

Figure 12. *(a) Geometry of S_1 and S_2 foliations and small-scale F_{2a} folds in the Ilivertalik granitoid gneiss; (b) Small-scale F_{2b} folds in the TTG gneiss.*

Geology of the high strain zone between Grædefjord and Quvnerup ilua

Lithology

Between Grædefjord in the north and Quvnerup ilua in the south, a NE-SW trending high strain zone at the contact between the 500 m wide and 10 km long mafic granulite lens and the surrounding TTG gneiss was studied (Fig. 1). From SE to NW, the exposed rocks comprise enderbitic gneiss, a thin NE-trending belt mainly composed of mafic granulite and the ca. 2.8-3.0 Ga TTG gneiss.
The enderbitic gneiss in the SW is fine- to medium-grained and has a well-developed subvertical foliation. The rocks consist of quartz, plagioclase, orthopyroxene, clinopyroxene and minor amounts of biotite and K-feldspar. Enderbitic gneiss also occurs as foliation-parallel, cm- to dm-thick layers within the mafic granulite. The contact between the two rock types is tectonic, primary intrusive contact relationships are not preserved. The mostly fine-grained mafic granulites (Fig. 13a, b) in the central parts of the study area have a typical medium-pressure granulite facies mineral assemblage of clinopyroxene, orthopyroxene, plagioclase, quartz, hornblende and magnetite. Many of the samples investigated also contain biotite. Clinopyroxene is locally replaced by epidote-quartz symplectites along its rims, especially where in contact with TTG gneiss. A characteristic feature of the mafic granulites is the presence of cm- to dm large, coarse-grained mafic boudins that are aligned parallel to the foliation (Fig. 13a). The boudins are dominated by mafic minerals such as clinopyroxene, orthopyroxene, garnet and non-magnetic opaque phases. Quartz and plagioclase occur in cm-wide networks within the boudins, suggesting that these represent the former leucosomes. Hornblende locally replaces clinopyroxene, especially where in contact with quartz and plagioclase. The fine- to medium-grained TTG gneiss to the NW of the mafic granulites is made up of quartz, plagioclase and biotite, pointing to amphibolite facies conditions. The mineral assemblage is consistent with the work of previous studies, which documented a major break in metamorphic grade across the mafic granulite belt. Amphibolite facies metamorphism is also indicated by the presence of banded amphibolite at e.g. locality 09JKOL055, composed of hornblende, plagioclase, quartz, clinopyroxene and titanite. The NE-trending high-strain zone has been intruded by numerous, foliation-parallel pegmatite dykes, which are particularly abundant in the mafic granulites close to the contact with the TTG gneisses in the NW (Fig. 13c). The majority of the medium- to coarse-grained pegmatite dykes contain a well-developed foliation. They mainly consist of quartz, plagioclase, K-feldspar, garnet, clinopyroxene, magnetite and hornblende, suggesting that they were emplaced during the peak of metamorphism. In two instances, however, pegmatite dykes with a mineral assemblage of quartz, plagioclase, K-feldspar, biotite and, locally, garnet have been identified, pointing to lower grade (amphibolite facies) conditions.

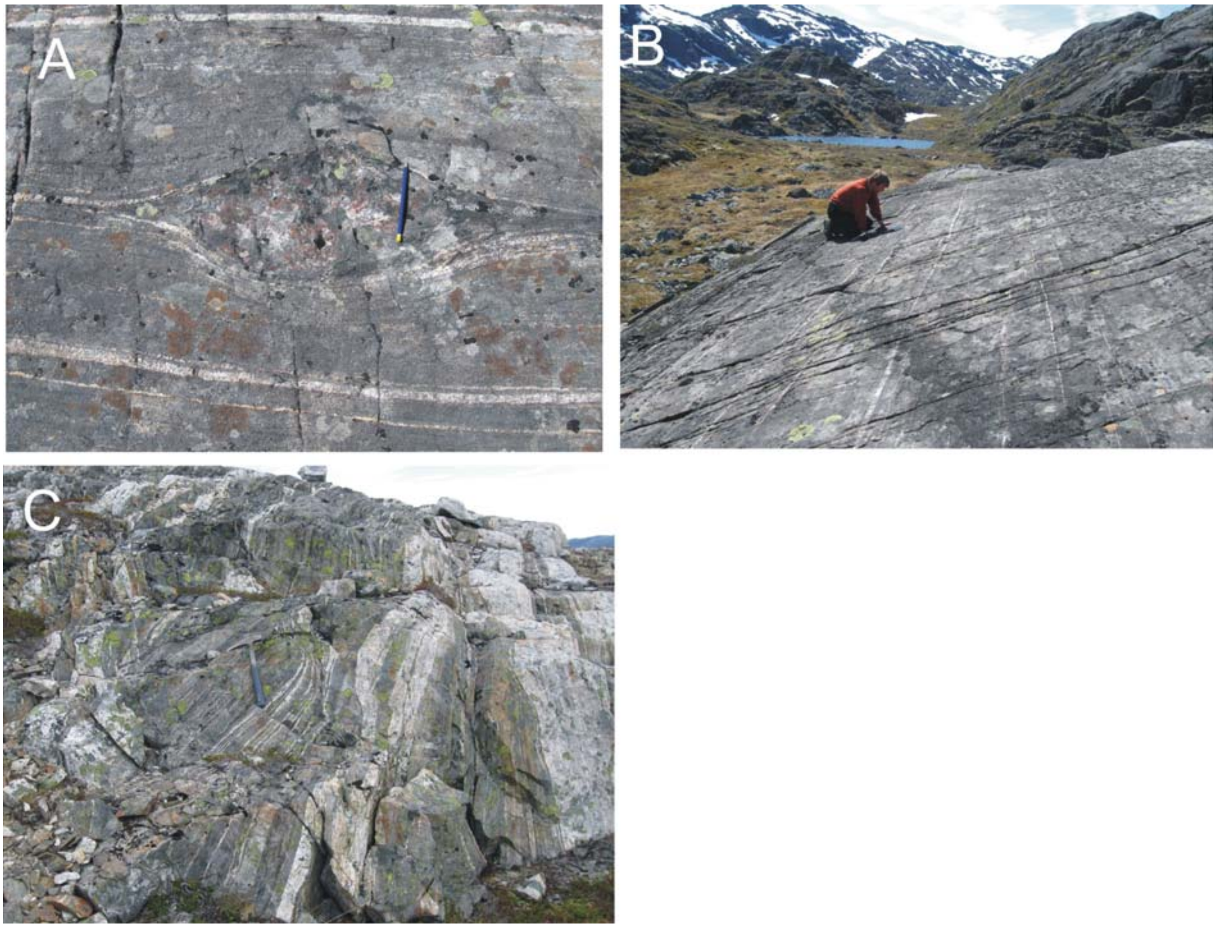

Figure 13. *(a) Boudins of more competent mafic granulites with Cpx-Opx-Grt in a well foliated (S_2) matrix of the characteristic Cpx-Opx-Pl-Qtz-Hbl-Mag granulites. (b) Same outcrop as (a), showing the well-developed S_2 foliation parallel to a banding in the mafic granulite. (c) Foliation-parallel (S_2) pegmatites in mafic-granulite of the high-strain zone.*

Structural geology

Between Grædefjord in the north and Quvnerup ilua in the south, the NE-SW trending high strain zone at the contact between the 500 m wide and 10 km long mafic granulite lens and the surrounding TTG gneiss was studied. The rocks are characterised by a penetrative, near-vertical NE-SW trending foliation. The mafic granulites show generally a shallower dip of the foliation to the SE compared to the TTG gneiss. Two foliations are distinguished and labelled with S_1 and S_2 (Fig. 14a, b). A correlation with D_1 and D_2 deformation stages further north that are described above is uncertain. A later normal D_3 shear zone is located about 1 km to the west of the high strain zone (Fig. 14c). A regional scheme for deformation stages has to await further U-Pb Zrn dating of syn-tectonic intrusive rocks. The structural data collected from the Grædefjord area by A. Kisters and A. Bergen can most probably correlated as follows (see below): D_1 is D_2 in Grædefjord, D_2 is D_3 in Grædefjord and D_3 is D_4 in Grædefjord.

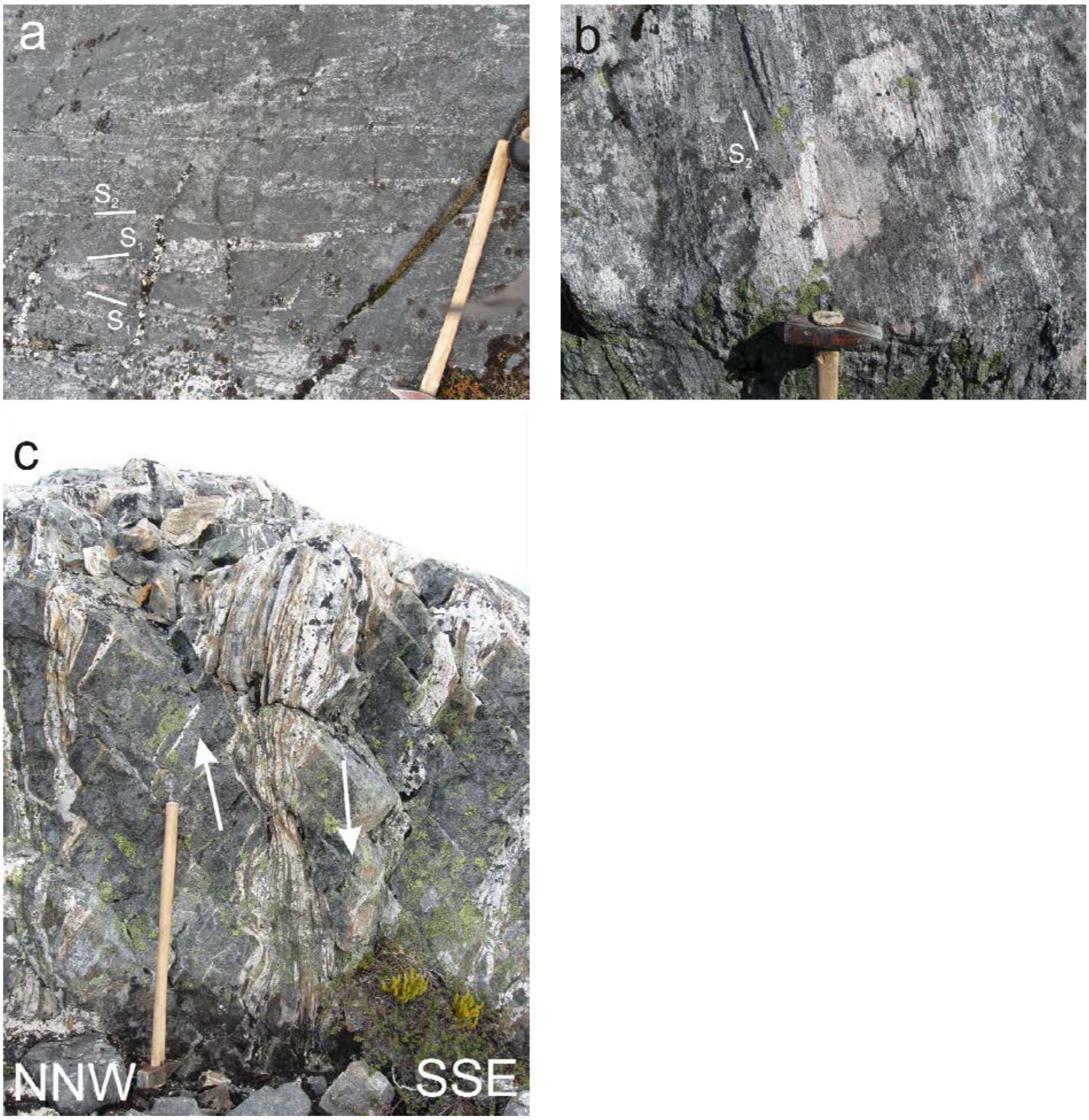

Figure 14. *(a) F_2 folds showing the slightly oblique geometry between S_1 and S_2 foliations in mafic granulite; (b) Characteristic high-strain S_2-fabric in the mafic granulite; (c) Late normal fault associated with pegmatite intrusion during the D_3 deformation stage.*

An early S_1 foliation is only locally developed in tight to isoclinal F_2 folds with a wavelength of about 50 cm and an amplitude of up to 40 cm. The F_2 folds are upright and have gently NNE or SSW plunging fold axes (Fig. 15a). The limbs and axial planes of the F_2 folds are parallel to the penetrative S_2 foliation.

Mainly along the contact of the mafic granulite lens and the TTG gneiss, the S_2 foliation is closely spaced trending NE-SW and generally dipping steeply to the SE (Fig. 15b). Locally, steep dips to the NW are also observed. Gneiss and pegmatite form cm- to dm-scale lit-par-lit intrusions parallel to the S_2 foliation (Fig. 15c). Moderately NW-dipping S_2 is developed in low-strain areas within the mafic granulite representing duplex structures. Up to 1 m wide Cpx-rich lenses form m-scale boudins parallel to S_2 (Fig. 14a). Mineral stretching lineation is weak, only observed in places and shows variable orientation (Fig. 15b). The foliation and mineral stretching lineation are defined by Opx, Cpx, Hbl and, locally, Bt in both gneiss and mafic granulite. The duplex structures and S-C fabrics suggest a general reverse to oblique reverse sense of movement, consistent with various microstructures in oriented thin sections (Fig. 15b). The regional pattern shows that S_2 is transposed from more ENE-WSW strike to NE-SW in the high strain zone. This is consistent with the shear sense in the outcrops, indicating an oblique sinistral reverse sense.

About 1 km west of the D_2 high strain zone, pegmatite dykes intrude the S_2 foliation planes of mafic granulite. The strong rheology contrast between the two lithologies led to the formation of bookshelf structures of the mafic granulite (Fig. 14c). The mafic granulite deformed by brittle deformation, whereas the pegmatite was ductile. The shear sense is normal and indicates that the D_2 high strain zone was reactivated as a normal shear zone during a D_3 deformation stage.

Locally, the D_2 high-strain zone was reactivated by deformation along regional D_5 faults as indicated by Ep alteration and slickensides on the foliation planes.

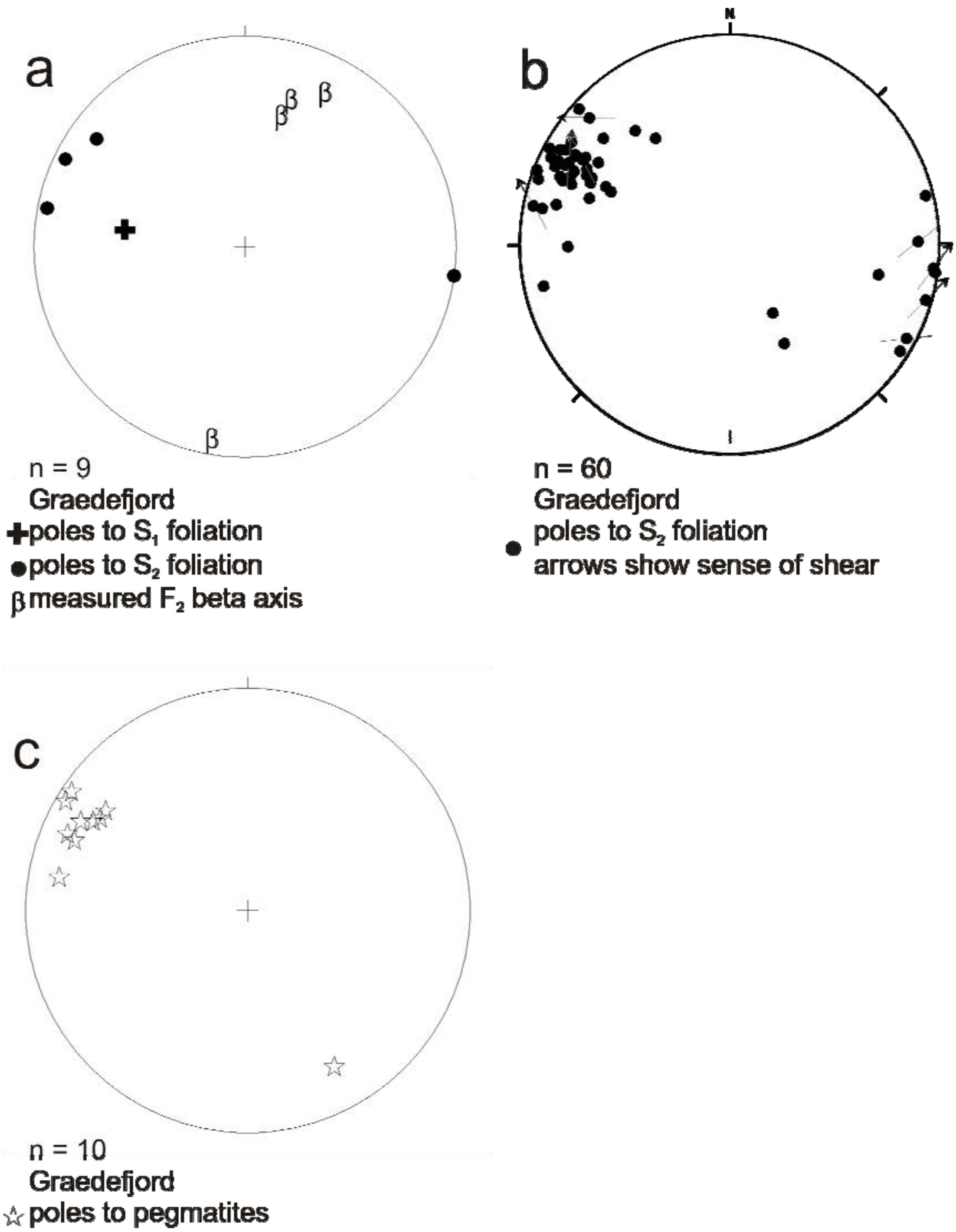

Figure 15. *(a) Poles to the S_1 and S_2 foliations indicating F_2 fold geometry; (b) Hoeppener diagram showing poles of S_2 foliation together with L_2 mineral stretching lineation and sense of shear; (c) Poles to pegmatites. Pegmatites are parallel to the S_2 foliation.*

Hydrothermal mineralisation

Two about 50 m wide gossan zones formed in the mafic granulite lens parallel to the S_2 foliation. These zones are continuous along strike for more than 2 km. The gossan is always located between two larger S_2-parallel pegmatites (Fig. 16). The hydrothermal alteration halo is centred on several S_2-parallel, mm- to cm-scale quartz vein stringers. The quartz veins contain minor Pl, Hbl, Ccp, Po and Py. Proximal to the quartz veins, the mafic granulite comprises a hydrothermal alteration assemblage of Hbl-Qtz-Grt-Po-Ccp-Ilm, locally Bt and Ms, in an about 2 m wide zone (Fig. 16). The distal hydrothermal alteration assemblage comprises Bt-Qtz-Py-Po-Mag and locally Grt and Ccp. Microstructures defined by the alteration assemblage are consistent with the sinistral oblique reverse sense of deformation during the D_2 stage. This indicates that hydrothermal alteration was contemporaneous with deformation during the D_2 stage. Whole rock analyses of 11 hydrothermal alteration samples of which four contain quartz vein stringers yield gold values between < 2 ppb and 30 ppb. This suggests that this area is not endowed with hydrothermal gold in quartz veins.

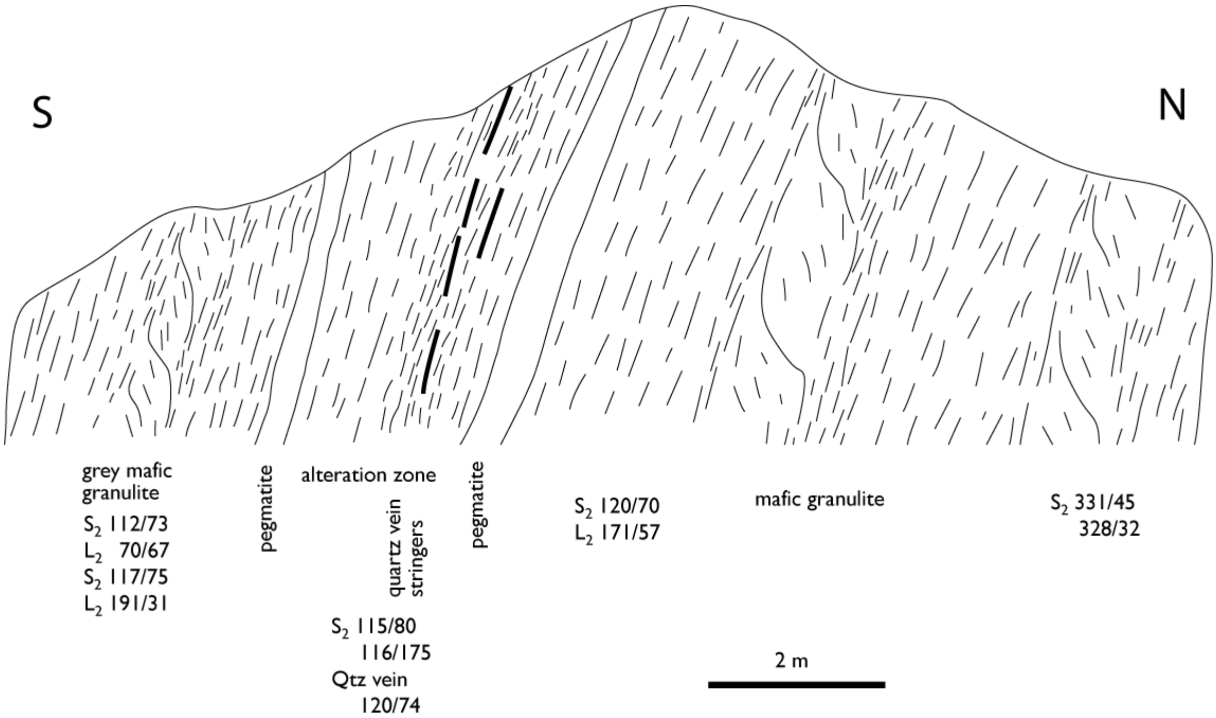

Figure 16. *Sketch of a cliff wall transecting the high-strain zone in the mafic granulite. The hydrothermal alteration zone and S_2-parallel quartz vein stringers are centred between two S_2-parallel pegmatites. Note the duplex structures in lower-strain zones.*

Another type of hydrothermal alteration was studied during a reconnaissance stop about 8 km to the east of the occurrence described above. The area north of Kangnaitsoq is characterised by several gossan zones that are aligned on a NE-SW strike (Fig. 1, 17). The gossan is developed in breccias of the host TTG gneiss. The gneiss comprises a hydrothermal alteration assemblage of Bt-Qtz-Po and rare Py and Ccp, replacing the peak metamorphic Opx-Pl-Kfs-Qtz assemblage. Hydrothermal veins in the breccias are composed of Qtz-Pl-Bt-Po-Py-Ccp-Sp and have a Bt alteration halo. Recrystallisation and deformation fabrics of Qtz indicate a formation in the greenschist facies. Whole rock geochemistry of the altered breccias shows enriched values for Ag (up to 2.2 ppm), Sn (up to 7 ppm) and Th (up to 13 ppm), which, however, are too low to be regarded economically interesting.

The alignment of the gossan spots along a NE-SW array and the brittle nature of the mineralised breccias suggest a relationship between hydrothermal alteration and regional faults (Fig. 17). The geometry indicates that the hydrothermal alteration and gossans are concentrated at complex fault intersections (Fig. 17). The absolute timing is, however, unclear, because the age of the faults is not determined in the area. On a larger regional scale in southern West Greenland similar faults are Proterozoic (Nutman *et al.* 1989b).

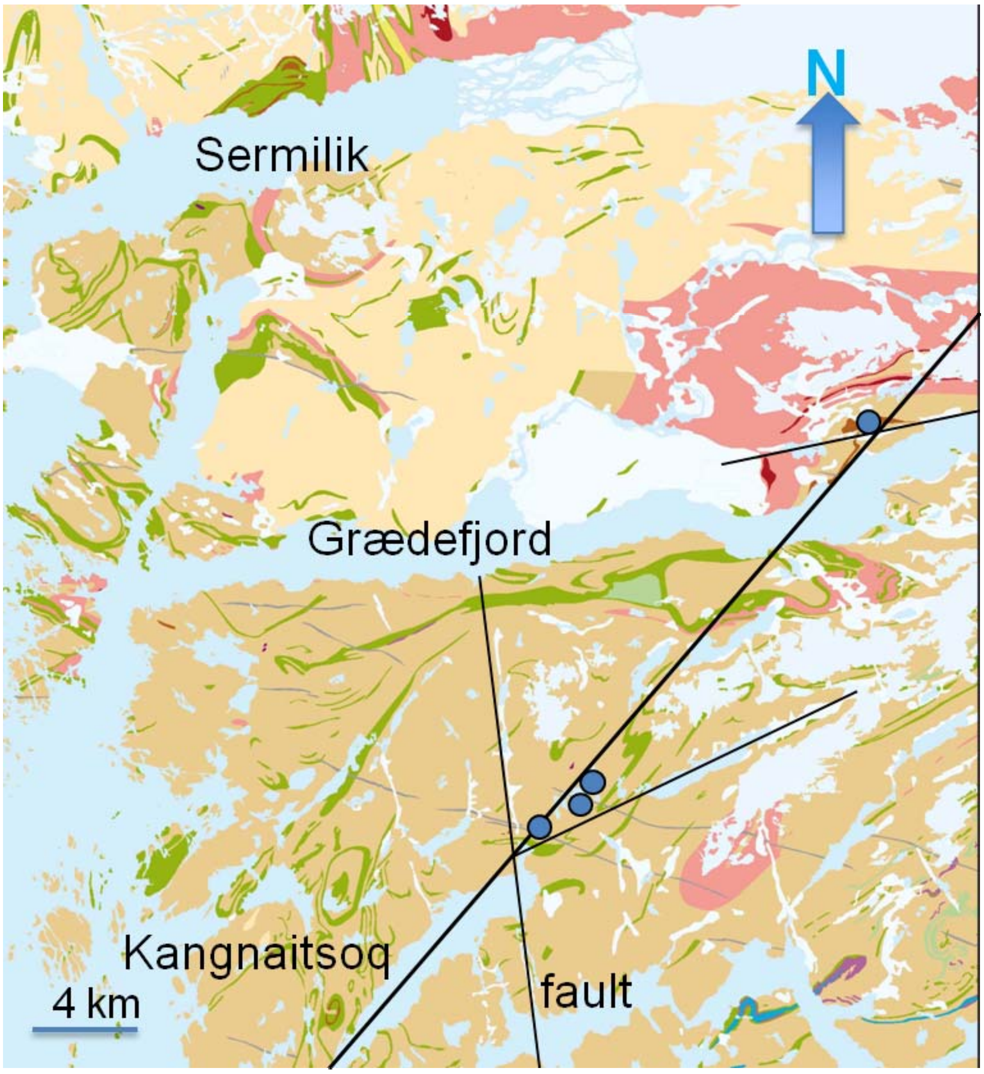

Figure 17. *Detail from the Grædefjord 1:100000 map sheet, showing the gossans with blue dots and interpreted faults as black lines (legend see Fig. 1). Note that the hydrothermal zones and gossans are concentrated at complex fault intersections. The occurrence north of Grædefjord is described in more detail below (Camp IV of Kisters & Bergen).*

Geology of the Sarfaat Aariaat area

Lithology

The geology of the Fiskenæsset Complex was investigated at two localities in the Sarfaat Aariaat area, which are situated 12 km north of Fiskenæsset (Fig. 1, 19, 20). The Sarfaat Aariaat area consists of three major components, including mafic granulite, a variety of meta-ultramafic rocks, meta-leucogabbro of the Fiskenæsset Complex and TTG gneiss. The contacts between the rocks are mainly tectonic, although primary intrusive contact relationships have locally been preserved between the TTG gneiss and the mafic granulite.

The white and greenish black, fine- to medium-grained mafic granulite has a well-developed foliation (Fig. 18a). The rock consists mainly of hornblende, plagioclase, ortho- and clinopyroxene and accessory magnetite. Leucosomes composed of plagioclase, quartz and large crystals of idiomorphic ortho- and clinopyroxene point to in situ partial melting during the peak of metamorphism. The green to black meta-ultramafic rocks are medium grained (Fig. 18b-d). In general, the rocks consist of pyroxene, hornblende, olivine and, locally, magnetite and serpentine. Based on the Streckeisen classification for ultramafic igneous rocks, most of the samples investigated can be classified as olivine-hornblende-pyroxenite. Based on different mineral assemblages and weathering surfaces, three different types of meta-ultramafic rock have been distinguished. The most common rock is medium- to coarse-grained and mainly consists of olivine, clino- and orthopyroxene and hornblende in decreasing order of abundance. This type of rock is characterised by rough, porous weathering surfaces (Fig. 18b). The second type is fine- to medium-grained and has been intruded by abundant, cm- to dm-thick hornblendite dykes (Fig. 18c). The mineral assemblage is clinopyroxene, orthopyroxene, olivine and hornblende. A third type is grey, medium-grained and relatively poor in olivine (< 10%; Fig. 18d). This type of rock consists mainly of clino- and orthopyroxene and hornblende and is often found at the contact between the meta-ultramafic rocks and the mafic granulite.

The medium- to coarse-grained meta-leucogabbro is black and white in colour and occurs in two different varieties. In a large proportion of this unit, the original (igneous) mineralogy and cumulate texture have been preserved, particularly in the central parts of this lithology (Fig. 18e). At or close to lithological contacts, the meta-leucogabbro is considerably finer-grained and contains a well-developed foliation. The rock consists of plagioclase, hornblende, ortho- and clinopyroxene in decreasing order of abundance. In coarse-grained varieties, plagioclase is often zoned. Many plagioclase grains have a grey, relict magmatic core that is surrounded by a white, recrystallised, fine-grained margin containing plagioclase and hornblende. The leucocratic TTG gneiss is medium-grained and has a well-developed foliation. It consists of plagioclase, quartz, biotite and, occasionally, rare tourmaline.

The whole sequence has been intruded by several generations of pegmatite dykes (Fig. 18f). The earliest generation is foliation-parallel and varies in thickness between ca. 1 m and more than 10 m. The foliation-parallel pegmatites occur especially within the meta-leucogabbro, but also along the contact between the meta-leucogabbro and the meta-ultramafic rocks. In addition, numerous, ca. 10 cm thick N-S and NE-SW trending pegmatite dykes have been identified within the meta-ultramafic rocks and the mafic granulite.

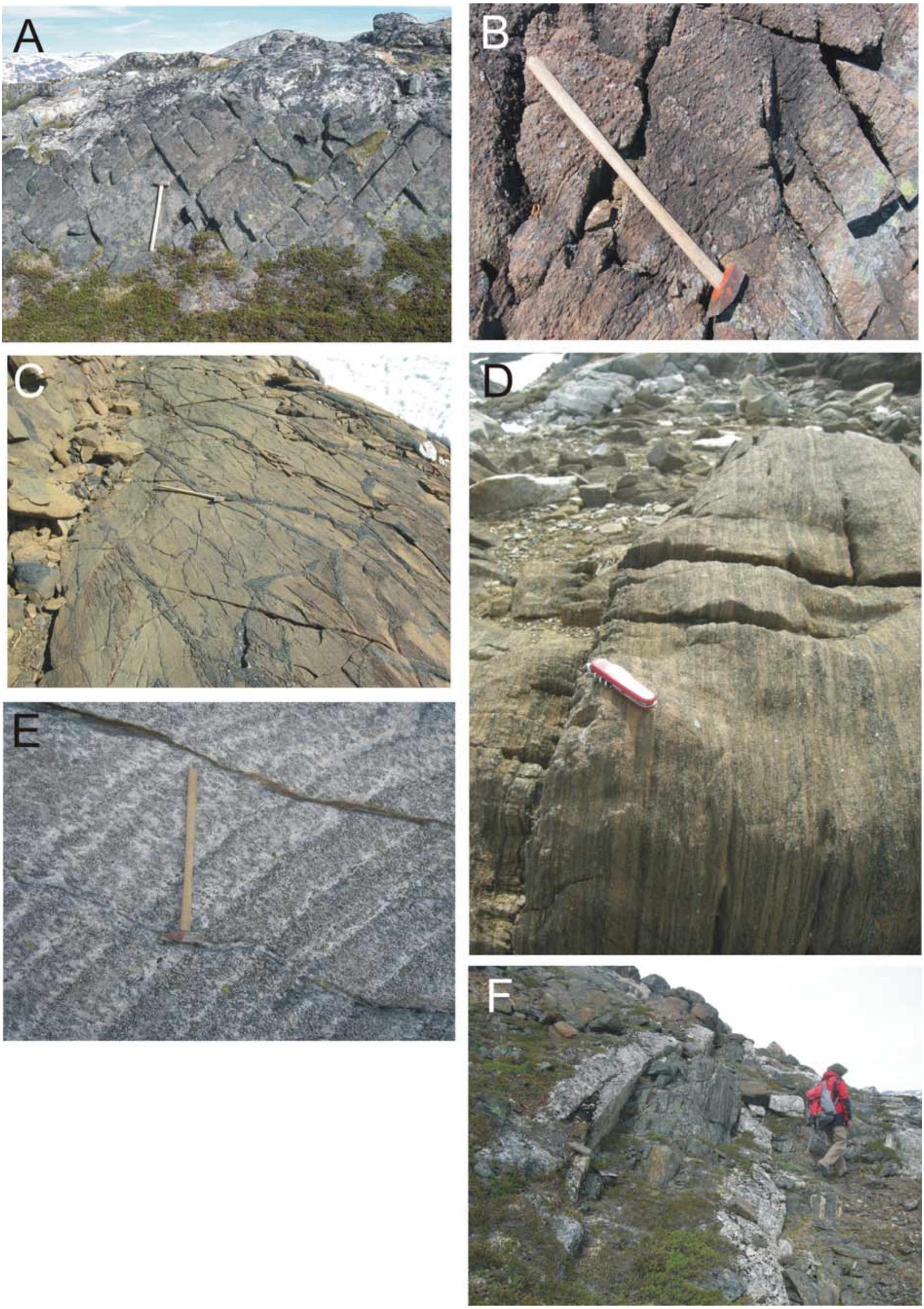

Figure 18. *(a) Mafic granulite and the characteristic blocky weathering. The near vertical foliation is hard to see in outcrop; (b) Meta-ultramafic rock with rough weathering surface; (c) Meta-ultramafic rock intruded by numerous hornblendite dykes; (d) Grey, banded meta-ultramafic rock; (e) Meta-leucogabbro showing cumulate texture; (f) Foliation-parallel pegmatites that intruded the mafic-ultramafic sequence.*

Structural geology

An S_1-foliation is only preserved in low strain domains mainly in the mafic granulite but also in the core of F_2 folds. The granulite facies mineral assemblages of orthopyroxene, clinopyroxene and hornblende define D_1 fabrics. The dominant fabric in the Sarfaat Aariaat area is a pervasive, mainly NE-SW trending S_2 foliation that dips moderately to the SE and E (Fig. 19, 20). The S_2 foliation is also defined by granulite facies mineral assemblages, suggesting that D_1 and D_2 occurred under similar PT-conditions. The D_2 deformation is characterised by tight to isoclinal F_2 folds with fold axes that plunge moderately to the SW (Fig. 19, 20). In the eastern part of the Sarfaat Aariaat area, felsic pegmatite dykes intruded parallel to the S_2 foliation (Fig. 19). The D_3 deformation refolds the S_2 foliation into open to tight F_3 folds. F_3 folding dominates the structural pattern in the western part of the Sarfaat Aariaat area, which is dominated by a tight F_3 syncline that plunges at 50-60° to the SE (Fig. 20). Further east, the F_3 folding is only weakly developed and characterised by open folds. A weak axial planar, NW-SE trending S_3 foliation is locally developed. Along the limbs of the F_3 syncline in the western part of the Sarfaat Aariaat area, it is often parallel to S_2 and thus, not easy to distinguish (Fig. 20). During D_4, NW-SE trending brittle faults developed in the eastern part of the area. The D_4 faults are mainly developed in competent lithologies such as meta-ultramafic rocks and meta-leucogabbro (Fig. 19, 20). The faults have mainly a strike-slip component, vertical displacement is minor. Thin (5-10 cm) N-S and NE-SW trending D_4 faults are intruded by pegmatite dykes and also show only minor displacement. An exception to this is a roughly E-W trending fault in the eastern part of the area, which cuts the SE limb of the F_2 fold. The field relations suggest a strong vertical displacement, which unfortunately could not be quantified due to the lack of exposure.

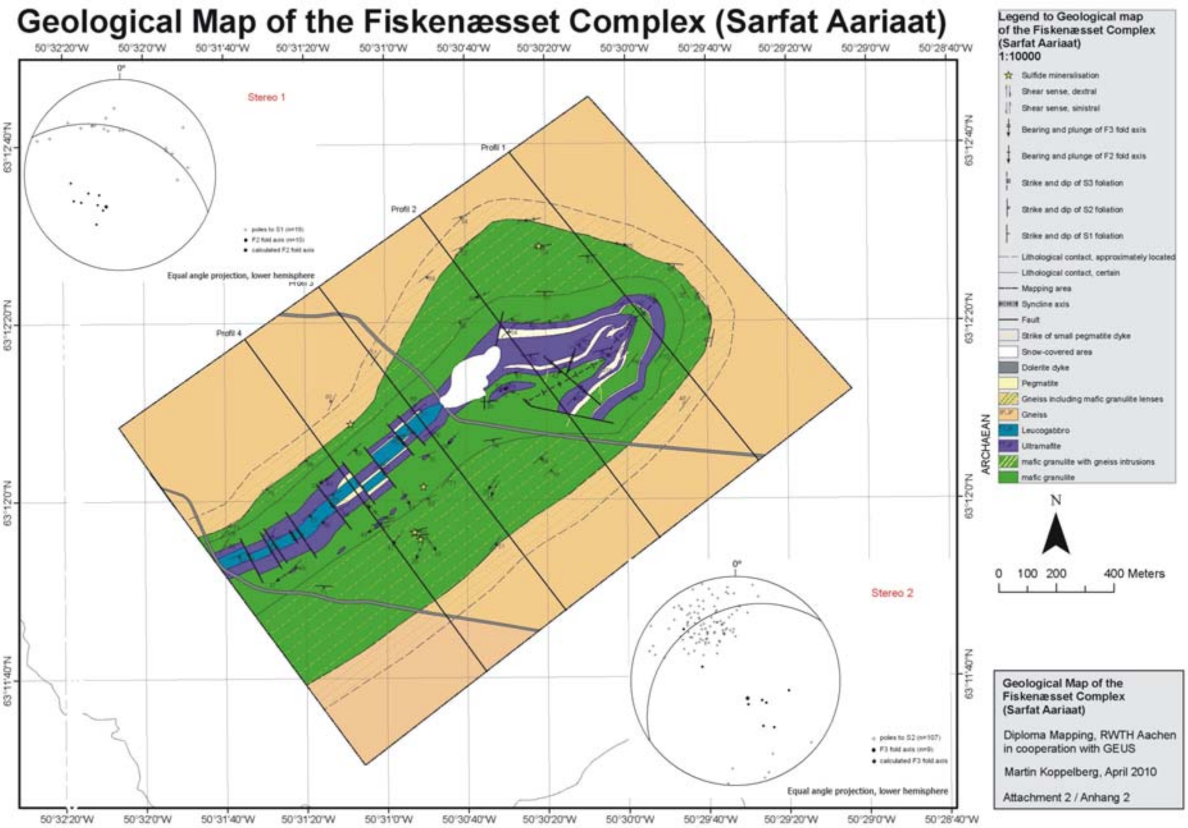

Figure 19. *Geological map of the eastern Sarfaat Aariaat area and stereoplots of the various structures (mapped by M. Koppelberg).*

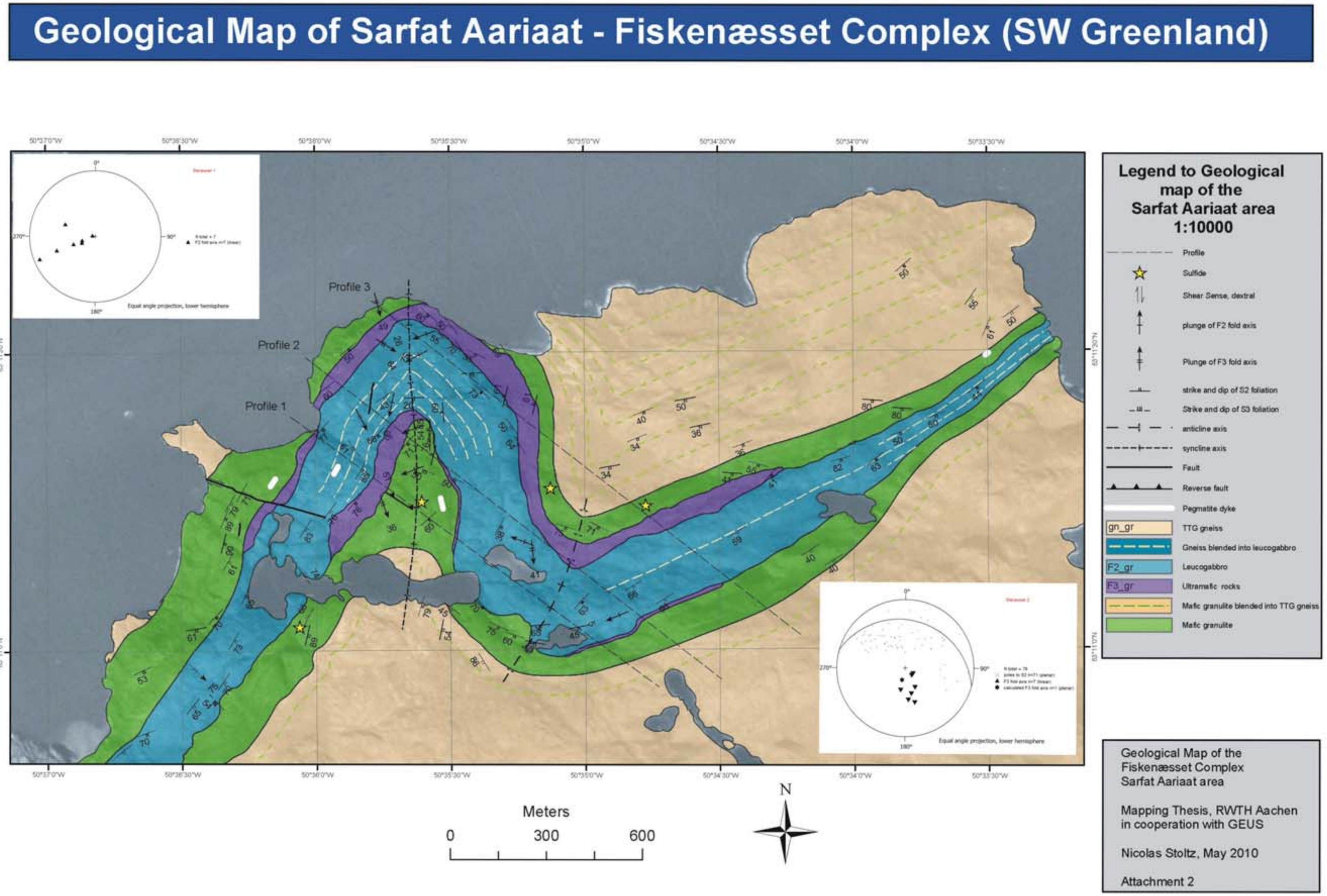

Figure 20. *Geological map of the western Sarfaat Aariaat area and stereoplots of the various structures (mapped by N.B. Stoltz).*

Hydrothermal mineralisation

About 2 – 10 m wide gossan zones formed at the contact between rocks of the Fiskenæsset complex and surrounding TTG gneiss parallel to the S_2 foliation. Locally, up to 5 cm wide quartz veins are developed parallel to the S_2 foliation (Fig. 21). These zones are continuous along strike over several 100 m. The wall rocks are layered mafic rocks. Individual layers are 1 – 2 cm wide and comprise Pl±Qtz-Bt layers and Cpx-Opx-Pl±Hbl layers. Hydrothermal alteration at the layer contact and along small oblique shear zones cross cutting the layers formed a Bt-Qtz-Po-Ccp-Sp-Ilm assemblage. The geometry of micro-structures, i.e. Bt forming a foliation parallel to the layering and in C' orientation cross cutting layering, suggests that during hydrothermal alteration shearing was layer- and S_2-parallel. Shearing was dextral at the northwestern limb of the fold structure N of Itise, consistent with flexural slip folding. It is, therefore, proposed that hydrothermal fluids altered the rocks during the formation of the map-scale D_2 folds with the NE-SW-trending axial traces (cf.; Fig. 19, 20). The hydrothermal mineral assemblage indicates that the hydrothermal alteration occurred retrograde in the lower amphibolite facies. Whole rock geochemistry yields values in the low ppb-range for Au, Pt and Pd, suggesting that no enrichment of precious metals is related to this hydrothermal alteration stage.

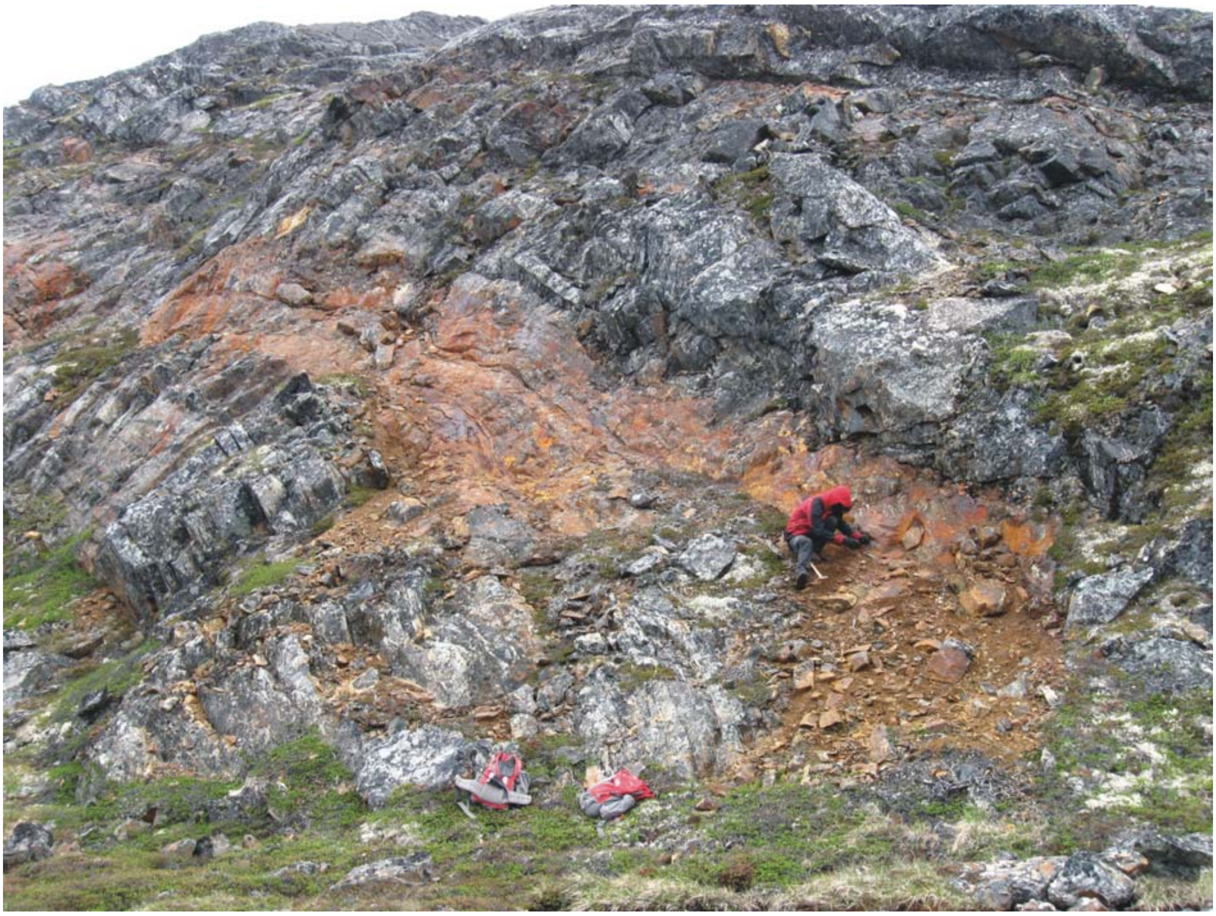

Figure 21. *Gossaneous hydrothermal alteration zone continuous along strike and parallel to the S_2 foliation.*

Structural reconnaissance mapping and mineralisation of the Graedefjord region

A.F.M. Kisters & A. Bergen

Abstract

Structural mapping around the Graedefjord, SW-Greenland was undertaken in order to (1) better constrain the significance of the Graedefjord structure, which, in recent years, has been likened to a possible terrane boundary, and (2) characterise and delineate potential areas of mineralization.

The lithological inventory and structural geology of areas N and S of the Graedefjord are similar. The volumetrically subordinate (< 5 vol. %) supracrustal assemblage includes predominantly amphibolites with minor felsic schists (pyroclastic, volcanoclastic rocks?) and ultramafic rocks. The supracrustal rocks occur mostly as highly attenuated, up to several kilometre long slivers. Two main generations of earlier grey gneisses and later leucogranites and pegmatites intrude the supracrustal rocks in a lit-par-lit manner. Intrusive breccias are only locally preserved.

At least three phases of bedding and fold transposition can be identified in individual outcrops. This includes (1) an early phase of bedding (layer-) parallel transposition, mainly confined to supracrustal rocks, (2) transposition of earlier mesoscopic upright, N-S trending F_2 folds by upright, E-W trending F_3 folds in the area around the Graedefjord, and (3) transposition of F_3 folds into E-W (NW-SE) trending striped gneisses in the central parts of the Graedefjord. D_3 strains in the central striped gneisses (the "Graedefjord structure") are characterised by N-S directed, subhorizontal bulk shortening and concomitant steep extrusion of the rocks. Non-coaxial fabrics are conspicuous by their absence. Kilometre-scale type 3 (refolded folds) fold interference patterns are only indicated by regional outcrop patterns of supracrustal belts. TTG gneisses, in contrast form steeply plunging, tubular folds, corresponding to the steep E to SE stretch recorded by linear fabrics and the steep extrusion of the gneisses. The main phases of D_2 and D_3 deformation were accompanied by melts and the synkinematic emplacement of TTG's and leucogranites. Later structural events include the formation of regionally prominent, E-W trending, steeply dipping, up to 500 m wide belts of brittle-ductile mylonites and cataclasites (D_4). D_4 shear/fault zones show predominantly dextral strike-slip kinematics, with only locally developed top-to-the-S thrust kinematics, or top-to-the-N normal movement. Brittle (D_5) faults trend N-S or form a conjugate pattern around N trends indicative of late-stage E-W extension.

Evidence of mineralisation is mainly found in form of ferruginous staining, spatially associated with late-stage pegmatites and, in particular, D_4 cataclasite zones. There is only minor quartz veining associated with the iron staining. D_5 brittle faults show extensive low-temperature alteration and retrogression of high-grade gneisses around the fault core, together with quartz veining, but no visible mineralisation.

Introduction

This field report presents results of a mainly structural study of selected areas around the Graedefjord (Fig. 1). The aim of the field work was to (1) document and characterise the structural significance of the “Graedefjord structure” that has, in recent years, been linked to a terrane boundary between two separate or parautochtonous crustal blocks of the Sermilik block to the north, the Bjørnesund block in the south (e.g., Windley & Garde 2009), and (2) characterise showings of mineralisation, spatially related to either late-stage shear and fault zones or supracrustal belts in the Neoarchaean, TTG-dominated, mid- to deep-crustal terrain.

The field team consisted of Alex Kisters (University of Stellenbosch) and Anders Bergen (University of Copenhagen). Field work was undertaken from five separate field camps that covered the Graedefjord region over an along-strike (E-W) distance of ca. 40 km from the far W to the E (Fig. 15). Samples were taken for geochronological and petrographic work, the results of which will be communicated in a later report. The 1:100.000 scale geological map of the Graedefjord region (Graedefjord 63V.1SYD) served as a basis for the more regional work and proved to be highly valuable and mapping results of this study largely conform to the regional map compilation. Differences between previous and this study are mainly related to (1) the diversity and abundance/occurrence of regionally mappable rock types that have not been differentiated on the regional map – in places, as a result of the spatial resolution on the 1:100.000 scale map, and (2) structural detail, i.e. while regional lithological and foliation trends are depicted with great accuracy, the structural complexity of the region cannot be fully appreciated on this regional scale of mapping.

The field report is structured into three parts:

(1) a very brief regional account compiled from the literature and previous GEUS reports,

(2) a presentation of field results obtained on field camps I to V, and

(3) a brief discussion and interpretation of these results with respect to the aims of the project formulated above.

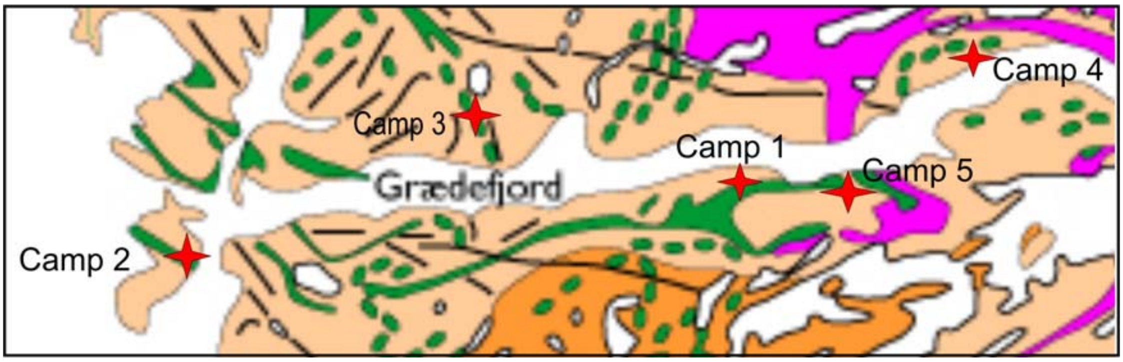

Figure 15. *The 2009 field area centred around the Graedefjord is highlighted, indicating the location of camps (red stars) presented and discussed in this report (Geological map after GEUS files; cf.; Fig. 1).*

Geological background

Recent works suggest SW Greenland to be made up of a number of distinct tectonostratigraphic terranes or crustal blocks (e.g., Nutman & Friend 2007; Nutman *et al.* 1989a; Windley & Garde 2009). Each of these blocks is interpreted to record prolonged histories of magmatic and tectonic accretion between > 3.2 Ga and ca. 2.8 Ga, culminating in a major accretionary event at ca 2.7 Ga during which the different crustal blocks were amalgamated. One of these accretionary sutures is believed to be located in and around the Graedefjord, separating a northern Sermilik block (the Tasiusarsuaq terrane) from a southern Bjørnesund block (Windley & Garde 2009). The actual terrane boundary is supposed to be located within 2-5 km to the S of the Graedefjord. The Graedefjord itself supposedly contains the boundary between upper, amphibolite-facies crustal levels and lower, granulite-facies crust in the northern Sermilik block.

Structural work undertaken in the Graedefjord region was first reported by (Myers 1978) who identified three main fold phases. The work of Myers (op cit.) highlighted, in particular, the complexity of fabric forming events and the highly differing degrees of transposition with respect to high-strain zones.

Results

Camp I: S of the Graedefjord

Coordinates 50°40'30.79 W 63°20'33.62 N

Camp I was shared with three further groups, but fieldwork was done, for the most part, independently.

- <u>Lithological inventory:</u>

1. The area is dominated by banded, dark- to medium grey biotite- (and/or hornblende) bearing TTG gneiss. This gneiss variety is very widespread in the Graedefjord region. In low-strain domains, the gneisses contain abundant folded and/or foliation-parallel mm- to cm- wide leucosomes (Fig. 16a, the term leucosome is used here and throughout the report to describe quartz-feldspar dominated, mainly stringer- or pocket-shaped bodies, without necessary invoking the in-situ partial melting origin of the leucosome, i.e. leucosomes may be intrusive). As a result of the small-scale folding, gneisses appear commonly crenulated. In high-strain domains, banded and striped gneisses dominate, but the actual fabric development is more complex (see below).
2. Camp I was located at the northern margin of a prominent, amphibolite-dominated greenstone sliver that describes a km-scale, closed structure. The supracrustal rocks include, in decreasing order of abundance, amphibolite (massive to banded, black – to grey-greenish, typically strongly foliated, locally garnetiferous), felsic schist (quartz-feldspar with minor biotite, foliated and/or finely laminated, locally

with fragments (tuff-like origin, bombs (?)), and meta-ultramafic rocks (dark-brown, weathered to talc-carbonate rocks). Dark-green calc-silicate fels (diopside, garnet, quartz and plagioclase) occurs as isolated, boudinaged layers in the felsic schist units, but are rare. The supracrustal rocks are intruded by (a) a variety of grey TTG gneisses, (b) leucogranite gneisses, and (c) pegmatoids. Foliation-parallel lit-par-lit intrusion is most common, but crosscutting dykes are also present. The dykes preferentially follow the axial planes of folds (Fig. 16b, see below) but irregular stockwork-type patterns also occur.

3. A mappable, ca. 200-300 wide unit of very leucocratic, coarse- to medium-grained leucogranite occurs between the Graedefjord and Camp I. The unit trends E-W, parallel to the regional grain of lithologies and the main foliation (S_3, see below). This leucogranite is not shown on regional maps. A similar leucogranite was mapped some 10-12 km along strike in Camp V and it seems likely that this sheet-like leucogranite gneiss is continuous over at least this distance. The leucogranite contains abundant angular xenoliths of amphibolite. The fragments range in size from merely deci- to decametres and contain an earlier isoclinal fold generation. The foliation in the leucogranite gneiss wraps around the xenoliths.
4. Leucocratic, mainly E-W trending pegmatites are volumetrically subordinate but widespread. The pegmatites occur mainly as dykes or irregularly shaped, anastomosing stringers, but are too small to be shown on regional maps. They intrude all lithologies and are the last, regionally significant felsic intrusive phase in the region.

- <u>Structural Geology</u>

Deformation events are listed as D_1 to D_5 in order to highlight the relative chronological order. However, overprinting relationships suggest the progressive nature of individual deformation events.

D_1:

S_1 and F_1 in supracrustal rocks

S_1 - is the earliest, bedding (compositional layering (S_0)) parallel foliation in supracrustal rocks, such as felsic schists or amphibolites. S_1 is defined by flattened quartz-discs and ribbons and elongated quartz-feldspar aggregates in felsic units and a grain-shape preferred orientation of e.g. amphibole or highly-elongated leucosome stringers in meta-mafic units, mainly amphibolites. Isoclinal, often rootless and, in places, intrafolial folds occur on a cm- to m-scale and testify to the transposition of fabrics. More commonly small-scale folds can be seen to refold the S_1 gneissosity (Fig. 16b). Strictly speaking, these folds should then not be referred to as F_1 folds, but the early S_1 fabric is characterised by multiple episodes of intrafolial folding and refolding. F_1 folds are mainly contained in the composite S_1. The actual degree of fabric transposition and resulting duplication of strata cannot be ascertained.

This complex development of an early high-strain transposed fabric seems to be confined to the supracrustal rocks. The earliest grey gneisses show a layer-parallel foliation (S_1) and occasional intrafolial folds (F_1), but fabric development does not show the same complexity compared to the supracrustal rocks.

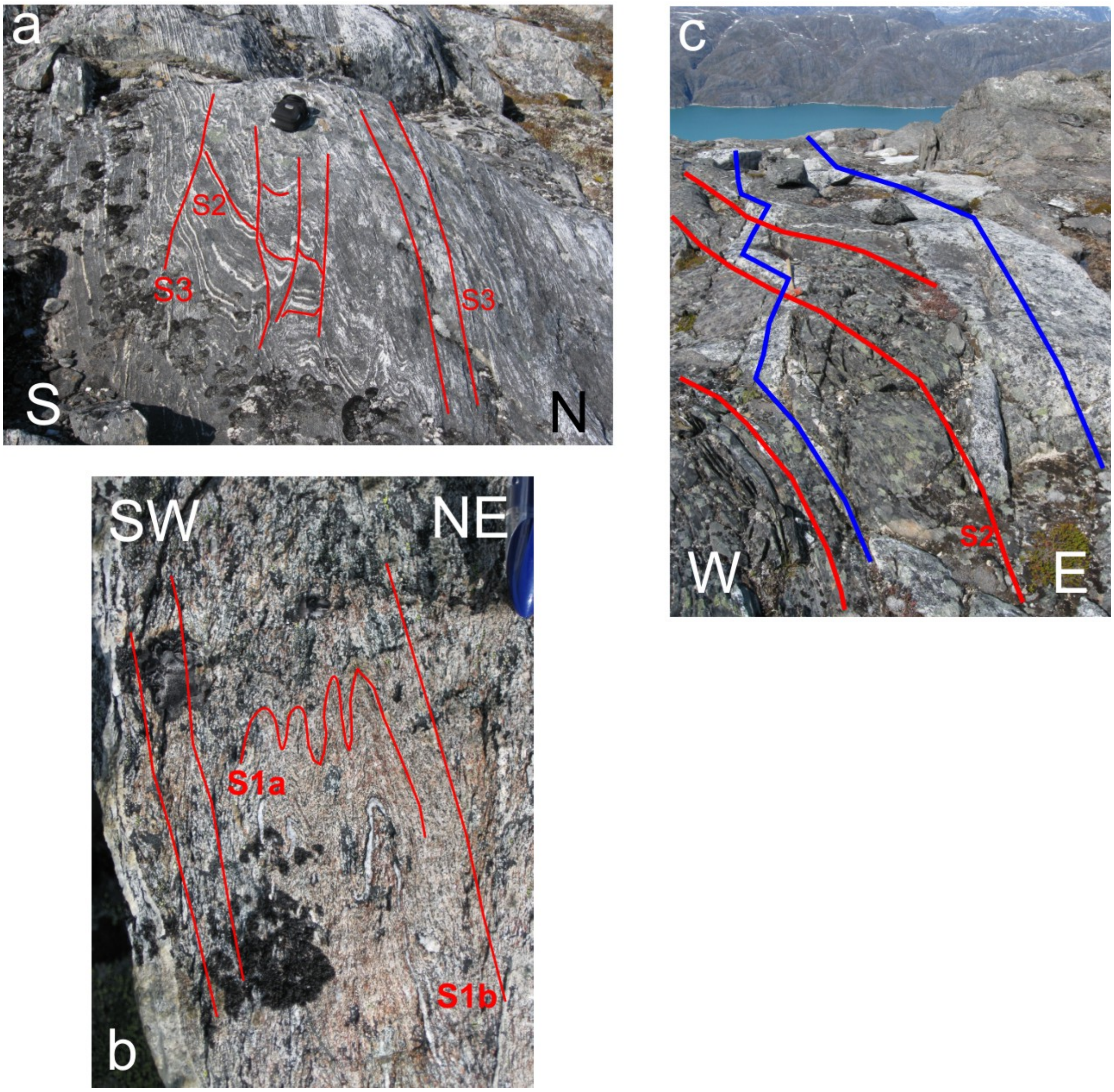

Figure 16. *(a) Early-generation grey gneiss (camera pouch for scale). Foliation planes are commonly lined with mm- to cm-wide leucosome stringers, accentuating an earlier S_2 gneissosity. The refolding and crenulation of the S_2 gneissosity by an E-W trending, sub-vertical S_3 foliation is very widespread and may lead to the complete transposition of S_2 into S_3 in high-strain domains. (S_2 and S_3 annotated by red lines, oblique plan view). (b) Felsic quartzo-feldspathic schist. The schists form narrow (5-25 m wide) units within the amphibolite-dominated supracrustal succession. Supracrustal rocks show evidence of an earlier transposition of fabrics (here: S_{1a} into S_{1b}) that is not observed in the intrusive TTG gneisses (cross-sectional view). (c) Oblique plan view of folded amphibolites (S_1 fabric annotated by red lines, only one limb shown on photo), intruded by N-trending TTG dykes that show an axial planar orientation with respect to the folds (F_2), Graedefjord in the background.*

D_2:

F_2 folds – N-S trending axial planes, subvertical plunges

An earlier, mesoscopic fold generation (F_2) is defined by the folding of the compositional layering, S_0, and S1. These folds are particularly well preserved in amphibolitic units where they are intruded by TTG gneisses. The folds show N-S trending axial planes and subvertical plunges. An axial planar foliation is only very weakly developed, but dykes of grey TTG's commonly intrude parallel to the axial planes of these folds. Fold half-wavelengths range from 1 to ca. 50 m. This fold generation is well preserved to the S of Camp I (50° 40.386W 63° 20.858N), but the folds are progressively transposed over a distance of ca. 500 m by E-W trending fabrics (S_3, see below). Similar N-S trending folds are preserved e.g. at coordinates 50° 34.968W 63° 21.129N, some 10-12 km to the E, indicating the regional significance of this fold generation.

D_3:

F_3 folds – E-W trending axial planes, steep plunges, strong stretching L, E-W high-strain zones

D_3-related fabrics describe a progression from S to N, whereby N-trending F_2 folds are progressively refolded and transposed by E-W trending fabrics (F_3, S_3; Fig. 17). The transition from N trending folds and fabrics (D_2 domain) to E trending fabrics (D_3 dominated) occurs over a distance of only several hundred metres. Fold transposition is initiated along undulating, E-trending, subvertical high-strain zones that anastomose around and enclose fabric domains with D_2 fabrics. These D_3 high-strain zones are often intruded by E-W trending TTG dykes. Both TTG gneisses and supracrustal rocks are open to isoclinally folded in the lozenge-shaped D_2 domains between the D_3 high-strain zones, clearly preserving evidence of earlier D_2 fabric elements. Notably, there is no consistent sense of rotation (drag) of the D_2 fabric elements into S_3 fabrics that would indicate a significant simple shear component along S_3 high-strain zones (Fig. 17). Similarly, non-coaxial fabrics are not recorded in S_3 fabric domains.

F_3 folds trend E-W and show steep to subvertical plunges. A pervasive mineral stretching lineation plunges at steep angles to the E (ENE-ESE) and subparallel to F_3 fold hinges. In places, L fabrics result in rodding fabrics (L>S), defined by stretched quartz-feldspar aggregates in TTG's and rodded amphibole in mafic supracrustal rocks. F_3 folds occur on a wide range of scales from mm- to cm-scale crenulations to folds with amplitudes and half-wavelengths > 100 m. S_3 is axial planar to F_3 folds (Fig. 16a), trending E-W with subvertical dips. In relatively low-strain domains, S_3 is developed as a cm- to dm-spaced crenulation cleavage (Fig. 16a). In areas of higher strain, S_3 is closely spaced and pervasive, progressively transposing F_3 folds into the E-W trending gneissosity (Fig. 17). It should be noted that this is the third transposition event recorded in gneisses of the Graedefjord, including (1) the early S_1 fabric forming event S_0/S_1 (Fig. 16b), (2) the transposition of N-S trending F_2 folds into S_3, and (3) the transposition of F_3 folds into banded gneisses (S_3) in high-strain domains (Fig. 17). This has obvious implications for the correlation of fabrics in the region. The progressive transposition can be observed on outcrop scale, but fold transposition into high-strain S_3 fabrics is most prominent on a km-scale, illustrated in the schematic N-S traverse depicted in figure 17.

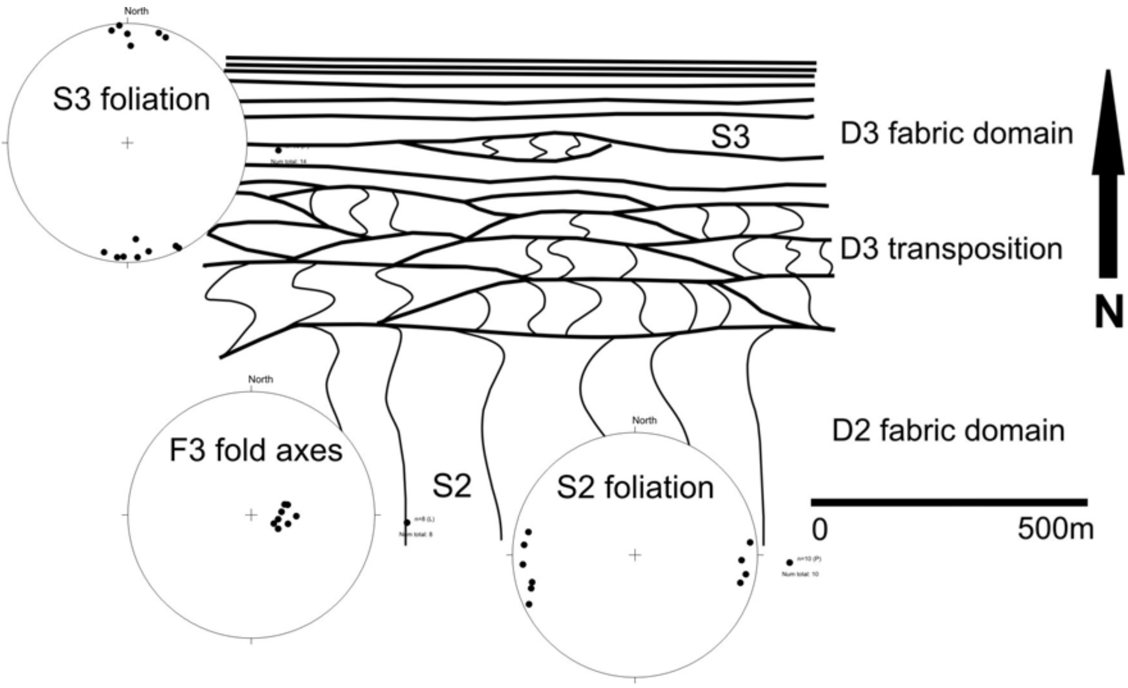

Figure 17. *Schematic formline map showing the progressive refolding and refoliation of N-S trending D_2 domains, containing N-S trending folds (not shown) and axial planar foliation (S_2), by E-W trending S_3 fabrics to the immediate S of the Graedefjord. Stereonets show poles to the S_3 foliation (top left), plunge of F_3 fold axes, parallel to mineral stretching lineation (bottom left), and poles to S_2 foliation (bottom right; all stereonets are equal area projections into the lower hemisphere).*

The highest fabric intensities and, thus, presumably strain intensities are found at and within ca. 500m of the Graedefjord where banded and striped gneisses are developed (Figs. 17 and 18a-c). Here, the foliation is subvertical, showing dips both to the N and S. Boudinage between different gneiss units is common. Conjugate shear bands occur on a cm- to m-scale and are ubiquitous, both in cross-section as well as in plan view (Fig. 18a, b). Conjugate shear bands and the commonly chocolate-tablet type boudinage indicate a large component of layer-normal (N-S, subhorizontal) shortening to be responsible for the development of the high-strain fabrics (Fig. 18a-c). Non-coaxial fabrics are conspicuous by their absence and are only localised in e.g. conjugate shear zones/bands. The exposed width of the high-strain fabrics and striped gneisses is 500-700 m, the full width being obscured by the Graedefjord that borders this zone in the N.

Two more features characterise deformation in these high-strain striped gneisses. Firstly, melt seems to have been present throughout the deformation and deformation is melt-assisted. Leucosome stringers are developed in e.g. shear bands, boudin necks, as folded and/or boudinaged veins and veinlets, irregularly shaped and only partly transposed pockets and stringers, etc. (Fig. 18b, c). In places, the striped gneisses contain breccia-like textures of angular, rotated blocks, but with hardly any melt present, suggesting melt extraction. Secondly, despite the pervasive fabric development and high strain, mylonitic fabrics are not developed. This may, in turn, reflect the melt-assisted deformation, assisting diffusion transfer under the high temperature conditions.

D_4:

E-W trending mylonites and cataclasites

Decimetre to several m-wide, mixed brittle-ductile shear zone/fault rocks occur throughout the area. The E-W trending, subvertical shear zones commonly show mm- to cm-large rounded and occasionally rotated porphyroclasts of feldspar set in a very fine-grained grey matrix. Quartz- and quartz-feldspar ribbons are common. There is a close spatial correlation between the occurrence of the shear zones and late-stage leucocratic feldspar-quartz pegmatites. Iron staining is common along these zones.

D_5:

Late, brittle faults

Late, brittle faults show predominantly N trends and steep dips. The central parts of the faults show brecciation and minor quartz veining plus epidote veinlets, commonly surrounded by a prominent chloritisation halo in which the wall-rock gneisses and/or supracrustal rocks are retrogressed. These alteration halos can extend for up to 50 m into the wall rocks and may pervasively overprint the high-grade assemblages of e.g. TTG gneisses and amphibolites. As a result, wall rock gneisses show milky feldspars (saussuritisation) and muscovite growth, whereas mafic rocks are chloritised. The faults and associated alteration are prone to weathering and smaller, tributary streams channelling melt water and feeding into the Graedefjord can often be seen to follow the faults.

- <u>Mineralisation</u>

Mineralization is indicated by localised iron staining, but primary sulphides could not be identified. The ferruginous zones are closely associated with late-stage pegmatites and particularly pegmatites that have been affected by D_4 brittle-ductile shear zones. This is a regional feature that is found in all but one locality visited in the 2009 field season around the Graedefjord. Retrograde alteration in the form of chloritisation and sericitisation and associated quartz veining is developed around D_5 brittle faults, but evidence of mineralisation was not observed.

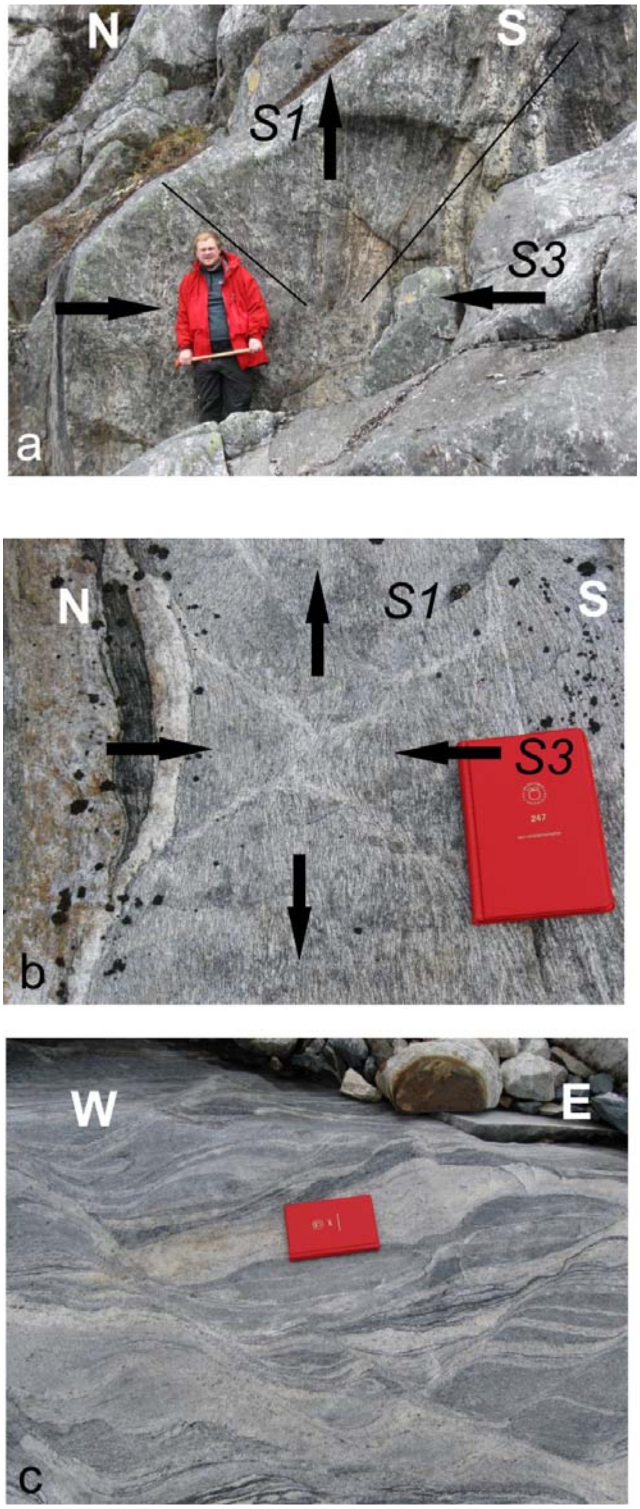

Figure 18. *(a) Cross-sectional view of grey gneisses close to the Graedefjord. Conjugate shear bands (annotated by black lines) indicate a horizontal, N-S directed, foliation-normal shortening strain and vertical, foliation-parallel extension (arrows indicate direction of S_1: maximum stretch, and S_3: maximum shortening). (b) Plan view of small-scale conjugate shear zones (S_1 and S_3 as in (a)), indicate N-S horizontal shortening and E-W, foliation parallel extension. Foliation (S3) is vertical. Note that small-scale shear bands contain leucocratic melt stringers. (c) Plan view of gneisses, showing progressively overprinting, but*

conjugate shear zones as in 17b. All photos suggest fabric formation during N-S subhorizontal shortening, accompanied by horizontal and vertical extension. The fabric symmetry indicates largely co-axial strains.

Camp II: Ikerasarssup Island, at the mouth of the Graedefjord.

<u>Coordinates: 51° 8.7599’ W 62° 19.8375’ N</u>

- <u>Lithological inventory:</u>

Most observations were made along the coast, where outcrop conditions are superb. Outcrop conditions in the interior of the island are equally good, but the exposures are invariably overgrown by a near-continuous lichen and moss cover. Three main rock types are developed, listed from old to young, based on cross cutting relationships.

1) Supracrustal rocks are dominated by a variety of amphibolites. Amphibolites occur as rafts in younger intrusive TTG’s, but are most abundant in up to several hundred metre wide and km-long belts in which amphibolites have been intruded by later TTG’s and granites in a lit-par-lit fashion (Fig. 19a). Amphibolites and TTG’s occur in roughly equal abundance in these belts. Amphibolites display a wide variety of textures and also composition. The latter is mainly a function of the relative abundance of amphibole over plagioclase and compositions range from highly melanocratic amphibolites (> 90% amphibole) to mesocratic and even leucocratic varieties (Amph/Pl ca. 50:50, Fig. 19b). Amphibolites may be massive, banded and layered and are invariably strongly foliated and lineated. Fabric intensities in amphibolites are almost invariably higher compared to the surrounding plutonic suite and intrafolial folds of either leucosomes or the compositional banding indicate fold transposition. The compositional layering is commonly expressed by varying amounts of plagioclase and amphibole, but boudinaged and internally layered cm- to dm-wide, greenish-black calc-silicate felses (clinopyroxene, plagioclase, occasional garnet) are common, albeit volumetrically subordinate, and testify to the compositional variation within the otherwise relatively monotonous supracrustal units. Numerous amphibolites show evidence of partial melting, ranging from small-scale, interconnected leucosomes, to isolated and interconnected dyke stockworks to collapsed, breccia-like textures that indicate melt loss from the rocks (Fig. 19b).

2) Grey, medium-grained, banded, biotite-hornblende gneisses are widespread. The mm- to dm-wide compositional banding is defined by alternating biotite/hornblende-rich domains and quartz/feldspar-dominated domains (Fig. 19c). A pervasive foliation is parallel to the compositional banding. Thin (mm- to cm- wide) foliation-parallel quartz-feldspar leucosomes are developed throughout the gneisses and accentuate the gneissosity. The gneisses are clearly intrusive into amphibolites, either cross-cutting or containing xenoliths of folded amphibolites.

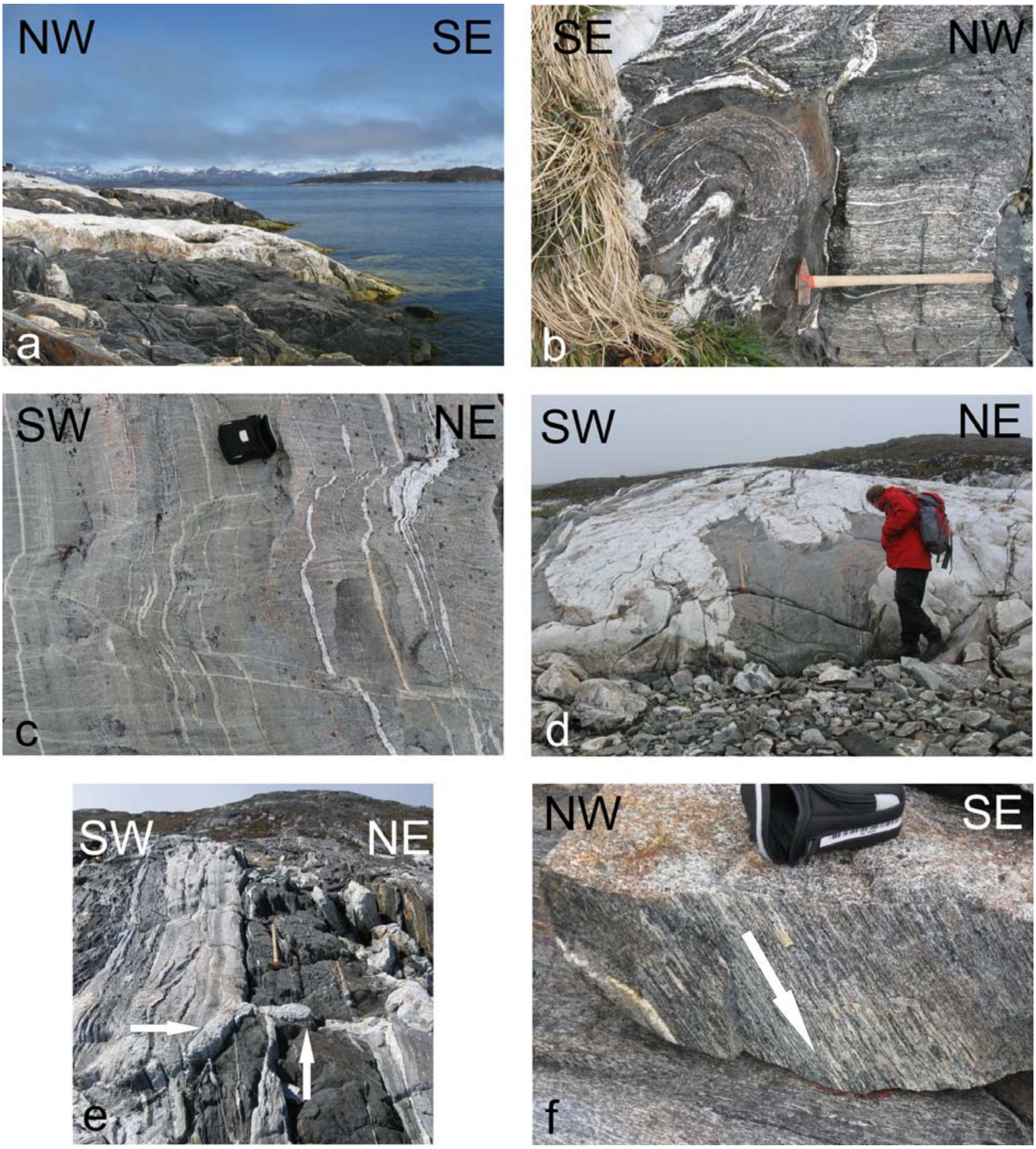

Figure 19. *(a) Large-scale lit-par-lit intrusive relationships between amphibolites, grey gneisses and leucogranites along the SW coastline of Ikerasarssup Island. (b) Banded amphibolites. Note the isolated and seemingly detached fold closure in the lower left hand corner of the photo, which is interpreted to indicate melt loss from the partially molten amphibolites. (c) Banded grey gneisses make up the bulk of gneisses on the island. Here, the gneisses show small-scale, brittle conjugate faults that are common in the area. (d) Xenolith of foliated grey gneiss in leucogranite gneiss (the Marraq Leuco-Granite). (e) Detail of lit-par-lit intrusive relationships illustrating the late-kinematic timing of leucogranites that intrude predominantly as steeply dipping, layer-parallel sills (horizontal arrows) connecting into cross-cutting dykes that occupy boudin necks and extensional fractures in amphibolites (vertical arrow). (f) Steep SE plunging rodding fabric (parallel to arrow) developed in am-*

phibolite. Prolate fabrics and L>S tectonites are common, despite the pronounced banded nature of the rocks imparted by the lit-par-lit intrusive relationships between supracrustal rocks and different TTG gneiss varieties.

3) Banded, highly leucocratic gneisses are volumetrically most abundant on the northern parts of the island, but are also developed elsewhere. These gneisses are indicated as Marraq Leuco-Granite on the 1:100.000 scale geological map of the Graedefjord. The leucogneisses are virtually devoid of any mafic minerals (only very minor biotite) and consist almost entirely of quartz and feldspar. As a general rule, coarse-grained varieties contain more biotite than fine-grained varieties. The foliation in the gneisses is defined by the grain-shape preferred orientation of quartz discs and quartz-feldspar aggregates. The leucogneisses represent the last, volumetrically significant intrusive phase in this area, containing xenoliths of both amphibolites and grey gneisses (Fig. 19d). A syn- to late-kinematic emplacement of the leucogneisses is, in places, indicated by cross-cutting apophyses of the granites in amphibolites in lit-par-lit contact zones between the two rock types (Fig. 19e). The cross cutting dykes commonly occupy extensional fractures or inter-boudin spaces, but without being progressively transposed as is the case with most other fabric elements and intrusive units.

4) Quartz-feldspar pegmatites are volumetrically subordinate, but common, occurring as dykes and sills, intruding all of the major rock units.

5) Mafic dykes mark the last intrusive event. NE, E and ESE dykes have been mapped. Their width ranges from thin, cm-wide dykelets up to 100 m wide, massive dykes. Contacts are sharp with, in places, cm-wide chilled margins against the wall-rock gneisses.

- Structural geology:

D_1: S_1, L_1 and F_1

The earliest foliation is a transposition fabric in amphibolites, enveloping isoclinal, intrafolial and often rootless folds in amphibolites.

$D_{2/3}$:

Gneisses and amphibolites contain pervasive, layer-parallel solid-state fabrics. The typical crenulation folding and transposition associated with the main fabric-forming events observed elsewhere around the Graedefjord (e.g. Fig. 16a, and see below) is not observed. Instead, planar high-strain fabrics dominate both gneisses and supracrustal rocks. Rodding fabrics and very prominent mineral stretching lineations are prominent in most outcrops. Lineations ($L_{2/3}$) show invariably steep plunges to the E and SE (Fig 19f). In essence, fabric development is similar compared to that observed in other camps around the Graedefjord, with differences probably related to stronger fabric intensities and, thus, strain intensities on Ikerasarssup Island.

D_4:

The coastal outcrops showed no evidence for the presence of D_4 deformation zones.

D_5:

Late-stage brittle faulting is abundant throughout the coastal outcrops. Faults range from narrow (1-5 cm wide), often closely spaced cataclastic zones to several m-wide breccia zones or fault arrays. Faults are subvertical and show N trends with both (apparent) dextral and sinistral offsets on horizontal surfaces (the island provides only limited vertical outcrop). Conjugate faults sets are a very common and faults trend NNW and NNE, showing dextral and sinistral apparent displacements, respectively (Fig. 19c). This orientation of faults, their conjugate arrangement and displacement are indicative of E-W extensional strains.

Camp III: N of Graedefjord,

coordinates: 50° 53.5649'W 63° 23.0719' N

- Lithological inventory:

Two main rock types are developed in this area N of the Graedefjord including (1) grey, banded TTG gneisses (Fig. 20a-f), and (2) amphibolites. The field appearance of the plutonic suite is virtually identical from the low-strain TTG gneisses described from Camp I from the S shores of the Graedefjord. They are banded, dark to light-grey, biotite/hornblende bearing gneisses containing ubiquitous, open- to isoclinally folded leucosome stringers (Fig. 20). The crenulation-type folding of the foliation/banding and parallel leucosomes and the formation of new leucosomes along the axial planar foliation of folds is equally similar to that observed at Camp I some 12 kilometres to the SE (Figs. 16a and 20a, b, d, and e).

Amphibolites are massive to banded, similar to other occurrences of supracrustal rocks around the Graedefjord. They occur as isolated rafts, or trains of rafts in the TTG's. Larger amphibolite exposures are up to 200 hundred metres wide and can be traced for several kilometres along strike, showing lit-par-lit contact relationships with intrusive gneisses.

Quartz-feldspar dominated leucogranites are the last, regionally developed intrusive phase. They occur as foliation-parallel (Fig. 20a, b and e) or low-angle cross-cutting sheets, as thin, interconnected stringers (Fig. 20d) or as intrusive stockworks that brecciate older gneisses (Fig. 20c). Similarly, large, mappable leucogranite bodies as they developed around Camps I, II and V were not observed. Deformation of the leucogranite stringers ranges from tightly folded and boudinaged (Fig. 20a, b, d and e) to sharply cross cutting and undeformed (Fig. 20c), indicating their late- to post-tectonic timing. This relative timing is consistent with observations made in other locations around the Graedefjord.

Mafic dykes are prominent in this area. They show mostly NW trends, sharply cross cutting all fabric elements in the Archaean rocks.

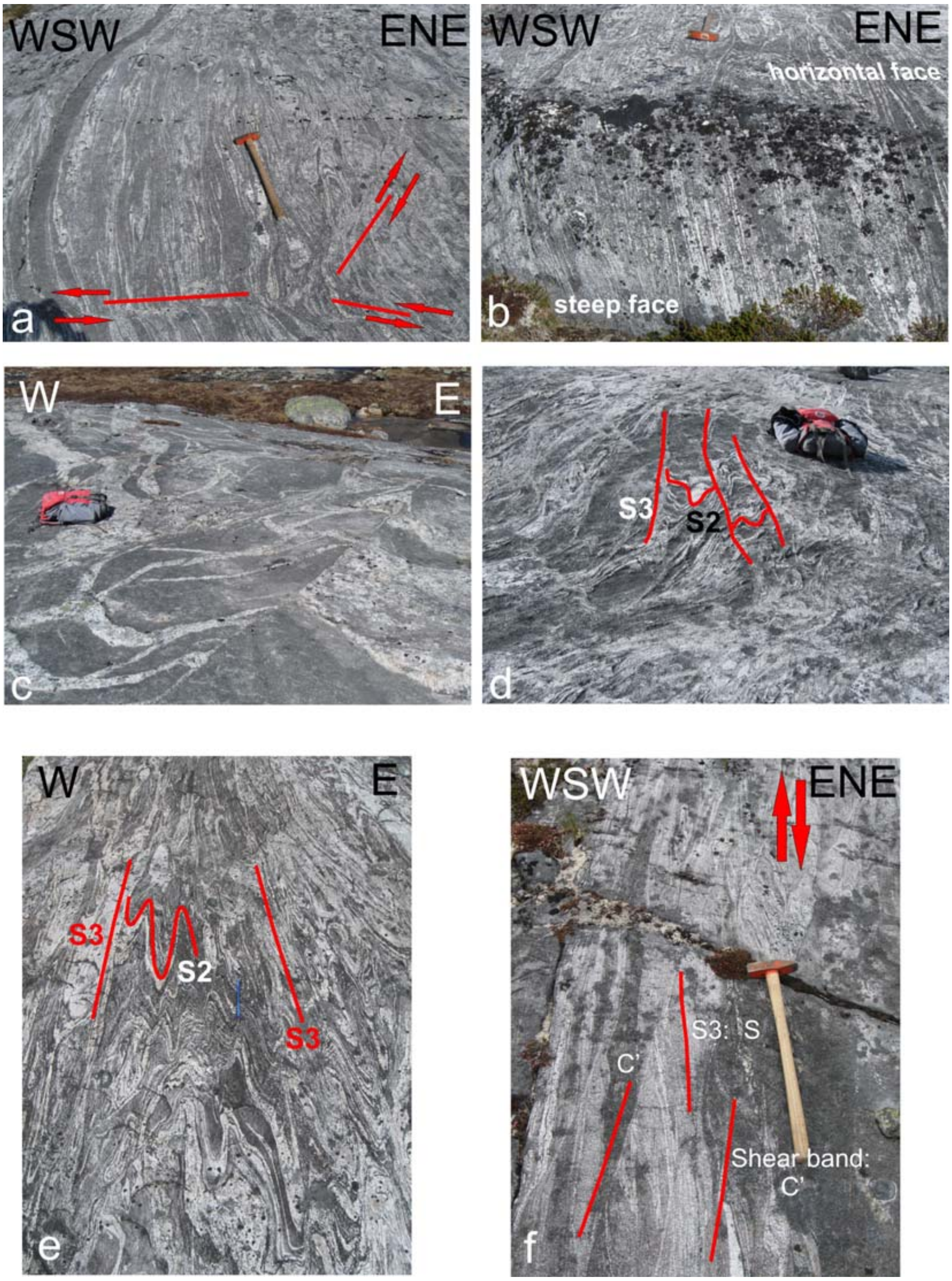

Figure 20. *(a) Oblique plan view of the subvertical, composite S_2/S_3 fabric in grey gneisses. The NNW trending fabric is, at this locality, truncated by high-angle, in places, conjugate shear bands that indicate a large component of layer-normal shortening during fabric development. (b) 3D outcrop of grey gneisses showing multiple crenulation folding on horizontal faces, but banded gneisses on steep faces. This suggests a steep, down-dip plunge of linear elements and the main stretch. (c) Intrusive stockwork of late-stage leucogranites brecciating grey gneisses. (d-e) Progressive development of S_2/S_3 transposition from low strain (d) to higher strains (e and f); (d) Late-stage leucogranites are intrusive into grey gneisses, but have been affected by S_2/S_3 transposition. (e) Tightening of F_3 folds between*

S_3 fabric domains. (f) Complete transposition of S_2 (no longer observed) into S_3 and development of oblique shear bands in the high-strain S_3 fabric.

- <u>Structural geology:</u>

Fabric development and details of the structural geology in and around Camp V are near identical to those described for Camp I with the exceptions that (1) the regional structures show different orientations, and (2) the high-strain gneiss belt characterised by E-W trending S_3 fabrics in the Graedefjord (e.g. Camp I) is not developed. Amphibolites contain a pervasive foliation and/or banding, containing intrafolial folds. The surrounding gneisses are crenulated, displaying all degrees of progressive fold transposition from open crenulation folding to isoclinal folding and near-complete transposition (Fig. 20a, b, d, e and f)).
The very well-exposed, clean, whale-back-type outcrops in this area illustrate the progressive nature of the fabric (foliation) development, in that earlier foliations are coaxially refolded, progressively transposed to form a new foliation, and again refolded (Fig. 20d, e and f). Hence, the use of S_1, S_2, etc. can only distinguish overprinting fabric relationships on a local scale, but is not considered to be helpful in regional correlations as it ignores the progressive nature of foliation development.
The glaciated 3-D morphology of the mainly whaleback-type outcrops provides some important additional information (Fig. 20b). Crenulation folding and refolding of the gneissosity is almost exclusively observed on horizontal or shallowly inclined surfaces. Vertical surfaces of the same outcrops, in contrast, do not display this folding, but are, instead, developed as straight, banded gneisses (Fig. 20b). This suggests a steep- to subvertical and down-dip plunge of crenulation fold axes throughout these outcrops. Fold axes are parallel to a strong stretching lineation (L_2). Fold hinges and stretching lineations plunge, for the most part, at steep angles to the SE.
During the three days in Camp III, structural work focused on the mapping of a large-scale fold structure clearly visible and outlined on the 1:100.000 scale geological map. A simplified formline map is shown in figure 21.
First-order structure: The structure is almost entirely developed in banded TTG gneiss. A train of amphibolites only occurs in the NE parts of the fold, where it can be traced as a marker for > 5 km along strike. In plan view, the structure is defined by the folding of the $S_{2/3}$ gneissosity (*note: the gneissosity has been termed S_2/S_3 here and for this particular structure, in order distinguish this folded fabric from later fabrics*). In places, the S_2/S_3 gneissosity contains an earlier generation of m-scale intrafolial folds. The folds are preserved in relatively low-strain sections of the gneiss, but progressive fold transposition is again evident in higher strained parts, which agrees with the regionally observed fabric development. The enveloping S_2/S_3 gneissosity describes a closed, somewhat triangularly-shaped geometry (Fig. 21). The fold, thus, shows a relatively sharp hinge in the N and two equally sharp hinges in the S. The limbs between the hinges are straight. Dips of the enveloping gneissosity are steep and away from the core of the fold and define a dome-like geometry (Fig. 21). A stretching lineation is prominent, in places, and shows, for the most part, E to SE plunges. NW plunges are restricted to a small area in the N parts of the fold (Fig. 21). Shallow foliation dips that would indicate the presence of a fold closure are conspicuous by their absence. As a result, the structure has the geometry of a steeply plunging cone, which is also illustrated by foliation readings taken throughout the dome.

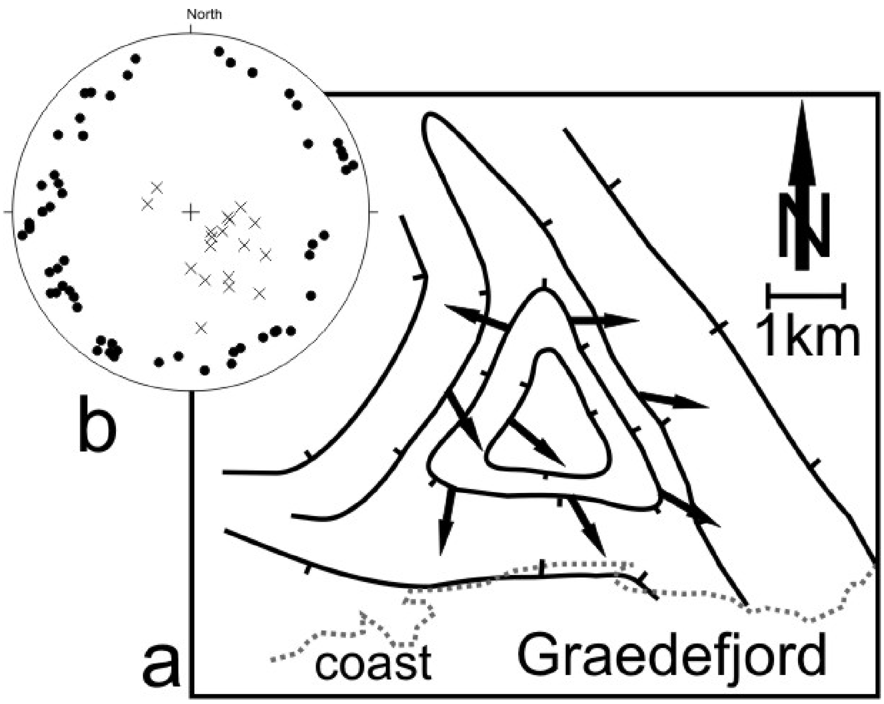

Figure 21. *(a) Simplified formline map of the central fold structure mapped at Camp III. Formlines illustrate the trend and mainly steep to subvertical dips of the S_2/S_3 foliation. Arrows show the regional plunge direction of the stretching lineation contained in the gneissosity. (b) Lower hemisphere, equal area projection of poles to S_2/S_3 (dots) and mineral stretching lineations (crosses). Note the small-circle distribution defined by poles to the gneissosity and the mainly steeply-plunging stretching lineation subparallel to the cone axis.*

*Minor structure*s: The rotation of the gneissosity from the straight limbs into the hinge zone is relatively sharp and occurs over only a few tens of metres. The first indication of folding closer to the hinge is given by a subtle rotation of the gneissosity by 10-20 degrees. Further rotation of the gneissosity closer to the hinge is accompanied by the formation of oblique shear bands (Fig. 20f). The shear-band and foliation relationships closely resemble S-C' fabric relationships, indicating a component of layer-parallel stretch during rotation.

Within the hinge, rotation of the gneissosity is achieved by high-angle shear bands and the rotation of foliation domains between shear bands, which results in almost breccia-like textures of high-angle, rotated foliation domains separated by thin, cm- to m-wide shear bands (Fig. 22). These shear bands show relatively consistent N trends (between N 30 E and N 30 W) and are found throughout the fold structure, but particularly common and closely spaced in the three hinges of the fold. The high-angle shear bands can be traced for several tens of metres along strike before commonly rotating and grading into the regional gneissosity. There is no consistent shear sense and shear bands bounding metre- to tens of metre wide domains of sigmoidally folded gneissosity resemble a large-scale crenulation.

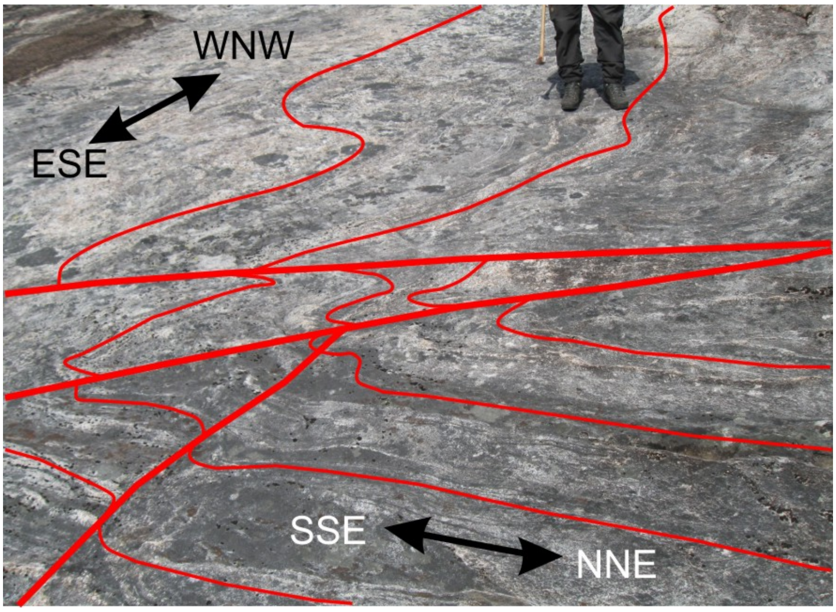

Figure 22. *The relatively sharp curvature and rotation of the regional gneissosity in the three hinges of the closed fold structure (Fig. 21) is achieved along high-angle, N-trending shear bands (here annotated by thicker red lines). Note the rotation of the gneissosity (S_2/S_3, annotated by thinner red lines) through an angle of 90° within only ca. 1 m. The high-angle shear bands are often filled with melts. Closely spaced shear bands (50 cm to 10 m) resemble a large-scale crenulation foliation.*

Camp IV: N of Graedefjord

<u>coordinates: 50° 29.431' W 63°24.332' N</u>

- <u>Lithological inventory and structural geology:</u>

Camp IV was located at the eastern extent of what has been mapped as a meta-sedimentary sliver south of the Illivertalik granite in the NE parts of the 1:100.000 scale geological map of the Graedefjord. The supracrustal sliver had been reported to show signs of mineralisation and alteration. The identification and delineation of potential mineralisation formed the main focus of the work around Camp IV. The area is dominated by relatively monotonous to banded, grey TTG gneisses. Amphibolites occur as up to several tens of metre large rafts. They are either massive or banded and, in places, brecciated by intrusive TTG phases. The Illivertalik granite forms a prominent, E-W trending topographic high towering over the area to the immediate N.

Rocks that constitute what is shown on the 1:100.000 scale geological map as a meta-sedimentary complex form a 250-300 m and up to 500 m wide succession that can be traced for at least 5 km along strike in an E-W direction. The rocks show a prominent foliation-parallel banding (Fig. 23a-d), expressed by alternating leucocratic layers, made of predominantly quartz and feldspar, showing foliated granitic textures and, on weathered surfaces, fine-grained brownish, iron-stained layers. This alternation imparts a closely-spaced (mm- to cm) banding on the rocks. On fresh surfaces, the brownish bands appear medium-to dark-grey, showing a very fine-grained matrix. There are number of features that suggest that this seemingly compositional banding is not of primary sedimentary origin, but tectonic in nature. The darker layers are, in outcrop, typically not continuous and can only be traced for several metres along strike, rather forming an anastomosing network than planar bedding (Fig. 23a, c). The fine-grained matrix contains mm- to cm-large, rounded to subangular feldspar porphyroclasts (Fig. 23b). In places, these porphyroclasts describe σ- and/or δ-clast geometries. Quartz forms, in places, quartz ribbons whereas large, cm-sized feldspars appear intensely fractured and dismembered. Moreover, elongate quartz-feldspar stringers are commonly deformed into tight- to isoclinal, intrafolial and rootless folds, but they may also show small-scale imbricate structures (Fig. 23b-d). S-C fabrics are locally developed. These features indicate that the darker bands represent anastomosing, mixed brittle-ductile cataclasite-mylonite zones that have imparted the banding on the rocks.

The foliation dips at steep- to moderate angles to the N throughout this zone. Despite the high-strain fabric of the rocks, linear fabrics are rare. Where observed, lineations show shallow E plunges. Shear sense indicators include σ- and δ-clasts, S-C and S-C' fabrics, small-scale duplexes and abundant asymmetrical folds. The majority of shear sense indicators points to an apparent dextral sense of displacement. However, down-dip, normal, top-to-the-N kinematics as well as reverse, top-to-the-S movement along the N-dipping foliation can also be recorded (e.g. Fig. 23d). The latter would correspond with the S- to SE vergent folds enveloped by the N-dipping cataclasite and regional foliation (see below). The S boundary of this zone is relatively sharp and made up of grey, relatively monotonous TTG gneisses that form the footwall of the brittle-ductile shear zone complex. The N hangingwall boundary, in turn, is made up of strongly mylonitised, banded TTG gneisses and intercalated granites and pegmatites, characterised pervasively-developed crystal-plastic textures (Fig. 23e). Shear-sense indicators on the mainly horizontal surfaces indicate an apparent dextral sense of displacement, similar to that recorded in the brittle-ductile mylonite-cataclasite complex in the footwall.

The N-dipping foliation forms the enveloping surface to S and SE verging folds that refold the banding in the mylonite-cataclasite (Fig. 24a, b). This suggests that shearing (i.e. mylonitisation and cataclastic deformation) formed a progressive deformation, refolding earlier shear- and fault zones. The N-dip and S- to SE-vergence of folds is most readily explained by a top-to-the-S sense of shear, as is locally recorded, but clearly subordinate to the near-ubiquitous dextral shear sense indicators.

- Mineralisation:

The mylonite-cataclasite zone shows a number of foliation/banding-parallel zones of ferruginous alteration. The most pronounced alteration is recorded in up to 2 m wide foliation parallel zones that can be traced for several hundred metres along strike (Fig. 25). Up to 5 of these distinct alteration zones can be distinguished. Alteration is localised around the cores of more massive, brittle cataclasite zones. Quartz veining is only rarely associated with the cataclastic cores and mineralisation (e.g. sulphides) was not observed. Although quite prominent in outcrop, iron staining seems to be a rather surficial feature, penetrating along joints and fractures into the cores of cataclastic fault zones.

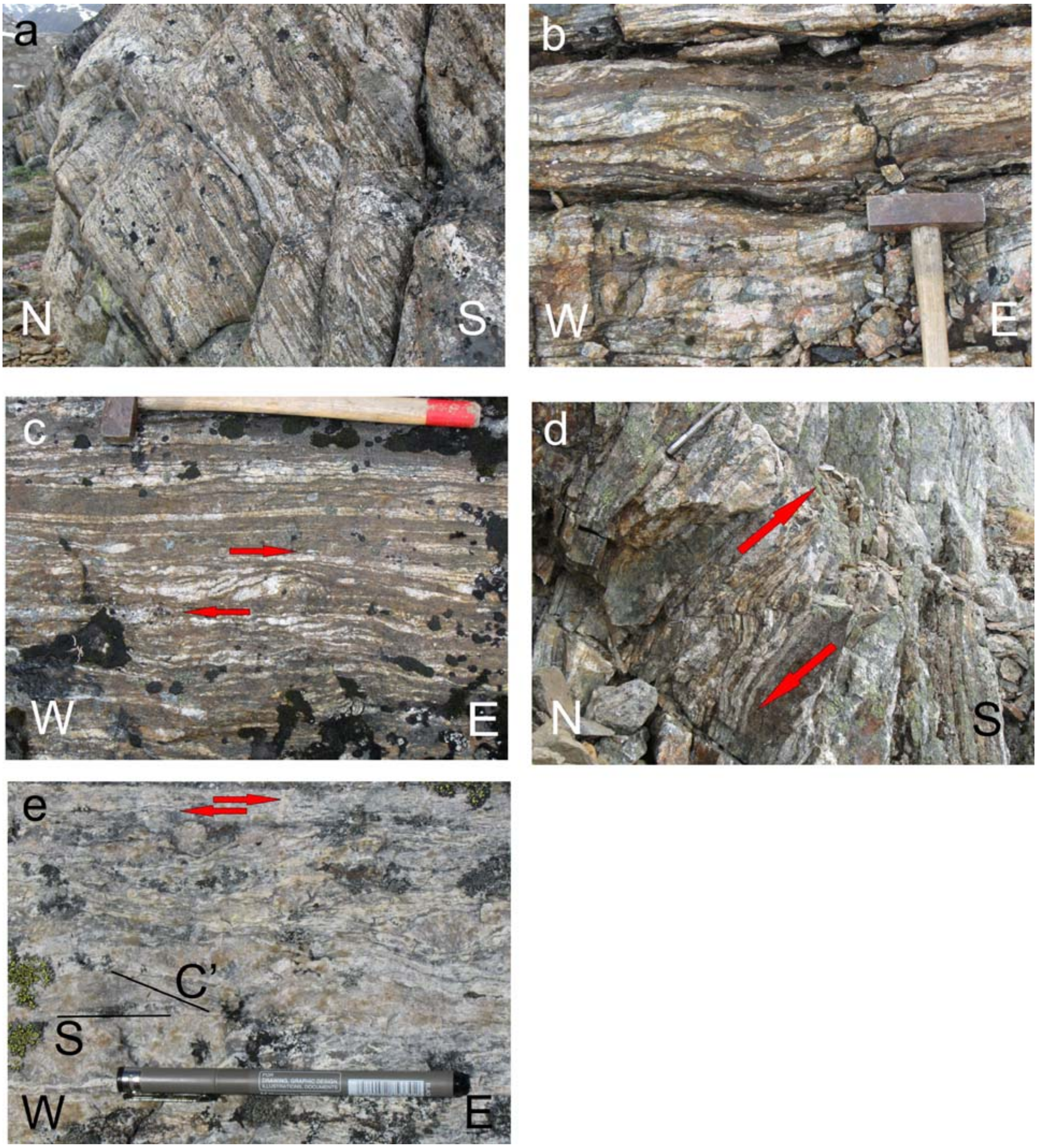

Figure 23. *(a) Banded gneisses (cross-sectional view) at Camp IV. The banding can be confused with sedimentary layering, but consists of, in detail, alternating cataclasite/mylonite bands. (b) Close-up of brownish weathering cataclasites containing rounded feldspar-porphyroclasts. Iron staining is widespread in this deformation zone, but is not pervasive and rather restricted to weathered surfaces and joints (pan view). (c) Plan view of banded cataclasite. Imbrication of quartz-feldspar ribbons indicates apparent dextral sense of displacement. (d) Cross-sectional view of banded cataclasites, showing small-scale duplex, indicating top-to-the-S sense of thrusting. (e) Plan view of mylonitic gneisses and mylonitised pegmatites. These mylonites are developed to the immediate N of the cataclasite zone. Pervasive crystal-plastic deformation features indicate higher temperature conditions during deformation than the cataclasite zones in the footwall of the mylonites. A dextral*

sense of displacement is indicated by a number of shear sense indicators (here: S-C' fabrics).

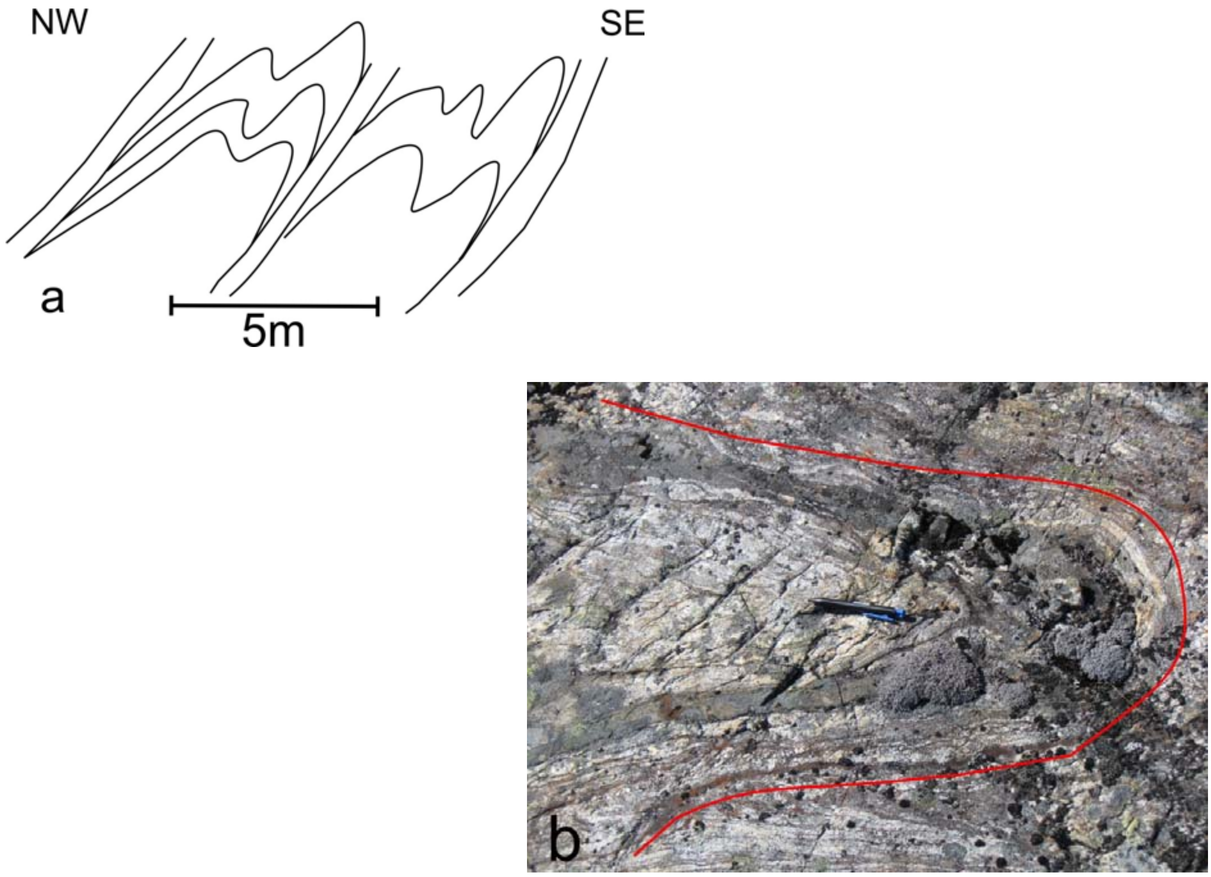

Figure 24. *(a) Simplified line drawing (cross-section) of S- to SE-verging folds enveloped by the regionally developed N-dipping gneissosity (e.g. Fig. 23d); (b) Plan view of refolded cataclasite/mylonite banding by a S-verging fold. Pen trends E-W and parallel to the axial plane of the fold.*

The alteration zone comprises a Grt-Bt-Qtz-Sil-Mag-Ilm-gahnite($ZnAl_2O_4$) assemblage with minor Pl, Kfs and Po. The whole rock analysis yield 3260 ppm Zn and minor enrichment for elements like As, Ag, In, Sn, Th and U. No Zn sulphides were observed and all the Zn is probably bound to gahnite, which is a Zn spinel that forms during metamorphism of primary Zn sulphide deposits. This suggests that at least some of the enrichment of different elements occurred prior to metamorphism.

Figure 25. *Overview of the E-W trending and N-dipping, banded cataclasite zone above Camp IV. Red ellipses indicate the presence of pods with prominent iron staining.*

Camp V: S of Graedefjord, Camp V was located some 10-12 km to the E of Camp I

coordinates: 50° 34.968 W 63° 21.129 N

- Lithological inventory:

Four main lithologies can be distinguished.

1. A medium- to dark grey gneiss is the oldest TTG phase. The gneiss contains a solid-state gneissosity that is parallel to a compositional banding. Macroscopically, the gneiss consists of quartz, feldspar, biotite and hornblende. The grey gneiss can be very melanocratic and the compositional banding is commonly highlighted by leucocratic quartz-feldspar stringers.
2. Amphibolites are locally abundant and intricately interlayered on a dm- to m-scale with the grey gneiss and later leucogneiss. Amphibolites consist macroscopically of mainly amphibole and varying amounts of plagioclase, locally developed garnet and, in one occurrence, post-kinematic orthoamphibole. Ultramafic and highly weathered talc-carbonate schists were mapped at one locality, interlayered with amphibolites and intrusive TTG's. The gneisses commonly intrude amphibolites in a lit-par-lit fashion and trains of interlayered amphibolites and gneisses are up to several hundred metres wide and can be traced along strike for several kilometres. Interlayered amphibolite and gneiss are also exposed in large pavements showing spectacular superposed folding and progressive transposition of fabrics (see below). In places, isolated and rotated rafts of amphibolites float within enveloping grey gneiss and leucogneiss.

3. Leucocratic granite gneisses are intrusive into both the older grey gneisses and amphibolites. Intrusive and cross cutting relationships are still preserved in low-strain domains, but the leucogneisses are commonly bedding-and foliation-parallel suggesting that they have experienced much of the strain paths of the older rocks. The leucogneisses are volumetrically subordinate, though ubiquitous in the E of the area, around the campsite. They become volumetrically more abundant towards the W and towards Camp I, forming initially larger, E-W trending continuous sheets and, eventually mappable (200-400 m wide, several kilometres long), subvertical, E-W trending sheet-like bodies.
4. Leucogranites and pegmatites form the last intrusive phases, except for post-tectonic mafic dykes. They are volumetrically minor, but ubiquitous. Cross cutting relationships and progressive deformation of the intrusives indicate a late-tectonic timing of emplacement.

Cross cutting relationships and the progressive deformation have been used to establish this generalised sequence of intrusion. However, it should be noted that particularly phases 3 and 4 (leuocratic granite gneisses and leucogranites/pegmatites) seem to have been emplaced over a protracted period of time and through much of, at least, the last deformation stages.

- <u>Structural Geology:</u>

Camp V was situated in a relatively low-strain domain, bordering against high-strain banded gneiss and amphibolite domains to the N and E. This allowed the details of the actual fabric development in the TTG-amphibolite sequence to be traced. The progressive fabric evolution sketched in the following occurs over a distance of commonly less the 1 to 1.5 km. It is, in essence, identical to what was described for the structural evolution at Camp I, some 10 km further W, underlining the regional significance of this fabric development.

The earliest fabric, S_1, is a bedding-/layering-parallel foliation in amphibolites and grey gneisses (Fig. 26a). This foliation and intrusive contacts are folded into an early generation of N-S trending, upright, commonly steep, but also doubly-plunging folds (F_1). The presence of relatively wide (10-25 m) subhorizontal foliation domains (i.e. the S_1 foliation and lit-par-lit layering) gently folded between the steep limbs of F_1 folds points to the originally subhorizontal orientation of S_1 and the lit-par-lit layering (Fig. 26a). Rare type 2 (mushroom-type) fold interference patterns also point to the presence of earlier subhorizontal domains that were subsequently refolded by upright (F_1) folds (Fig. 26b). This seems noteworthy since this is the only location mapped during this field season, where shallowly-dipping fabrics have been recorded.

Towards the N and E (i.e. with increasing fabric intensity), the northerly-trending folds are cut by steeply-dipping, 50 cm to 2 m wide, E-W trending high-strain zones and earlier folds are progressively refolded by a later generation of upright, E-W trending folds (F_2), resulting in spectacular dome-and-basin fold interference patterns (Fig. 26c, d). Leucogranites and pegmatites intrude during this deformation. The sheet-like granites show mainly E-W trends and intrude along the axial planes of F_2 folds and into the high-strain zones (Fig. 26e). The high-strain zones do not show any preferred sense of shear or fabric asymmetry that would point to a significant non-coaxial component of deformation. In fact, opposite sense of wall-rock drag into the shear zones is common (also recorded at Camp I), rather indicating co-axial shortening at high angles to the shear zones (Fig. 26e).

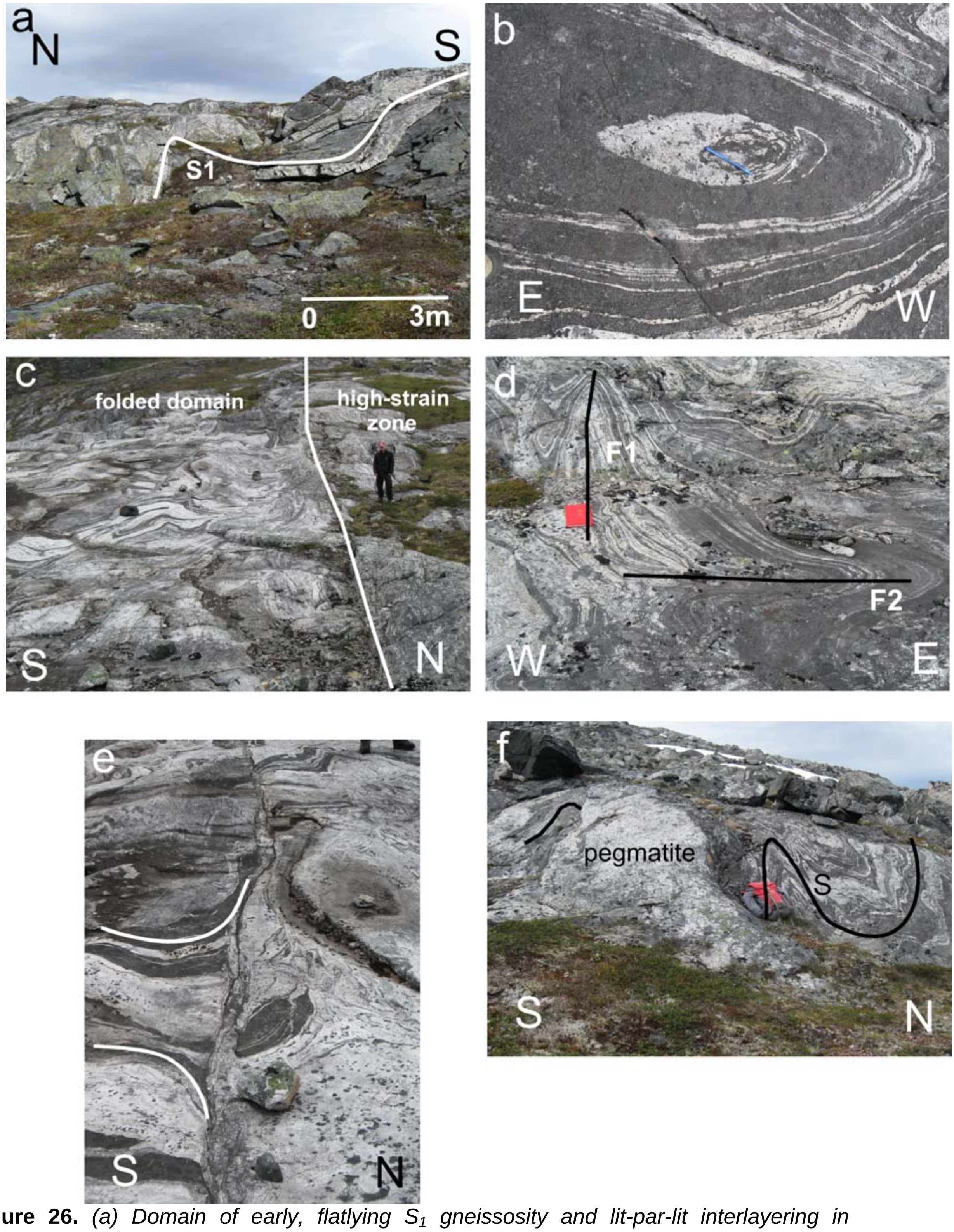

Figure 26. *(a) Domain of early, flatlying S_1 gneissosity and lit-par-lit interlayering in gneisses and amphibolites. (b) Type 2 (mushroom-type) fold interference in grey gneisses. (c) Dome-and-basin interference patterns in grey gneisses are transected and progressively transposed by E-W trending high-strain zones. (d) Oblique plan view of interference between N-S trending folds (black lines annotate traces of axial surfaces) and later-generation E-W trending folds. (e) The pure-shear, flattening-dominated deformation along the E-W trending melt-filled high strain zones is here illustrated for a smaller-scale example by the opposite sense of rotation of the foliation on the S side of the shear zone. Compare*

this image to the overall structural evolution of the Graedefjord sketched in Fig. 17. (f) Intrusion of leucogranites and pegmatites along the axial planes of the late-generation E-W-trending folds is common throughout the area.

Further fold tightening about E-W trends occurs mainly parallel to m-wide, E-W trending high-strain zones (banded gneisses), resulting in highly elongate, E-W trending domes and basins. Eventually, earlier-generation folds are completely obliterated and transposed into E-W to NW-SE trending, subvertical banded and/or striped gneisses that may attain widths of up to 25 metres, grading to the N and E into then several hundred metre wide zones of striped gneisses and interlayered amphibolites (Fig. 27a). In vertical sections, the gneisses show dm- large shear bands (asymmetric and symmetrical) indicating a subvertical stretch (Fig. 27b). This corresponds to an invariably steep E to SE plunging mineral stretching lineation developed on foliation planes (Fig. 27c). Mylonitic textures (e.g. quartz ribbons, grain-size reduction, etc.) are only observed in coarse-grained pegmatites, whereas leucogranites and TTG’s show a pervasive solid-state fabric, but no mylonitic textures (sensu stricto). The emplacement of leucogranitic and/or pegmatitic, mainly foliation-parallel stringers seems to have occurred throughout the deformation history.

The progressive fabric development that can be illustrated for TTG gneisses at both Camps I and V illustrate that seemingly simple looking banded gneisses may contain a composite and possibly longlived structural evolution. In this case, the transposition fabric of banded gneisses of the Graedefjord region records of three previous fabric-forming events.

The latest phase or deformation is marked by the occurrence of brittle-ductile cataclasite-mylonite zones (Fig. 27d, e). The fault zones trend E-W and show a strong spatial correlation with the late-stage pegmatite sheets of the area. The faults are almost identical to those described at Camp IV, imparting a banded texture on the rocks, commonly leucogranites and pegmatites (Fig. 27e). Shear sense indicators are abundant and point to consistently dextral strike-slip kinematics (Fig. 27d). The brittle-ductile mylonites form an anastomosing pattern. Individual mylonites may reach several metres in width, but combined, they from an up to 200 m wide zone that can be traced for at least 5 km along strike.

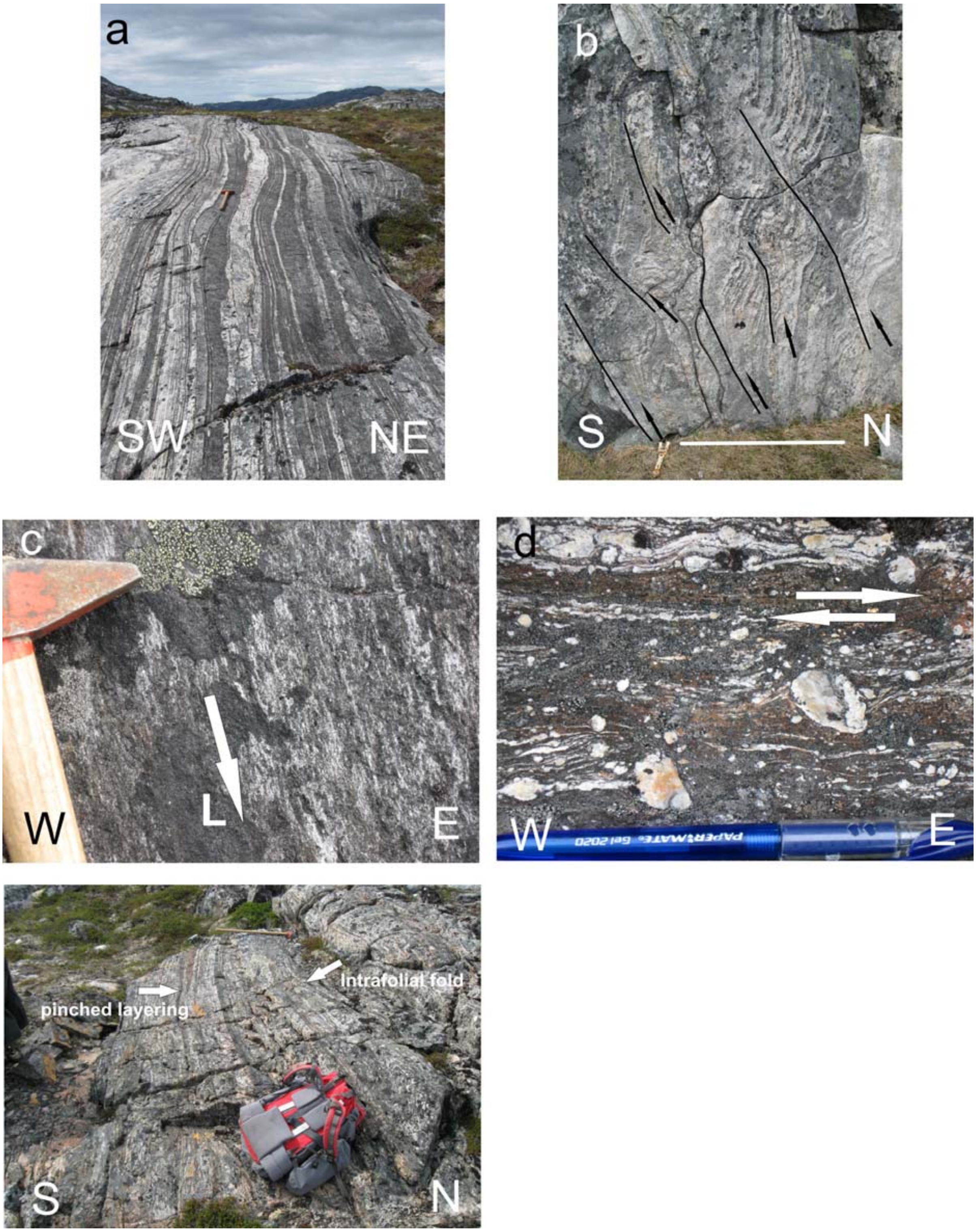

Figure 27. *(a) Structurally seemingly striped gneisses are the result several phases (here at least three phases) of fold- and layer-transposition. (b) Cross-sectional view of oblique shear bands, indicating vertical stretch along the steep E-W trending gneissosity (Fig. 18 shows a near-identical stretch in gneisses some 12 km to the W). (c) Steep E and SE plunging mineral stretching lineation in amphibolite. (d) Ductile-brittle mylonite/cataclasite zone. Large feldspar porphyroclasts indicate that the protolith of the mylonites were pegmatites. There is a close spatial association between late pegmatites and mylonite/cataclasite*

zones throughout the area. (e) E-W trending, banded mylonites/cataclasites. The late-stage shear zones are identical to those recorded at Camp IV (compare Fig. 23).

Summary and Discussion

The area around the Graedefjord is a TTG dominated (> 90-95 vol.%) terrain. Supracrustal rocks are massive to banded amphibolites with very subordinate meta-ultramafic rocks, felsic meta-volcanic- and/or volcanoclastic rocks and meta-sedimentary rocks. Primary volcanic textures are rare, but felsic schists contain textural evidence that may point to their origin as crystal tuffs and/or volcanoclastic rocks.

Throughout the Graedefjord region, the sequence of TTG intrusion is characterised by an early phase of grey, banded TTG gneisses (most likely representing a multitude of intrusive events), followed by mainly sheet-like leucogranite gneisses and a last stage of leucogranites and pegmatites. The Illivertalik granite along the NE parts of the Graedefjord is a mappable, although texturally and compositionally very heterogeneous pluton. Based on regional correlations, its relative age is between that of the early grey gneisses and later leucogranites. Except for the oldest, commonly highly transposed phases, all TTG and granite phases show evidence for a synkinematic (D_2/D_3/D_4) emplacement, underlining the polyphase tectonic history of the terrain. Detailed geochronology is required to identify whether deformation was part of one progressive event or whether distinct tectonic episodes can be distinguished.

Structural Geology

Deformation phases and structural styles are similar in all investigated areas, with the exception of Camp IV (see below). The deformation phases outlined by the present report broadly correspond to the deformation episodes described by Myers (1978) during his regional field work in the Graedefjord region to the immediate E of the present field area. Variations in structural styles between different camps can be related to different fabric (strain) intensities that may or may not have overprinted previous deformation phases. The D_3 deformation episode is the dominant phase of deformation responsible for the E-W trending structural grain of the area. The main deformation phases around the Graedefjord can be conceptualised as follows:

D_1: early phase of recumbent folding and layer-parallel transposition. This phase is only observed in supracrustal rocks and the earliest grey gneisses. It is preserved on an outcrop scale in the supracrustal rocks. On a regional scale, it is indicated by the type 3 fold interference pattern outlined by supracrustal belts that suggests an early recumbent fold phase refolded by a subsequent upright fold phase. Relics of the probably early horizontal fabric domains are locally preserved (e.g. Camp V, Fig. 26a).

D_2: a second fold phase characterised by upright, N-S trending, mainly steeply plunging folds (F_2). Mesoscopic F_2 folds are well preserved in low-strain (D_3) domains around e.g. Camps 1 and 5. Leucogranites and pegmatites commonly intrude axial planar to F_2 folds. On a regional scale, the approximately N-S trending folds are evidenced by the type 3 fold interference outlined by amphibolite belts (see above).

D_3: characterised by E-W trending, upright, steeply plunging folds that refold. In D_3 high-strain zones, all earlier fold generations (F_1-F_3) are completely transposed into a subvertical, E-W trending gneissosity. Fabric development indicates that D_3 strains are characterised by bulk N-S subhorizontal shortening. Layer-normal shortening is associated with a steep stretch and foliation-parallel extension, indicated by shear bands and the near ubiquitous steep SE- to E-plunging mineral stretching lineation. In places, prolate fabrics are dominant (e.g. Camp II). Deformation is accompanied by emplacement of commonly sheet-like leucogranites and pegmatites, often axial planar to F_3 folds or parallel to the E-W trending gneissosity (S_3). Despite the high-strain fabrics, mylonitic textures are rare, probably pointing to the high T-conditions of deformation and the presence of melts in the rocks, both facilitating recovery processes. D_3 high-strain fabrics (gneiss belts, striped gneisses and interlayered amphibolites) dominate the area around the Graedefjord. Away from the central high-strain belts (e.g. Camp II to the north), the D_3 deformation is interpreted to have resulted in the refolding of earlier fabrics (D_2 and D_3) by steeply plunging tubular folds (D_3 late). These folds are interpreted to have formed in response to the vertical extrusion of material on the margins of the D_3 high-strain Graedefjord structure.
D_4: is characterised by the formation of E-W trending, subvertical to steep N dipping high-strain zones. D_4 high-strain zones were mapped at Camps I, IV and V. Ductile-brittle conditions of deformation in D_4 high-strain zones are indicated by pervasive crystal plastic textures in e.g. mylonites next to and overprinted by brittle-ductile cataclasites (e.g. Figs. 26b, e; 27e). The high-strain zones show a close spatial association with late-stage pegmatites and leucogranites. Kinematic indicators point to predominantly dextral strike-slip kinematics, although top-the-S reverse movement (Camp IV, see also Windley 2009) and top-the-N normal movement were recorded. The D_4 deformation is the most prominent deformation phase at Camp IV, also associated with SE verging folds, and evidence for the earlier deformation phases is not as clear as in other camps. D_4 deformation zones and associated pegmatites are commonly associated with iron staining.
D_5: the last regionally significant phase of deformation is related to the formation of brittle faults. These faults were recorded in all Camps, but are particularly abundant at Camp II, off the coast. Faults are invariably steep, trend N-S or define a conjugate pattern around N trends, corresponding to an episode of E-W extension. Greenschist-facies retrogression of high-grade gneisses and supracrustal rocks may extend for up to 50 m around the faults.

The structural evolution of this area and deformational style suggest a rheologically extremely weak crustal section during the D_2/D_3 deformation. The style of deformation (particularly during D_3) recorded in the Graedefjord region indicates bulk shortening and predominantly vertical extrusion of the weakened crust, with a subordinate lateral component. This agrees with theoretical considerations and modelling of weak lithospheric structures during collisional tectonics (e.g., Touissant *et al.* 2004), that predict bulk flow of weakened crustal levels rather than deformation localised to discrete thrusts or detachments. The implication is that conditions during peak-metamorphic temperatures were not conducive to large-scale thrusting and imbrication of blocks as might be expected along a terrane boundary.
Pervasive crystal-plastic textures of e.g. feldspars in D_4 mylonites point to relatively high-temperature conditions during at least the onset of D_4, but these conditions are clearly retrograde compared D_2/D_3. D_4 cataclasites indicate that the last strain increments occurred when the terrain had cooled to below ca. 450°C, i.e. the onset of feldspar plasticity. D_5

faults are possibly related to a very late stage of deformation such as the opening of the Atlantic.

Mineralisation

The most common manifestations of mineralisation are ferruginous zones and iron staining that are either associated with (1) late-stage brittle-ductile faults and shear zones (D_4), and/or (2) late-stage pegmatites. Incidentally, both late-stage pegmatites and faults are often associated with each other, showing predominantly E trends in the Graedefjord region. Quartz veining is mainly confined to N-trending, late-stage brittle faults. Fluid flow along these faults is also indicated by up to 50 m wide alteration halos and associated sericitisation of TTG wall-rock gneisses and chloritisation of amphibolites, but mineralisation could not be identified.

Summary and discussion

Hydrothermal quartz veins were observed in the Tasiusarsuaq terrane to the north and to the south of Grædefjord. The Grædefjord area itself is barren in terms of economically interesting quartz veins. The only hydrothermal mineralisation with slightly elevated metal contents is hosted in breccias that formed during D_5 faulting, probably in the Proterozoic. However, the conclusion is that the outcrop extent is limited and the metal content too low to be of any economic interest.

The hydrothermal quartz veins are 1–50 cm wide and are continuous along strike and down dip over several m to up to 40 m. Besides Qtz, they contain minor Fsp, Hbl, Py and Po. The quartz veins are surrounded by a 20 cm to 2 m wide alteration halo. The mafic granulites contain a Bt-Hbl-Grt-Qtz-Py±Kfs-Ms-Po-Ilm-Ccp-Mag-Au hydrothermal alteration assemblage. In meta-sedimentary rocks, the hydrothermal alteration comprises Bt-Grt-Sil-Qtz-Py. Composite systems of several parallel quartz veins together with alteration zones can be 50–200 m wide and can be followed along strike and down dip 250–2000 m if the outcrop situation allows that.

In the Sermilik area, one out of 7 quartz veins yield about 6 ppm Au, which makes this area interesting in terms of economic hydrothermal gold mineralisation. The veins formed most probably in the late stages of the D_2 deformation during F_{2b} folding. Quartz veins form a network of veins (1) parallel to F_{2b} fold limbs, (2) axial planar to F_{2b} folds and (3) in ac-orientation to F_{2b} folds.

Further north in the Tasiusarsuaq terrane, similar hydrothermal quartz vein and alteration systems formed during D_3 deformation and occupy the structures of F_3 folds (Kolb *et al.* 2009). A minimum age of this hydrothermal alteration stage is given by the age of a late-D_3 pegmatite yielding 2668 ± 4 Ma (U-Pb zircon age, Kolb *et al.* 2010).

Hydrothermal quartz veins and alteration zones between Grædefjord and Quvnerup ilua are controlled by local D_2 high strain zones, which probably correlate with the ca. 2.7 Ga D_3 high strain zone in Grædefjorden (A. Kisters unpubl. data).

In the Nuuk area further north, several gold occurrences are known from the strike extent along the Ivinnguit fault (IVF), namely Storø, Qussuk, Bjørneøen, Qilanngaarsuit and SW Isua. The quartz vein hosted gold mineralisation at Storø formed at about 2630 Ma and is, thus, spatially and genetically linked to terrane collision and deformation along the IVF at 2650–2600 Ma (Nutman *et al.* 2007; van Gool *et al.* 2007). One type of gold mineralisation at Storø occurs in quartz veins and alteration zones comprising Bt, Grt, Qtz, Di, Po and Apy (Eilu *et al.* 2006). The gold mineralisation in Qussuk similarly occurs in quartz veins with distinct alteration halos of Bt, Grt, Qtz and Po (Schlatter & Christensen 2010). A very similar alteration of Bt, Grt and Qtz associated with quartz veins is observed at SW Isua (Stensgaard 2008). On Qilanngaarsuit hydrothermal quartz veins are hosted in D_3 structures and are surrounded by hydrothermal alteration halos comprising Bt-Qtz-Grt-Po-Py-Ccp±Tur-Sil-Au (Kolb *et al.* 2009). Hydrothermal alteration and D_3 deformation postdate high-pressure metamorphism, which was dated at ca. 2715 Ma (Nutman & Friend 2007).

The IVF may represent a high permeability zone where hydrothermal alteration and gold mineralisation occurred around 2650–2600 Ma (Kolb *et al.* 2009). To the south between Ameralik and Fiskenæsset, hydrothermal alteration and gold mineralisation is most probably related to deformation around 2720–2670 Ma (Kolb *et al.* 2010; Nutman *et al.* 2007). The two stages of hydrothermal gold mineralisation are most probably related to major accretionary tectonism, (1) along the IVF and (2) between the Tasiusarsuaq terrane and the northern terrane assembly of the North Atlantic craton of southern West Greenland.

Conclusions and future work

Field work in 2009 has identified several occurrences of hydrothermal quartz veins and associated hydrothermal alteration zones. Quartz veins and hydrothermal alteration are structurally controlled and their location can be predicted based on the mapped structures. The footprint of the hydrothermal quartz veins in the Tasiusarsuaq terrane is characterised by:

- Structural control by the limbs and sheared limbs of the F_3 folds or F_{2b} fold structures in Sermilik;
- Quartz vein systems with various orientations of veins forming an interconnected network;
- Hydrothermal alteration assemblage comprising Bt-Hbl-Grt-Qtz-Py±Kfs-Ms-Po-Ilm-Ccp-Mag in meta-mafic rocks, Bt-Grt-Sil-Qtz-Py in meta-sedimentary rocks and Ms-Qtz-Po-Ccp in TTG gneiss
- Gold contents of up to 6 ppm; and
- Outcrop extent of up to 2 km strike length, up to 400 m width and up to 1.5 km down dip (where the outcrop situation allows observing that).

In spite of the similarity in the major characteristics listed above, the geochemical analysis of the whole rock samples yield very variable results on the gold content. Many of the samples returned Au values in the lower ppb range and also below the detection limit of 2 ppb. The question whether this reflects “true” variation in gold endowment cannot be answered unequivocally. Further studies are needed that are directed towards the following possible explanations:

- Different timing of hydrothermal alteration during D_2 and D_3 stages;
- Various hydrothermal fluid compositions, e.g. Kfs is hydrothermal alteration mineral only in the systems in Sermilik containing up to 6 ppm Au (on the other hand, low Au values are also recorded from here);
- Different host structures and host rocks;
- Remobilisation of Au during later greenschist facies hydrothermal overprint;
- Remobilisation of Au during supergene alteration; and
- Sampling was unsystematic, not taking into account the difficulties in solving the nugget effect problem for gold analysis.

The general approach that was used during field work in 2008 and 2009 will also be followed in the last season in 2010 of this 3-year joint BMP-GEUS project. The focus will be on the two known gold occurrences east of Paamiut and at Tartoq. GEUS geologists will be supported by external partners covering the following projects:

- Mapping of hydrothermal alteration and quartz vein systems of the Paamiut gold occurrence (University of Windsor, Canada);
- Metamorphic evolution of the rocks at Paamiut (Oxford University, UK);
- Geochemical variations and mass balance calculations of the hydrothermal alteration in the Tartoq gold occurrence (M.Sci. thesis, Imperial College, UK);
- Structural control of hydrothermal alteration in the Tartoq gold occurrence (University of Stellenbosch, South Africa);
- Metamorphic evolution of the rocks at Tartoq (RWTH Aachen University, Germany);

- Stratigraphy and geochemistry of host rocks at Tartoq (University of Windsor, Canada); and
- Quantitative mineralogy of hydrothermal alteration zones at Tartoq (Geocenter Danmark).

Some of the results from these projects will be produced later than the end of 2010 and, therefore, will be reported independently from the final report of this 3-year BMP-GEUS project to be expected in the first half of 2011, by scientific publications and theses.

Running and finished projects are:

- M.Sc. project on hydrothermal quartz veins in Kangiata Nuna and Sermilik (Copenhagen University);
- M.Sc. project on massive sulphides found on Simiutat, Qilanngaarsuit and close to Narssaq (Copenhagen University);
- Geochemical variations and mass balance calculations of the hydrothermal alteration in the Qilanngaarsuit gold occurrence (M.Sc. thesis, RWTH Aachen University)
- B.Sc. project: Marie-Isabelle M. Struck (2009), Die geochemische Charakterisierung von metamorphen Gesteinen der Færingehavn-, Tre Brødre-, und Tasiusarsuaq-Terrane, Südwestgrönland (RWTH Aachen University);
- M.Sc. mapping project: Martin Koppelberg (2010), Geological map of the Fiskenæsset complex: Sarfat Aariaat east (RWTH Aachen University); and
- M.Sc. mapping project: Nicolas Benjamin Stoltz (2010), Geological map of the Fiskenæsset complex: Sarfat Aariaat west (RWTH Aachen University).

References

Andersen, L.S. & Friend, C. 1973: Structure of the Ravns Storø amphibolite belt in the Fiskenæsset region. Rapport Grønlands Geologiske Undersøgelse **51**, 37-40.

Chadwick, B. & Coe, K. 1983: Buksefjorden 63 V1 Nord Descriptive text Geological map of Greenland 1:100 000 The regional geology of a segment of the Archaean block of southern West Greenland, 70. Copenhagen: Grønlands Geologiske Undersøgelse.

Crowley, J.L. 2002: Testing the model of late Archean terrane accretion in southern West Greenland: a comparison of the timing of geological events across the Qarliit nunaat fault, Buksefjorden region. Precambrian Research **116**, 57-79.

Eilu, P., Garofalo, P., Appel, P.W.U. & Heijlen, W. 2006: Alteration patterns in Au-mineralised zones of Storø, Nuuk region - West Greenland, 73. Copenhagen:

Escher, J.C. & Myers, J.S. 1975: New evidence concerning the original relationships of early Precambrian volcanics and anorthosites in the Fiskenæsset region, West Greenland. Rapport Grønlands Geologiske Undersøgelse **75**, 72-76.

Escher, J.C. & Pulvertaft, T.C.R. 1995: Geological map of Greenland, 1:2 500 000, Copenhagen: Geological Survey of Greenland.

Friend, C.R.L. & Nutman, A.P. 2001: U-Pb zircon study of tectonically bounded blocks of 2940-2840 Ma crust with different metamorphic histories, Paamiut region, South-West Greenland: implications for the tectonic assembly of the North Atlantic craton. Precambrian Research **105**, 143-164.

Friend, C.R.L., Nutman, A.P. & McGregor, V.R. 1987: Late-Archaean tectonics in the Færingehavn-Tre Brødre area, south of Buksefjorden, southern West Greenland. Journal of the Geological Society London **144**, 369–376.

Friend, C.R.L., Nutman, A.P. & McGregor, V.R. 1988: Late Archaean terrane accretion in the Godthåb region, southern West Greenland. Nature **335**, 535–538.

Friend, C.R.L., Nutman, A.P., Baadsgaard, H., Kinny, P.D. & McGregor, V.R. 1996: Timing of late Archaean terrane assembly, crustal thickening and granite emplacement in the

Nuuk region, southern West Greenland. Earth and Planetary Science Letters **142**, 353-365.

Ghisler, M. 1970: Pre-metamorphic folded chromite deposits of stratiform type in the early Precambrian of West Greenland. Mineralium Deposita **5**, 223-236.

Hopgood, A.M. 1976: Structures in an area north-east of Fiskenæsset, West Greenland. Rapport Grønlands Geologiske Undersøgelse **73**, 16–21.

Kalsbeek, F. & Myers, J.S. 1973: The geology of the Fiskenæsset region. Rapport Grønlands Geologiske Undersøgelse **51**, 5–18.

Kolb, J., Kokfelt, T. & Dziggel, A. 2010: Deformation history of an Archaean terrane at mid-crustal level: the Tasiusarsuaq terrane of southern West Greenland. Precambrian Research, in prep.

Kolb, J., Stensgaard, B.M., Schlatter, D.M. & Dziggel, A. 2009: Controls of hydrothermal quartz vein mineralisation and wall rock alteration between Ameralik and Sermilik, southern West Greenland, 76. Copenhagen:

Myers, J.S. 1976: Granitoid sheets, thrusting, and Archean crustal thickening in West Greenland. Geology **4**, 265–268.

Myers, J.S. 1978: Formation of banded gneisses by deformation of igneous rocks. Precambrian Research **6**, 43–64.

Myers, J.S. 1985: Stratigraphy and structure of the Fiskenæsset Complex, southern West Greenland. Bulletin Grønlands Geologiske Undersøgelse **150**, 72.

Næraa, T. & Scherstén, A. 2008: New zircon ages from the Tasiusarsuaq terrane, southern West Greenland. Geological Survey of Denmark and Greenland Bulletin **15**, 73-76.

Nutman, A.P. & Friend, C.R.L. 2007: Adjacent terranes with ca. 2715 and 2650 Ma high-pressure metamorphic assemblages in the Nuuk region of the North Atlantic Craton, southern West Greenland: Complexities of Neoarchaean collisional orogeny. Precambrian Research **155**, 159-203.

Nutman, A.P., Christiansen, O. & Friend, C.R.L. 2007: 2635 Ma amphibolite facies gold mineralisation near a terrane boundary (suture?) on Storo, Nuuk region, southern West Greenland. Precambrian Research **159**, 19-32.

Nutman, A.P., Friend, C.R.L., Baadsgaard, H. & McGregor, V.R. 1989a: Evolution and assembly of Archean gneiss terranes in the Godthåbsfjord region, southern West Greenland: structural, metamorphic, and isotopic evidence. Tectonics **8**, 573–589.

Nutman, A.P., Rivers, T., Longstaffe, F. & Park, J.F.W. 1989b: The Ataneq fault and mid-Proterozoic retrograde metamorphism of early Archaean tonalites of the Isukasia area, southern West Greenland: reactions, fluid compositions and implications for regional studies. In: Bridgwater, D. (ed.): Fluid movements - element transport and the composition of the deep crust, 151–170. Dordrecht: Kluwer Academic Publishers.

Pidgeon, R.T. & Kalsbeek, F. 1978: Dating of igneous and metamorphic events in the Fiskenaesset region of southern West Greenland. Canadian Journal of Earth Sciences **15**, 2021–2025.

Polat, A., Appel, P.W.U., Fryer, B., Windley, B.F., Frei, R., Samson, I.M. & Huang, H. 2009: Trace element systematics of the Neoarchean Fiskenæsset anorthosite complex and associated meta-volcanic rocks, SW Greenland: Evidence for a magmatic arc origin. Precambrian Research **175**, 87-115.

Ramsay, J.G. & Huber, M.I. 1987: Folds and fractures, 700. London: Academic Press Limited.

Riciputi, L.R., Valley, J.W. & McGregor, V.R. 1990: Conditions of Archean granulite metamorphism in the Godthab-Fiskenaesset region, southern West Greenland. Journal of Metamorphic Geology **8**, 171–190.

Schjøtte, L., Compston, W. & Bridgwater, D. 1989: U-Pb single-zircon age for the Tinissaq gneiss of southern West Greenland: a controversy resolved. Chemical Geology **79**, 21–30.

Schlatter, D.M. & Christensen, R. 2010: Geological, petrographical and lithogeochemical investigations on the Qussuk gold mineralisation, southern West Greenland, 53. Copenhagen:

Stensgaard, B.M. 2008: Gold favourability in the Nuuk region, southern West Greenland: results from fieldwork follow-up on multivariate statistical analysis, 74. Copenhagen: Danmarks og Grønlands Geologiske Undersøgelse Rapport.

Touissant, G., Burov, E. & Jolivet, L. 2004: Continental plate collision: Unstable vs. stable slab dynamics. Geology **32**, 33-36.

van Gool, J.A.M., Scherstén, A., Østergaard, C. & Neraa, T. 2007: Geological setting of the Storø gold prospect, Godthåbsfjord region, southern West Greenland; Results of detailed mapping, structural analysis, geochronology and geochemistry., København: Danmarks og Grønlands Geologiske Undersøgelse Rapport.

Wells, P. 1976: Late Archean metamorphism in the Buksefjorden region, Southwest Greenland. Contributions to Mineralogy and Petrology **56**, 229-242.

Windley, B.F. 2009: Shear zones and suture on tectonic boundaries in the Grædefjord region. In: Kolb, J. & Kokfelt, T. (eds): Annual workshop on the geology of southern West Greenland related to field work: abstract volume I **2009/21**, 29. Copenhagen: Danmarks og Grønlands Geologiske Undersøgelse Rapport.

Windley, B.F. & Garde, A.A. 2009: Arc-generated blocks with crustal sections in the North Atlantic craton of West Greenland: crustal growth in the Archean with modern analogues. Earth-Science Reviews **93**, 1-30.

Windley, B.F., Herd, R.K. & Bowden, A.A. 1973: The Fiskenæsset complex, West Greenland Part I A preliminary study of the stratigraphy, petrology, and whole rock chemistry from Qeqertarssuatsiaq, 80.